Design and Synthesis of Bicyclic Ligands for the FK506-Binding Proteins 51 and 52

Yansong Wang

aus

Nanchong, China

2012

Erklärung

Diese Dissertation wurde im Sinne von § 7 der Promotionsordnung vom 28. November 2011 von Herrn Prof. Dr. Christoph W. Turck betreut von der Fakultät für Chemie und Pharmazie vertreten.

Eidesstattliche Versicherung
Diese Dissertation wurde eigenständig und ohne unerlaubte Hilfe erarbeitet.

München, den 29.06.2012

....
Yansong Wang

Dissertation eingereicht am 29.06.2012

1. Gutachter: Prof. Dr. Christoph W. Turck

2. Gutachter: Prof. Dr. Roland Beckmann

Mündliche Prüfung am 18.07.2012

Acknowledgements

Contents

1. Abstract

The FK506-Binding Proteins 51 and 52 (FKBP51/52) belong to the immunophilin superfamily. Both proteins are highly homologous. They are composed of three domains and adopted similar conformations. They have cochaperone activity by participating in the Hsp90-steroid receptor complex to regulate the glucocorticoid receptor (GR) signal transduction. FKBP51 has been shown to be a negative regulator whereas FKBP52 is a positive regulator of the glucocorticoid receptor. FKBP51 is involved in the etiology of stress-related psychiatric disorders and has potential as a novel therapeutic target for psychiatric disorders. Few synthetic ligands for FKBP51 and FKBP52 were described and all of them display unfavorable pharmacokinetic profiles which make them unsuitable to study the biological roles of FKBP51 and FKBP52. In this project, the aim was to limit the ligand flexibility by ligand preorganization to mimic the FKBPs ligands active conformation and to focus on the improvement of their ligand efficiencies.

The bicyclic [3.3.1] aza-amide and bicyclic [4.3.1] aza-amide core structures were designed as rigid replacements for the pipecolyl-monocyclic scaffold. Their potential binding modes were first analyzed *in silico.* A synthetic route was then establised to prepare a series of bicyclic [3.3.1] aza-amide derivatives **4** and bicyclic [4.3.1] aza-amide derivatives **5**. Their activities were tested in a competition binding fluorescence polarization assay, by isothermal titration calorimetry and in a GR hormone radioactive binding assay. Ligand **5h** was indentified as the most efficient FKBP ligand known today. It is the first lead-like ligand (MW= 367Da, LE= 0.29, clogP= 0.95) for the clinically relevant FKBP51 and offers three rigidly defined attachment points (R^1, R^2 and C^8) for further lead optimization. The comparison of the three series compounds indicated that the bicyclic [4.3.1] aza-amide scaffold has a better degree of preorganization than the bicyclic [3.3.1] aza-amide scaffold which in turn is preferred over the monocyclic scaffold. The cocrystal structures of **4g**, **5g** and **5f** with FKBP51 FK1 domain showed their binding modes are similar to those observed for compound **2** in complex with FKBP51 FK1.

Based on the cocrystal structures of **5g** and **5f**, the C^8 substituted bicyclic [4.3.1] aza-amide scaffold was designed to increase the contact surface between ligand and protein to further enhance the binding affinity. A new stereoselective synthetic route

was established and optimised in which a stereoselective carbon-carbon bond formation by intramolecular N-acyliminium cyclization was the key step. The cocrystal structure of **71** with FKBP51 FK1 confirmed the desired conformation obtained from the stereoselective synthesis. A further racemic dihydroxylation of the C^8 vinyl group substantially improved the affinity for all FKBPs yielding ligands with low nanomolar potencies that rivalled those of the natural product FK506. The higher binding affinity was proposed to be obtained from a putative hydrogen bond between the C^{11}-OH of **73a** and Tyr^{57} which was to be confirmed in the future by the corresponding cocrystal structure.

These results provided valuable information for the further optimization of FKBP51 ligands.

2. Introduction

2.1 The FK506 binding protein (FKBPs) family

The FK506 binding proteins (FKBPs) belong to the immunophilin family with high binding affinity to the immunosuppressive drugs FK506 and Rapamycin. It is a highly conserved class of proteins found in all organisms with peptidyl prolyl isomerase (PPIase) activity[1-3]. The PPIase activity catalyzes cis–trans isomerization reactions of peptide bonds involving the amino acid proline (Figure 1) which is regarded to be necessary for the proper folding of several proteins.[4]
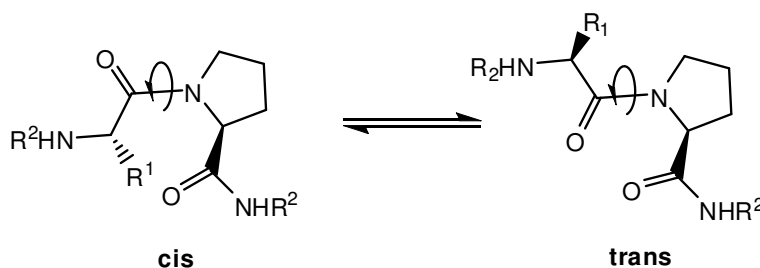
Figure 1: Peptidyl prolyl cis/trans-isomerization by PPIases.

In the nucleus, FKBPs regulate transcription[5, 6], histone chaperon activity[7, 8] and chromatin modification[9, 10], cancer progress[11, 12] and chemoresistance[13, 14]. In the cytoplasm, FKBPs play important roles in protein stability[15-17], protein trafficking[18, 19], receptor signaling[20, 21], kinase activity, intracellular Ca^{2+} homeostasis via interaction with calcium channels like the ryanodine receptor, regulation of inositol 1,4,5-triphosphate receptor[21, 22] and cation channel like TRPC1[23]. The human FKBP family consists of FKBP12, FKBP12.6, FKBP 13, FKBP15, FKBP22, FKBP24, FKBP25, FKBP36, FKBP38, FKBP51, FKBP52, FKBP60, FKBP65 and FKBP133 with their homologs usually also be found in other mammalian FKBP families[24-27] among which the FKBP12, FKBP12.6, FKBP38, FKBP51 and FKBP52 are the most studied and explored paralogs.[24, 25]

2.2 FKBP51 and 52 Structures

The amino acid sequences, domain organization and three-dimensional crystal structures of the full-length human FKBP51 and the overlapping fragments of human FKBP52 have been reported[28, 29]. They are homologous proteins with 60% identity and 75% similarity in their amino acid sequences. Both proteins are composed of three domains and adopt similar conformations (Figure 2).

The N-terminal FK1 domain has the PPIase and FK506 binding activity and it is the primary regulatory domain for steroid hormone receptors[20, 30]. Both the Hsp90 binding and the PPIase pocket are neccssary for the modulation of the SHRs[31], the PPIase activity per se is not necessary. The 40s and the 80s loop (residues 71-76 and 118-122 for FKBP51, respectively) represent the largest structural divergence in the FK1 domain between FKBP51 and 52. In the 40s loop, the Asn[74], Glu[75] and Pro[76] in FKBP51 is replaced by Lys[74], Asp[75] and Lys[76] in FKBP52. The proline rich loop (80 loop) which sits on top of the binding pocket with Leu[119] in FKBP51 and Pro[119] in FKBP52 was found to be a major cause for the different functions of FKBP51 and FKBP52 on the steroid hormone receptors. The mutations of A116V and L119P in FKBP51 was found to switch the activity to full FKBP52-like characteristics towards AR activation.[31]

The PPIase-like FK2 domain is structually similar to the FK1 domain but exhibits no PPIase activity or FK506 binding activity. Like the FK1 domain, FK2 also has the typical FKBP fold - an antiparallel six stranded β sheet around a central α helix. The function of the FK2 domain is still not clear. A mutant of FKBP51 containing a three amino acids deletion (D195, H196 and D197) deletion in the FK2 domain still binds to Hsp90 but the integration into progesterone receptor complexes is abnormal which might be due to the decreased interaction with the receptor complex.[29]

The C-terminal TPR domain is made up of three tetratricopeptide repeat (TPR) domain of a consensus 34-amino acid motif and is responsible for binding to Hsp90 through interaction with the EEVD motif in the C terminus of Hsp90.[28, 29, 32] The residues at the TPR/Hsp90 binding interface are highly conserved in both FKBP51 and FKBP52 with the exception of Q333, F335, A365 in FKBP52 and R331,Y333,L363 in FKBP51. These variations may account for the different binding activity of them to Hsp90.
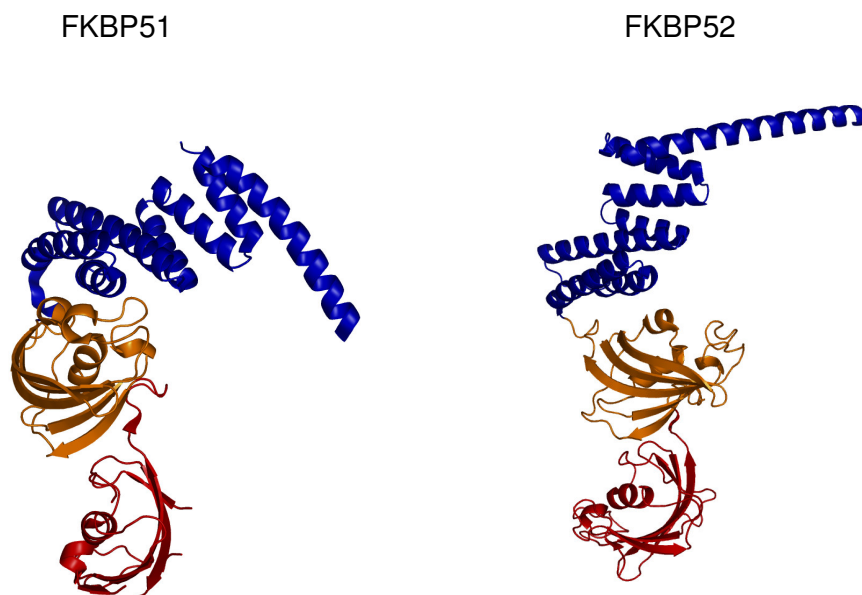
FKBP51   FKBP52

Figure 2 The crystal structure of FKBP51 (PDB number 1KT0) and a composite of two partial structures for human FKBP52 (PDB numbers 1Q1C and 1P5Q) are shown in ribbon format colored based on secondary structure. The C-terminal TPR domains are shown in blue, the FK2 domains are in organe, the FK1 domains are in red. The figure, including the overlay of the two partial FKBP52 structures, was created using pymol.

2.3 Cellular and Physiological Functions of FKBP51 and FKBP52

Although FKBP51 and FKBP52 share high sequence and structural similarity, their cellular and physiological functions are different.

2.3.1 The role of FKBP51 and FKBP52 in steroid receptor signaling

FKBP51 and FKBP52 were first identified in complex with the steroid hormone receptors[33, 34] and are best known as heat shock protein 90 (Hsp90) associated co-chaperone to regulate steroid hormone receptors (SHRs)[30]. They function antagonistically to each other. In most cell types, FKBP51 decreases the signal transduction of the SHRs[35] whereas FKBP52 increases it for androgen receptor (AR)[36], glucocorticoid receptor (GR)[20] and progesterone receptor (PR)[37]. As an exception FKBP51 was found to increase rather than decrease the signalling of the AR in prostate cancer cell lines[38, 39]. Most SHRs, especially the glucocorticoid receptor (GR), primarily stay in the cytoplasm in the ligand free state and migrate to

the nucleus upon ligand binding after a Hsp90-assisted maturation process[40, 41] (Figure 3).
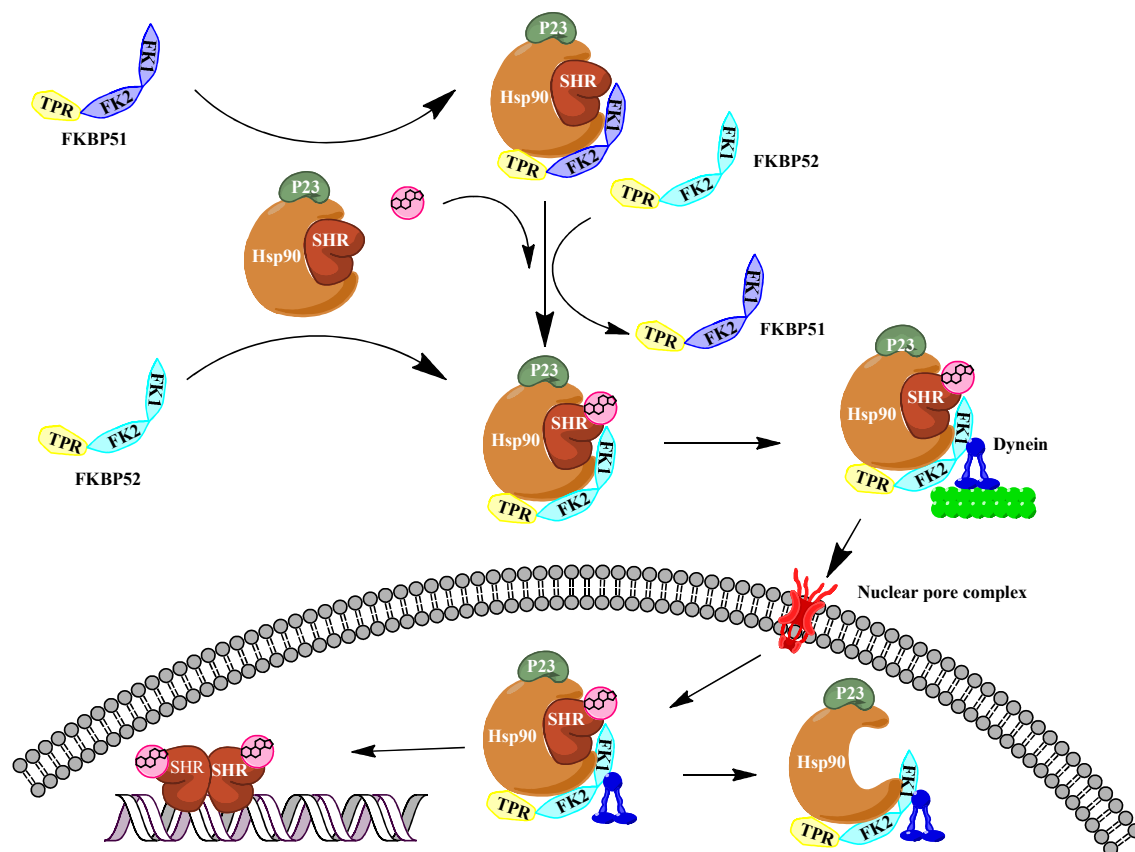
Figure 3: Model of FKBP51 and 52 on steroid hormone maturation, ligand binding and nuclear translocation.

The latest model of FKBP regulation of SHRs maturation, hormone binding and nuclear translocation was postulated as follows[42, 43]: The FKBP binds to the C-terminus of Hsp90 via the TPR domain to enter the Hsp90-dimer-SHR complex, which is stabilized by the p23 cochaperone[41]. It brings the FKBP FK1 domain into contact with the receptor ligand binding domain to directly influence hormone binding affinity. As a result of the differences in the FK1 domain especially the proline rich loop of FKBP51 and FKBP52, hormone binding is repressed in the presence of FKBP51 and potentiated in the presence of FKBP52. Upon steroid binding, the SHR heterocomplex exchanges FKBP51 for FKBP52, which is able to interact with dynein. The whole SHR–chaperone complex translocates through the nuclear pore complex

followed by receptor transformation, binding of the steroid-activated receptor to hormone response elements and gene transcription regulation. The Hsp90–FKBP52 complex further assists the cytoplasmic retrotransport of a number of Hsp90-associated factors.[43] In intact cells, FKBP51 was shown to slow down the nuclear translocation of the GR, possibly by blocking FKBP52 mediated recruitment of the dynactin motor complex. Through the active involvement of FKBP51 and FKBP52 in steroid receptor signaling, they play important roles in a variety of diseases which depend on these hormone signaling pathways.

2.3.2 Biological implications of FKBP51 and FKBP52 in diseases

2.3.2.1 Stress related diseases

The hypothalamus-pituitary-adrenal (HPA) axis is a stress hormone system triggering the physiological and behavioral response to chronic and acute stress in humans. Upon stress the hypothalamus secretes corticotropin releasing hormone (CRH) which triggers the synthesis and release of adrenocorticotropic hormone (ACTH) in the pituitary gland and results in secretion of cortisol in the adrenal gland into the blood to act on various tissues. The HPA axis is controlled by a negative feedback exerted by cortisol via the GR to inhibit the further release of CRH and ACTH thereby maintaining homeostasis of the HPA axis (Figure 4). The imbalance in the HPA axis was correlated with the risk for and course of diseases such as major depression, bipolar disorder, post-traumatic stress disorder (PTSD), schizophrenia and anxiety disorders.[44] One of the reasons for the inappropriate reaction of the HPA axis to stress was claimed to be the malfunction of GR[45]. FKBP51 and FKBP52 were shown to have opposing functions on GR[20, 46]. In clinical studies, the risk allele carriers of the single nucleotide polymorphisms rs1360780 in the FKBP51 -encoding gene showed higher FKBP51 protein levels. The same SNPs were also associated with a more rapid response to antidepressants and more lifetime depressive episodes[47-50]. FKBP51 polymorphisms have been reported to be correlated to bipolar disorders[50], suicidal events,[51-54] the recovery from psychosocial stress in healthy individuals[55], peritraumatic dissociation[56] and PTSD[57, 58]. In several independent animal model studies, FKBP51 has been shown to be an negative modulator of GR activity and

important in stress coping behavior and adaptation to stress[59-62]. The induced fkbp5 mRNA levels and the FKBP51 expression pattern in the brain after a stress or glucocorticoid challenge was shown to be region specific and correlates to the fkbp5 baseline level.[63] All these findings strongly indicated the important role of FKBP51 in the etiology of stress-related psychiatric disorders and the potential as a novel therapeutic target for psychiatric disorders.
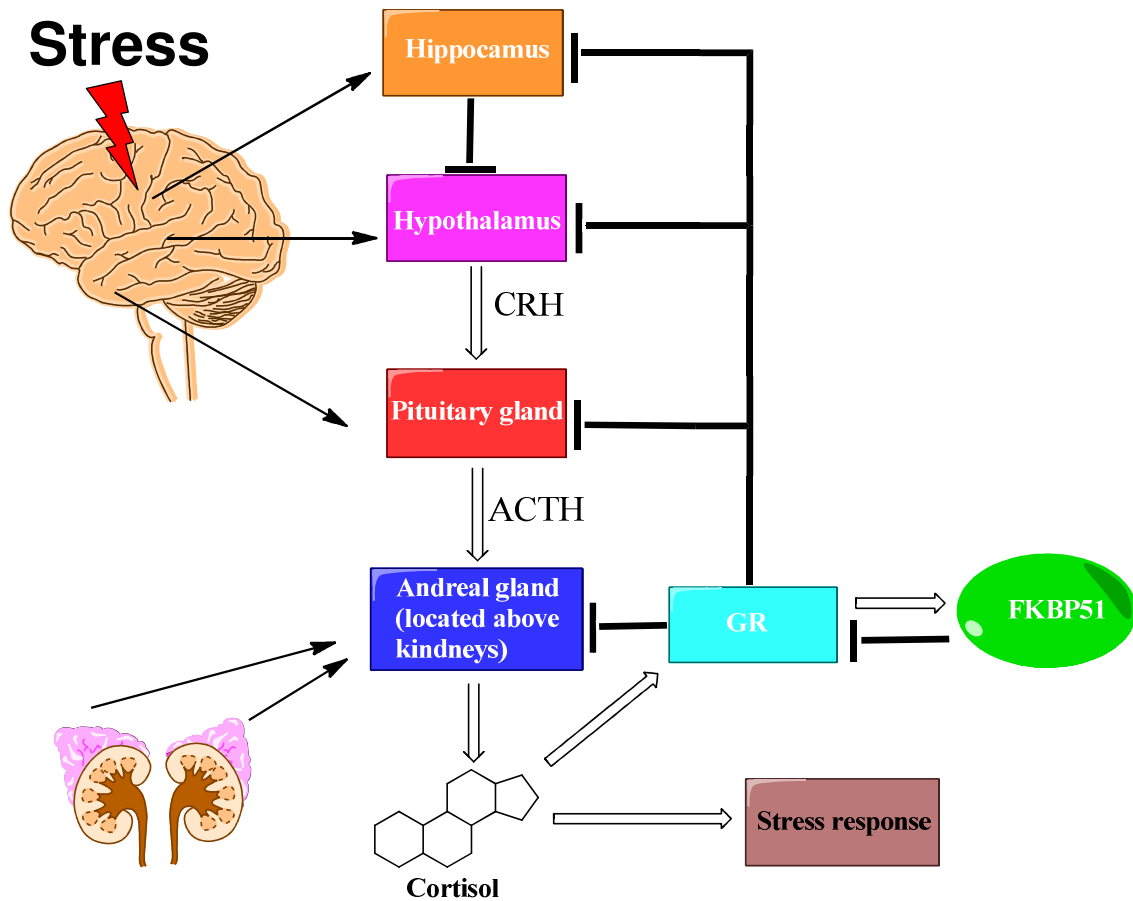
Figure 4: The Hypothalamic–Pituitary–Cortisol System[64]

2.3.2.2 Cell proliferation and cancer

FKBP51 is a protein with a progressively emerging role in cancer biology. The active role of FKBP51 in cell proliferation and cancer was shown by the increased level of FKBP51 in physiological conditions of cell growth and differentiation with preferential

expression in mitotically active cells[65-68] and in gliomas[69], retinal tumor cells[70], melanoma[71, 72], prostate cancer[73, 74] and prostatic hyperplasia [75]. In prostate cancer cells, FKBP51 was indentified as a positive regulator of AR and androgen-dependent cell growth, which is distinctly different from the effect observed on GR and PR, where FKBP51 is a negative modulator[39, 76-79]. FKBP51 was described to enhance NF-κB mediated transcription to protect from apoptosis upon a number of stimuli and to enhance cell viability or proliferation in leukemia[71] and melanocyte malignancy[80]. Via the action on GR, FKBP51 suppressed proliferation in colorectal adenocarcinoma[81] and the dexamethasone-induced expression of FKBP51 by the GR in myeloma cells has been interpreted as an adaptive process before cell death[82]. The decreased FKBP51 expression in several cancer cell lines and in pancreatic cancer tissue was correlated with increased AKT phosphorylation and a reduced cell sensitivity to chemotherapeutic agents[13, 14]. FKBP51 was proposed to negatively regulate the activity of the cell growth regulator AKT and serve as a scaffolding protein to recruit the phosphatase PHLPP[13]. Taken all together, the involvement of FKBP51 in a wide variety of cancers indicated FKBP51 as an important molecular player with divergent functions and represented a promising cancer therapy target.[39, 69, 71, 72, 83]

By contrast, less is known about the role of FKBP52 in cancer. The recently observed increased expression of FKBP52 in prostate needle biopsies from human patients[84], prostate cancer cells[85] and breast cancer cells[86] together with the androgen, progesterone and glucocorticoid insensitivity phenotypes observed in FKBP52 knockout mice[36, 37, 87-89] indicated FKBP52 as a potential therapeutic target in a variety of diseases dependent on these hormone signaling pathways.

2.3.2.3 Immune system

FKBP51 also plays a role in immune-related diseases and inflammation mainly through regulation of GR activity and modulation of NF-κB-dependent gene expression by FKBP51[69, 90-93]. It was shown that FKBP51 modulates the stability of IκB, the phosphorylation of NF-κB and enhances DNA binding of NF-κB. Enhanced FKBP51 expression in bone marrow cells was observed in rheumatoid arthritis[90] and in the treatment of chronic obstructive pulmonary disease[94]. The inhibiting of endogenous MHC class II-restricted antigen presentation by FK506 was also shown

to be mediated by FKBP51[95]. Additionally, like other smaller FKBPs, FKBP51 can bind to FK506 to mediate inhibition of the calcineurin which activates nuclear factor of activated T cells[96, 97].

2.3.2.4 Reproductive development and reproductive success

The important role of FKBP51 and FKBP52 in mammalian reproductive development and reproductive success was shown by the studies of FKBP51 knockout and FKBP52 knockout mouse lines.

Male FKBP52 knockout mice display phenotypes consistent with partial androgen insensitivity where the secondary sex organs are mainly affected with dysgenic prostate, smaller seminal vesicles, ambiguous external genitalia and retention of nipples into adulthood while the primary sex organs like testes remain unaffected.[36, 89] Female FKBP52 knockout mice seem to be morphologically normal but sterile.[37] A failure of embrynomic implantation and decidualization was found to be the reason for the infertility which indicated the crucial role for FKBP52 in female reproduction and uterine signaling[88].

FKBP51 knockout mice display no obvious morphologically phenotypes and reproduce normally compared to FKBP52 knockout mice. The double knockout of both FKBP51 and FKBP52 genes is embryonic lethal in mice[98] indicating that FKBP51 and FKBP52 have some crucial but redundant roles in embryonic development.

2.3.2.5 Neurodegenerative diseases

With their high expression in the central and peripheral nervous system, FKBP12, FKBP38, FKBP51, FKBP52 and FKBP65 also play important role in neurodegenerative disorders with neurotropic, neuroprotective and neurotransmitter releasing effects[15, 99-101]. In Parkinson's Diesease (PD), FKBP52 was found to be associated with RET51, which is a tyrosine kinase receptor important in the development and maintenance of the nervous system in a phospohorylation dependent manner. This was independent of Hsp90 or other chaperones[102]. In studies of PD and Alzheimer's Disease (AD), FKBP51 and FKBP52 showed

contrasting effect on tau stability. FKBP51 preserves tau levels but reduces its phosphorylation and enhances the tau mediated MT polymerization[15] whereas increased levels of FKBP52 is correlated with decreased tau stability[101, 103]. The PPIase activity of FKBP51 and FKBP52 are regarded critical for the regulation of tau[104, 105]. FKBP52 was also shown to interact with Atox1[106, 107] to modulate Aß pathogenesis by modulating Aß generation and toxiciy via copper homeostasis in AD[108, 109]. A transgenic mouse model of amyotrophic lateral sclerosis indicated the correlation of decreased expression of FKBP52 with degeneration of anterior lateral horn neurons and deregulation of axonal transport[110].

2.4 Chemical biology of FKBPs ligands

2.4.1 Immunosuppressive FKBPs ligands

Best known as immunosuppressive ligands used in the clinic as transplantation medicine, FK506 and rapamycin (Sirolimus) bind to FKBPs with very high affinity. Isolated from *Streptomyces tsukubaensis*, FK506 consists of a FKBP binding domain and an effector domain with which the FKBP-FK506 complex binds and allosterically inhibits the secondary target calcineurin to induce the immunosuppressive effect[111]. FKBP12, FKBP12.6 and FKBP51 are thought to be the primary FKBPs to mediate the immunosuppressive action of FK506[97, 112].
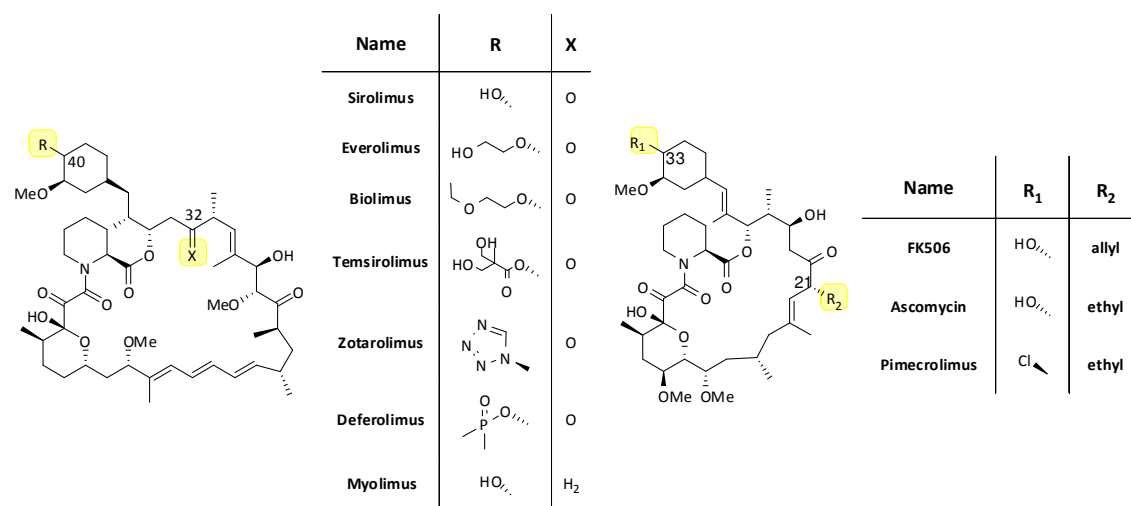
Figure 5: Clinically used immunosuppressive FKBPs ligands derived from FK506 and rapamycin.[113] The modified substructures were shaded in yellow.

Isolated from *Streptomyces hygro*scopicus, rapamycin binds to FKBPs and exhibits the immunosuppressive activity via a different ternary partner, the serine-threonine protein kinase mammalian target of rapamycin (mTOR). Many immunosuppressive FK506 and rapamycin analogs (Figure 5) were designed and used in various phases of clinical trials or in the clinic against various disorders like breast cancer, melanoma and advanced renal cell carcinoma, metastatic soft-tissue sarcomas etc. with improvement in terms of side effects, solubility and efficacy[113].

2.4.2 Non-immunosuppressive FKBPs ligands

Besides the immunosuppressive effects, FK506 and Rapamycin were also shown to have neuroprotective and neurotropic effects[114, 115]. The non-immnosuppressive FKBPs ligands were developed to reduce the suppression of immune responses of FK506 and Rapamycin but preserve or improve the neuroprotective and neurite outgrowth promotive activities in a variety of neuronal cell systems. These ligands were active in animal models of cerebral ischemia[116, 117], traumatic brain injury[118], diabetic neuropathy[119], Parkinson's disease[120-122], and other types of physical neuronal injury[123-126].

Semi- or biosynthetic analogs of FK506 or Rapamycin are one type of the non-immunosuppressive FKBPs ligands. Their bindings to calcineurin/ mTOR were abolished by modification of the effector domain (e.g., FK1706, meridamycin, normeridamycin, ILS920, Way-124466, Wye-592, L685-818) (Figure 6).

The second type of non-immunosuppressive FKBP ligands consists of small synthetic FKBPs ligands. They were designed to mimic the dicarbonyl pipecolyl moiety of the FK506 and rapamycin but lack the effector domain (Figure 7). VX-10,367 is the most potent synthetic FKBP12 ligands known to date[127] while its analogue biricodar (VX-710) was reported to retain high potency for FKBP12. It was investigated in several clinical trials as chemosensitizing agents but it displayed only modest affinity for FKBP51 and FKBP52[128]. GPI1046 and its analogs (GPI1485, JNJ460/GM284[129]) were reported to have neurotrophic and neuroprotective activities and high FKBP12 binding affinity although contrary results were also reported[116, 130-133]. GPI1046 was inactive for FKBP51 and FKBP52[134]. GPI1485 was claimed as the active form of its prodrug GPI1046 produced after in vivo ester hydrolysis[135].

Antascomycin A-E

	R1	R2	R3	n
A	H	H	H	2
B	OH	H	H	2
C	OH	Me	H	2
D	H	H	H	1
E	H	H	OH	2

Meridamycin (n = 2)
3-Normeridamycin (n = 1)
(Currently available stereo shown)

X,Y=CH$_2$: ILS-920
X,Y=CH: WYE-592

Way-124,466

WAY-179639

R1=Ethyl, R2=OH, R^3=OMe: L-685,818

R1=Ethyl, R2=OH, R^3=Me: 13Me-18OH-Ascomycin

R1= , R2=OH, R^3=OMe: FK1706
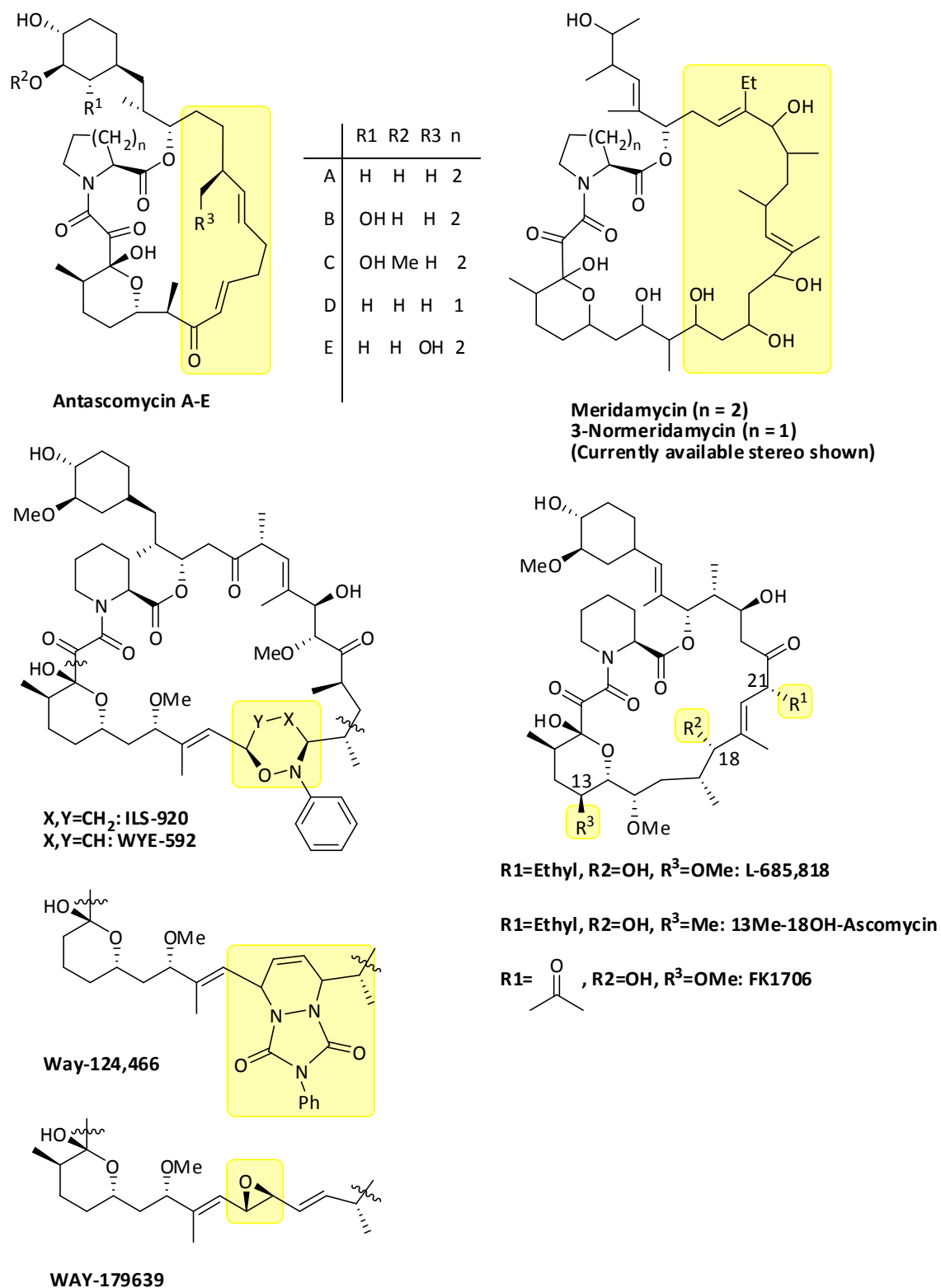
Figure 6: Representive biosynthetic or semi-synthetic analogs of FK506 or rapamycin as non-immunosuppressive FKBPs ligands [113]

13

GPI1485 failed to show activity in two phase II clinical trials[136] and was inactive in a PPIase assay of FKBP12[137]. Various FK506 analogs (VX-853, V-13,661 and V-13,670) were claimed not to bind FKBP12 but to other unidentified protein targets to produce at least some of the effects of FK506[126, 138]. VX-853 (Timcodar) was shown to be active in two animals mode of peripheral nerve diseases and advanced to a phase II clinical study for diabetic neuropathy[113]. It showed no affinity for for FKBP51 and FKBP52[134], the selectivity profile of these ligands for other FKBP family members are unknown. The cycloheximide analog DM-CHX was developed as a selective FKBP ligand for FKBP38 vs. other FKBP homologs and it was active in an animal model of focal cerebral ischemia[117]. Hudack et al. designed a tetrahydroisoquinoline moiety **A** via acyl iminium chemistry followed by systematic structure activity relationship study to give **A1** and **A2** with low nanomolar affinity for FKBP12[139].
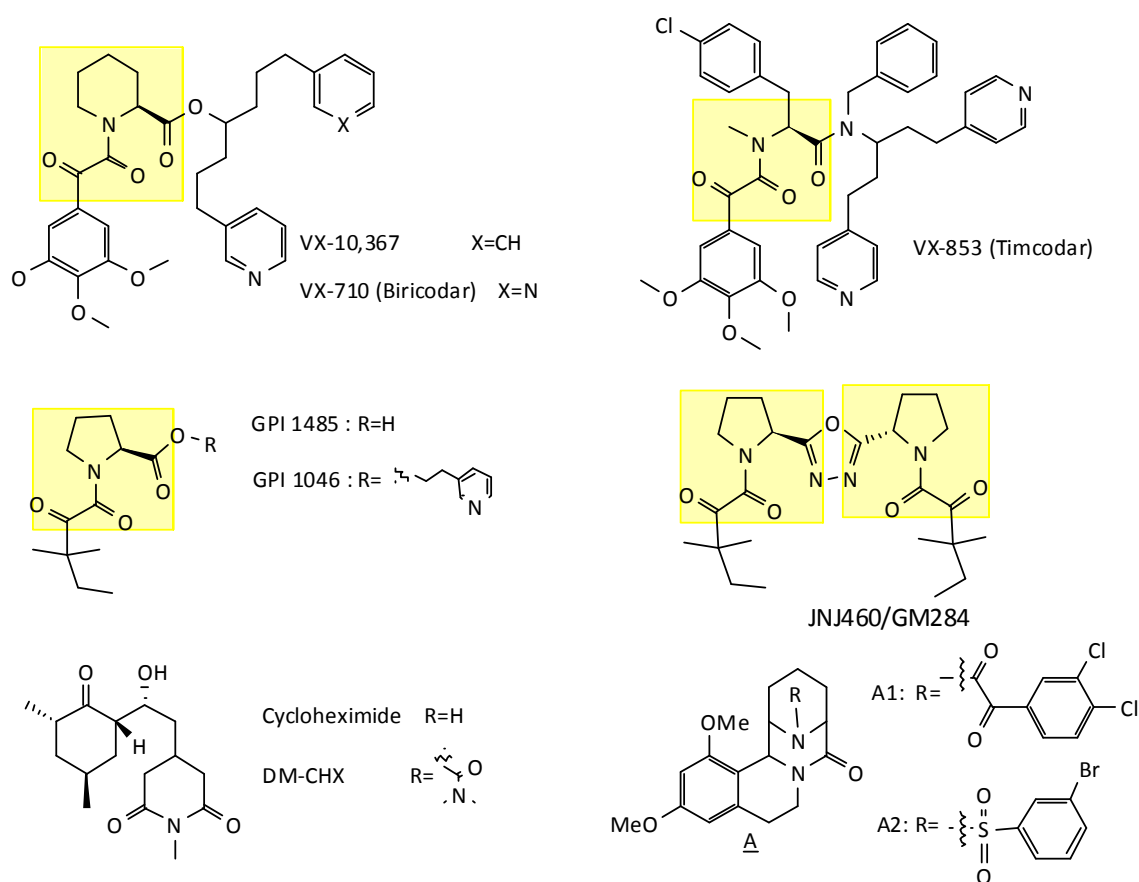
Figure 7: Synthetic neuroimmunophilin ligands. The core of FK506 or rapamycin or equivalent groups are shown in yellow[140].

2.4.3 FKBP51 and FKBP52 ligands

Compared to the active research on the biology of FKBP51 and FKBP52, few efforts for the discovery of novel synthetic FKBP51 and FKBP52 ligands were described. The first described synthetic ligand for FKBP51 and FKBP52 with low micromolar affinity was SLF[141], a simplified analogue of FK506 and rapamycin that was originally developed for FKBP12 with low nanomolar affinity[142]. Ranganath Gopalakrishnan et al. elaborated the first detailed first structure–activity relationship study for FKBP51 and FKBP52 ligands based on SLF[134]. Compared to FK506, SLF has the piperidine core derived from the diketoamide pipecolinic core of FK506 and rapamycin but it lacks the effector domain. Based on the co-crystal structure of SLF and FKBP51, a series of synthetic FK506 analogues for FKBP51 and 52 based on the pipecolate scaffold **C** were prepared. In particular, a cyclohexyl ring system which more closely resembles the pyranose ring in the high-affinity ligands rapamycin and FK506 was implemented instead of the tert-pentyl group to target the proline rich loop.

The best compounds of this series are **C1** and **C2** (Figure 8) with binding affinities of 1 µM to 4 µM. Furthermore, a focused sulfonamide library for FKBP51 and 52 were prepared using a solid phase strategy[143]. With the same pipecolate scaffold **C**, sulfonamids were attached at the R_2 position as bioisosteric replacement of the metabolic labile diketo amide moiety. Compound **C3** was claimed to be the best known ligand for the large FKBPs to date, albeit without selectivity while **C4** has exceptionally high affinity for FKBP12, rivaling those of the natural products FK506 and rapamycin. However, **C4** displayed but only low micromolar affinity for FKBP51 and FKBP52.

Unfortunately all of the described FKBP51 and 52 ligands are very large, show only modest binding affinity and suffer from low drug-like Properties.

As SLF and FK506 were the only two public known FKBP51 and FKBP52 ligands[141] at the start of this thesis, they were used as prototypes for our structure based rational ligand design.
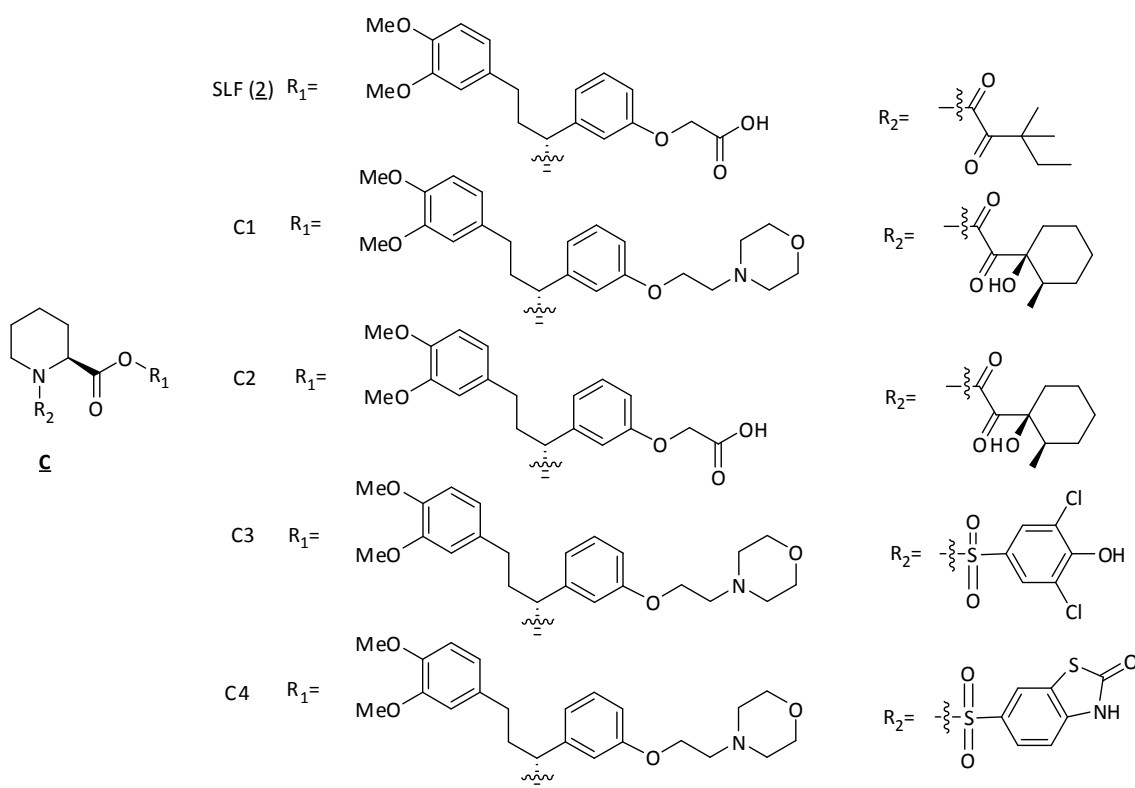
Figure 8: Representive FKBP51 and FKBP52 ligands.

2.5 Interactions of 2 (SLF) and polycyclic ligand 3a with FKBP51

FK506 (**1**) (Figure 9a) binds to the peptidyl prolyl isomerase (PPIase) domain of FKBP51/52 and inhibits their PPIase activity. SAR studies with synthetic FKBP ligands indicated the dicarbonyl pipecolyl-scaffold (shadowed in Figure 9) of FK506 as the most important group for their binding to FKBPs. The α-keto amide has been suggested as an analogue of the twisted amide in the transition state of the peptidyl-prolyl isomerisation catalyzed by FKBPs[144, 145].

SLF (**2**) (Figure 9b) is a simplified synthetic analogue of FK506 with micromolar affinity for FKBP51/52. Its cocrystal structure with the FK506-binding domain of FKBP51 and a first SAR study were recently reported[134]. Upon binding of compound **2**, FKBP51 adopts a very similar conformation as found in the FK506 complex. Most active site residues are virtually superimposable in the two co-crystal structures (Figure 9c). A comparison with the cocrystal structure of FK506[146] showed that most of the key interactions are conserved. The conserved interactions include hydrophobic contacts between the piperidine ring and the indole of Trp[90], hydrogen

bonds between the C^8-amide carbonyl and Tyr[113]-OH and between the C^1-amide carbonyl and Ile[87]-NH, a dipolar interaction between C^1 and Tyr[113]-OH (142°, 3.2Å) and aromatic hydrogen contacts of Tyr[57], Phe[67] and Phe[130] with the C^9-carbonyl. Part of the lower binding affinity of **2** may be due to its higher flexibility compared to FK506. Compound **2** and all other known FKBP51/52 ligands, including the natural products FK506 and rapamycin display unfavorable pharmacokinetic profiles and suffer from a very low ligand efficiency (<0.18). This is below the widely accepted lower limit of 0.3[147] (Figure 9a and 9b).

(a)			(b)		
1(FK506)			**2(SLF)**		
Protein	FKBP51	FKBP52	FKBP12	FKBP51	FKBP52	FKBP12
Ki(µM) (LE)	0.028±0.005[141] (0.18)	0.08±0.01[141] (0.17)	0.01±0.003[141] (0.24)	2.1±0.3[141] (0.19)	2.7±0.2[141] (0.18)	0.01±0.003[141] (0.26)

(c)

Figure 9: (a) Immunosuppressive drug FK506 (**1**). (b) A synthetic analog thereof SLF (**2**). The pipecolate and α-keto amide core structure as the key FKBP recognition motif is shaded gray with binding affinities for FKBP51, FKBP52 and FKBP12. The ligand efficiency (LE) is defined as the ratio of Gibbs free energy (ΔG) to the number of non-hydrogen atoms (N) of the compound: $LE = (\Delta G)/N$, where $\Delta G = -RT\ln K_i$ with RT equal to 0.6 kcal/mol. The unit of LE is kcal/mol/non-hydrogen atom[148]. (c) Surface representation of FKBP51 in complex with **2** (4DRK) (magenta). FK506 bound to FKBP51 (3O5R) is superimposed in cyan.

Figure 10: (a) The polycyclic ligand **3a** and its binding affinities for FKBP51, FKBP52 and FKBP12. (b) Cocrystal structure of 3a (marine blue) with the FK506-binding domain of FKBP51. Key residues of FKBP51 are show in orange, hydrogen bonds are dashed red. Dipolar-dipolar interactions are dashed in green, van-der-Waals contacts are dashed yellow.

Studies with the smaller homolog FKBP12 showed that binding affinity and ligand efficiency might be improved by macrocyclization[149] or by rigid polycyclic scaffolds[139]. Flexible ligands are thought to suffer an entropic penalty upon binding due to the freezing of rotatable bonds[150]. In turn, reducing ligand flexibility, e.g., by macrocyclization, is an appealing concept to improve potency. It is also well known that flexible ligands often adopt higher energy conformations upon binding to fine-tune ligand-protein interactions[151-154] Thus, in principle, additional binding energy could be gained by preorganizing or stabilizing these high-energy active conformations. Thus representative examples of the polycyclic scaffold **3a**-**3e** were synthesized (Table 1). Unfortunately, these did not enhance binding affinity and ligand efficiency for FKBP51/52.

To get an insight into the molecular binding mode, the polycyclic ligand **3a** was cocrystallized with the FK506-binding domain of FKBP51 (Figure 10). Compound **3a** bound to the FKBP51 FK1 domain in a similar way as the core of FK506 or the synthetic analog **2** with most of the key interactions conserved. The pipecolyl ring of the ligand sits atop the indole of Trp^{90} of FKBP51 which forms the floor of the hydrophobic binding pocket. Two hydrogen bonds between the C^{16}-amide carbonyl and Tyr^{113}-OH and between the C^1-amide carbonyl and Ile^{87}-NH are observed. These

two hydrogen bonds are a hallmark of FKBP ligands. Tyr^{113}-OH also approaches the C^1 carbonyl almost perpendicular (88.3°) at 3.4Å. This putative dipolar interaction has been observed previously in FKBP-ligand structures but might be less strong in case of **3a**[155]. The C^{17}-carbonyl engages the three ε-hydrogens of the aromatic residues Tyr^{57}, Phe^{67} and Phe^{130} which form the apparent carbonyl binding pocket of FKBPs. The C^8 of the bicyclic bridge system forms van-der-Waals contacts with the tip of Phe^{77}. Ring B and ring C stack on top of each other via π-π interactions. The preorganization by the rigid ring B might lock ring C into a conformation favourable for binding. The stacking of these two rings could represent a productive ligand hydrophobic collapse[156]. Favourable van-der-Waals interactions between Tyr^{57} and C^{15}-OMe, between Asp^{68} and C^{19}-OMe, and between Tyr^{113}, Ser^{118} and C^{20}-OMe also contribute to the binding of the ligand. This is supported by the inactive ring C analogs **3b**-**3e** where the aromatic ring C is replaced by an aliphatic moiety or sulfonamides aromatic ring (Table 1).
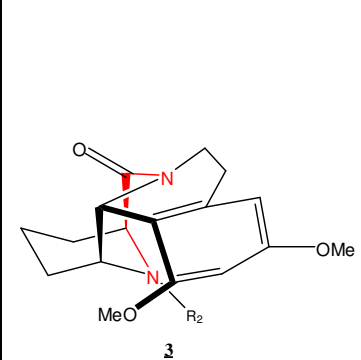
	Compound	R$_2$	FKBP51 IC50(μM) (LE)	FKBP52 IC50(μM) (LE)	FKBP12 IC50(μM) (LE)
	3a		18.1±1.2 (0.17)	19±1.5 (0.17)	0.5±0.1 (0.23)
	3b		>100	>100	2.8±4.5 (0.23)
	3c		>100	>100	27.7±11.4 (0.20)
	3d		>100	>100	0.87±2.5 (0.25)
	3e		>100	>100	2.1±0.3 (0.23)
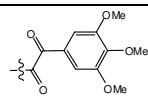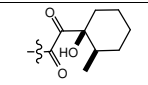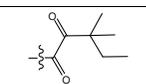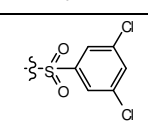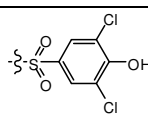
Table 1: Binding affinities and ligand efficiencies of polycyclic ligands **3a**-**3e** for FKBP51, 52 and 12.

Cyclohexyl rings that mimic the pyranose of FK506 or rapamycin were recently shown to be preferred substructures compared to the trimethoxyphenyl moieties in a monocyclic scaffold[134]. In contrast, in the polycyclic context a dramatic decrease of the binding affinity was observed when ring C was changed to the cyclohexyl α-keto amide substructure in **3b**. The lower affinity of **3b** might be due to less favourable

intramolecular interactions leading to the loss of the preorganized conformation. Likewise, derivative **3c** bearing the tert-penyl group present in **2** was also inactive. Although sulfonamides were suitable surrogates for the α-keto amide substructure in monocyclic FKBP51/52 ligands[143] , polycyclic aza-sulfonamide compounds **3d** and **3e** were both inactive. This might be because these sulfonamide aromatic rings were locked at different angles compared to the constrained sulfonamides due to π-π interactions with ring B.

2.6 Reported compounds with similar scaffolds as **4** and **5**

The proposed [3.3.1] aza-amide scaffold and [4.3.1] aza-amide scaffold were not found in nature. The closest natural products are exemplifed by the [4.2.1] alkaloids such as anatoxin A[157] and [3.2.1] aza-amide scaffolds in the tropane alkaloids[158] (Figure 11). The closest synthetic analogues of the [3.3.1] aza-amide scaffold were reported as part of the polycyclic scaffold **3**[139].
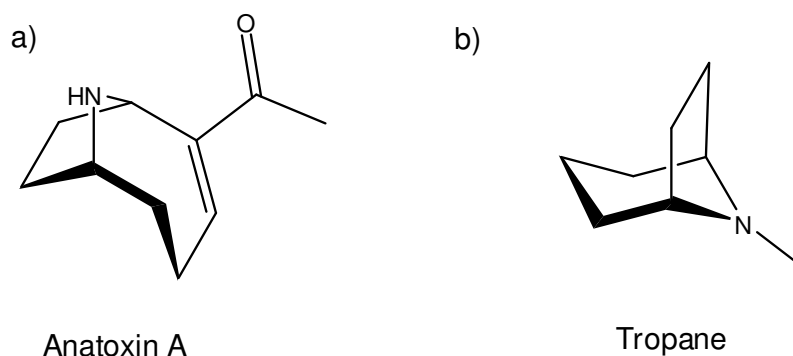
Figure 11: The chemcial structure of (a) Anatoxin A, (b) Tropane

In the synthesis of anatoxin A[159, 160], tropane alkaloids[161] and the polycyclic scaffold **3**[139], the intramolecular N-acyliminium cyclization was employed as a key step.

2.7 Intramolecular N-acyliminium cyclization

The N-acyliminium or N-acyliminium ion chemistry has been extensively employed for the synthesis of N-heterocyclic ring systems related to alkaloids. It has been systematically studied especially by Speckamp et al. based on the succinimide

system.[162] Under acidic condition, the hemiaminal D1 is converted to the N-acyliminium ion intermediate D2 (Scheme 1). Compared to the iminium ion which has been widely employed in the Mannich reaction, the Bischler-Napieralski reaction and the Pictet-Spengler reaction, the carbonyl group adjacent to the nitrogen atom greatly increased the electrophilic reactivity of the N-acyliminium ion which broadens the range of nucleophiles that can be used in carbon-carbon bond formation reactions. Because of its high activity, the N-acyliminium ion intermediate is seldom if ever isolated[162, 163] and usually is generated *in situ*. Intermediate D2 was found to be reactive towards a wide variety of π-nucleophiles including alkenes, allenes, alkynes and aromatic and heteroaromatic systems[162].
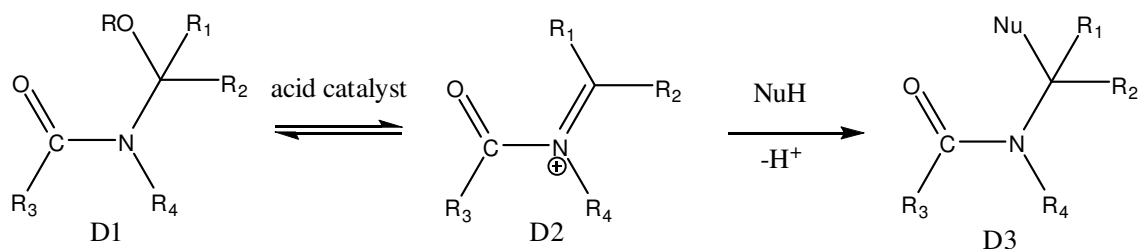
Scheme 1: Mechanism of N-acyliminium chemistry.

The intramolecular N-acyliminium cyclization is widely employed especially in the synthesis of bicyclic and polycyclic N-heterocyclic ring systems. Some examples even showed high stereocontrol during the C-nucleophilic additions to N-acyliminium species[164, 165] which makes the intramolecular N-acyliminium cyclization even more attractive for the synthesis of alkaloidal ring systems.

Generally, the N-acyliminium ion can be generated from three sources. α-Oxygenated amides is the most common source of N-acyliminium ions while the use of other α-substituted amides such as bisamides, α-chloroalkyl amides and α-thioalkyl amides were also reported[162]. The α-oxygenated amides can be prepare by addition of an amide to an aldehyde or ketone under acid condition (reaction 1 in Scheme 2)[164], electrochemical oxidation of amides or carbamates (reaction 2 in Scheme 2)[166], reduction of cyclic imides in the presence of an alcohol (reaction 3 in Scheme 2)[167], and addition of Grignard reagents to cyclic imides (reaction 4 in Scheme 2)[168]. Acylation of imines with an acid chloride or acid anhydride to afford acyliminum species was also reported (reaction 5 in Scheme 2)[169]. Although the protonation of N-acylimines is possible in principle, very few examples have been

described (reaction 6 in Scheme 2)[170]. The limitation is mainly due to the tautomerization of the N-acylimines to enamides when α-hydrogen atoms are present.
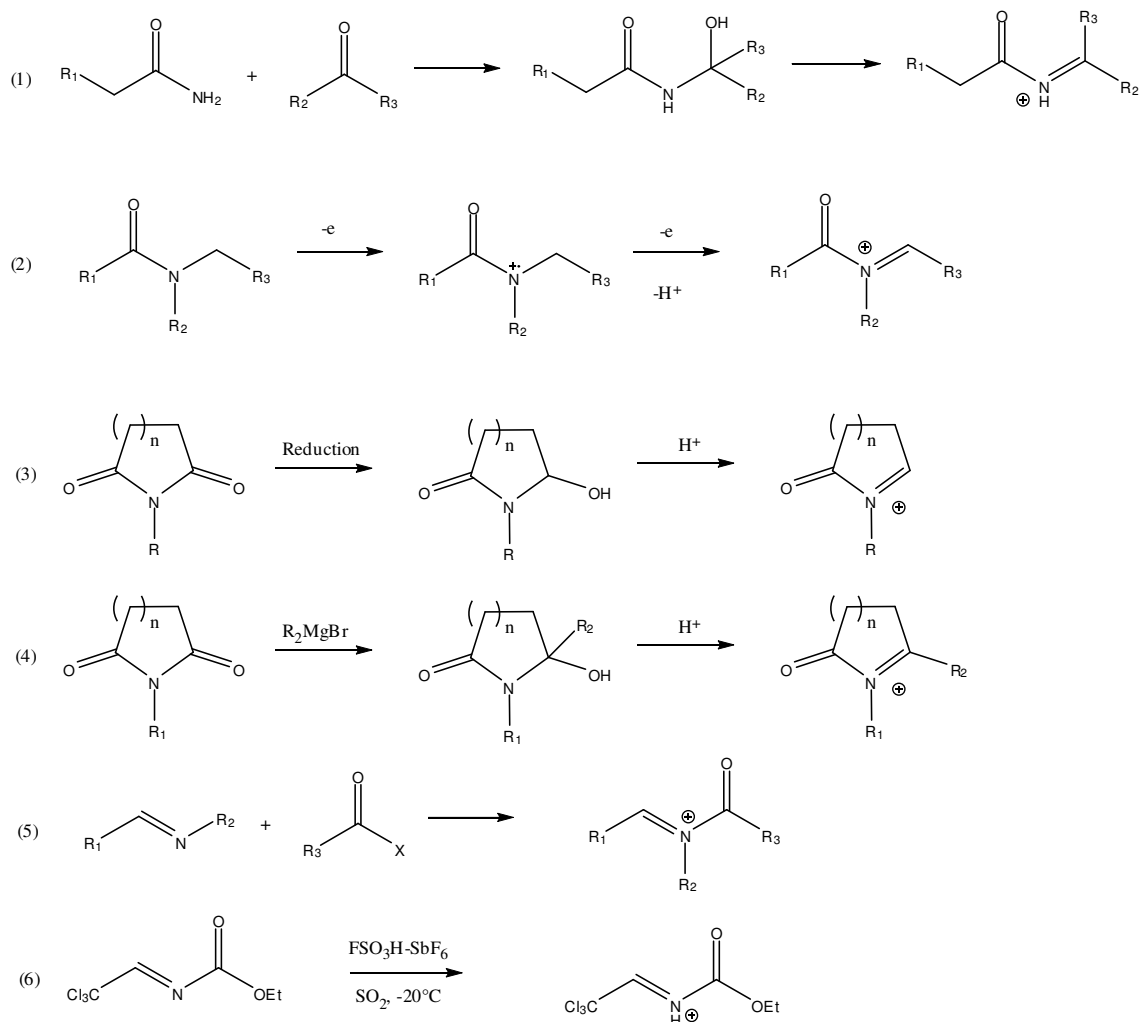
Scheme 2: Summary of the N-acyliminium ion generation.

The intramolecular N-acyliminium cyclization has been used to construct pyrrolidines, piperdines and related rings[171-174], pyrrolizidines[175], indolizidines[176, 177], spirocyclic systems[178], ring systems containing a seven-membered or eight-membered ring[179], polycyclic and bridged systems[180]. Some of its applications in preparaion of bicyclic or polycyclic N- heterocyclic ring systems of natural products are shown in Scheme 3.
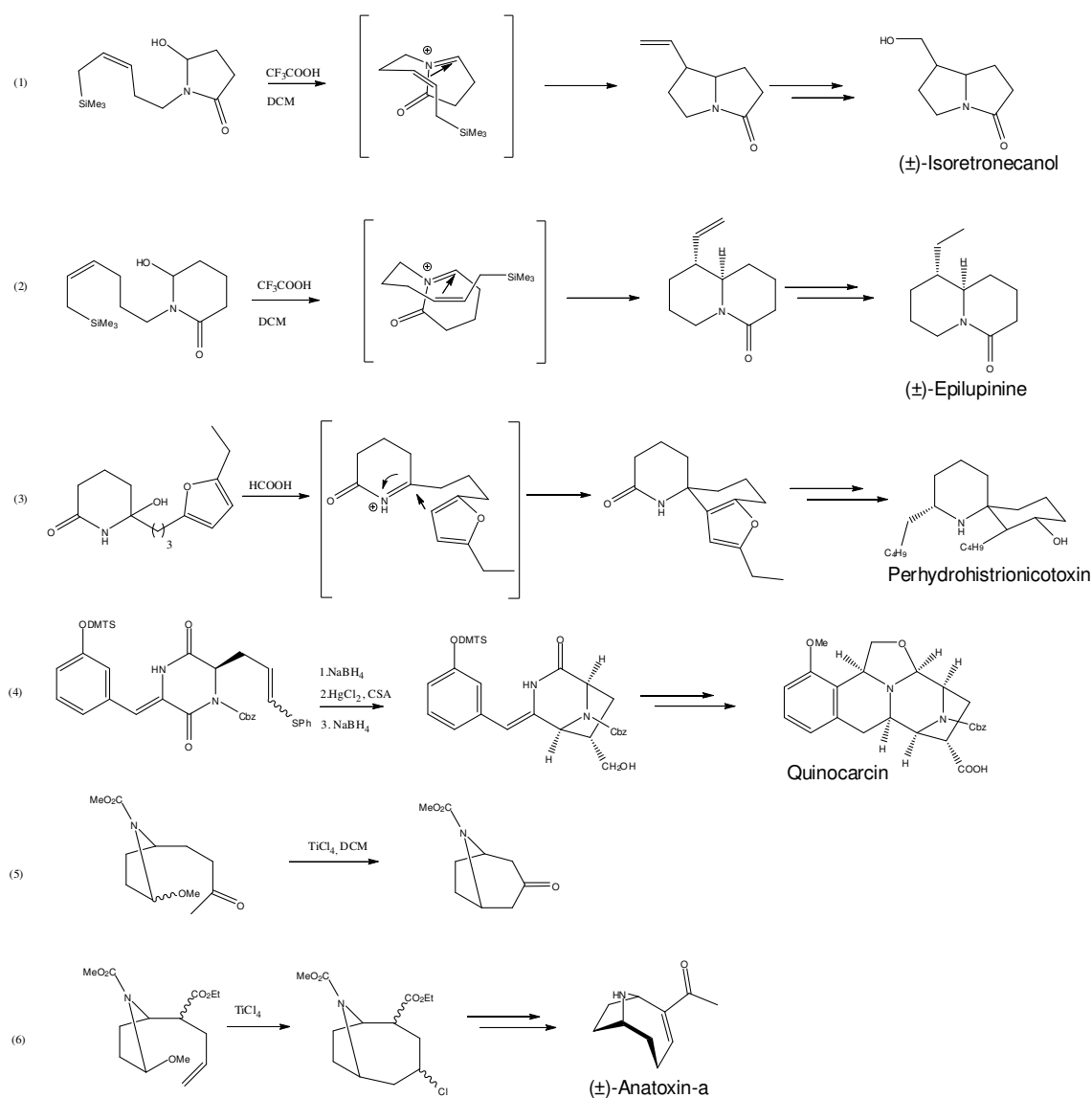
Scheme 3: Some examples of intramolecular N-acyliminium cyclization in preparation of bicyclic and polycyclic N- heterocyclic ring system of natural products.

A silicon-directed N-acyliminiun ion cyclization was employed to prepare the fused bicyclic structures of Isoretronecanol[177] and Epilupinine (reaction 1 and 2 in Scheme 3)[176]. For the spirocyclic systems of Perhydrohistrionicotoxin, the furan ring was found to be a good π-nucleophile for the intramolecular N-acyliminiun ion cyclization (reaction 3 in Scheme 3)[176]. The bridge bicyclic system in Quinocarcin was prepared through acylated amide reduction followed by cyclization (reaction 4 in Scheme 3)[181]. The lewis acid induced cyclization of enolic π-nucleophiles could easily afford the tropane-like system (reaction 5 in Scheme 3)[182]. An 8-Azabicyclo[4.2.1] system like in

Anatoxin-a was shown to be obtained by lewis acid-induced cyclization of an unfunctionalised alkene π-nucleophiles[159] (reaction 6 in Scheme 3).

The intramolecular N-acyliminium cyclization was also crucial in the synthesis of other natural products like Gephyrotoxin[183], Laudanosine[180], Yohimbine[184], Ajmalicine[185], Vindorosine[186], Gelsemine[187], Sarains[188] and so on.

3. Aim of this project

FKBP51 and FKBP52 have important implications in diseases like cancer and depression. However, all known FKBP51 and FKBP52 ligands display unfavorable pharmacokinetic profiles which make them unsuitable to study the biological roles of FKBP51 and FKBP52.

In this project, the aim was to limit the ligand flexibility by ligand preorganization to mimic the FKBPs ligands active conformation and to focus on improvement of their ligand affinities and efficiencies. Two new classes of conformationally defined pipecolyl analogs based on aza-amide bicycles as rigid replacements for the pipecolyl-monocyclic scaffold were designed. First, efficient synthetic procedures for the bicyclic [3.3.1] aza-amide and [4.3.1] aza-amide core structures had to be developed. Second, the bicyclic [3.3.1] and [4.3.1] aza-amide scaffold had to be derivatized to identifiy the best substituents and to probe the energetic contribution of the individual subgroups. Third, a detailed biological and biophysical characterization of selected analogs was intented to elucidate the molecular underpinnings of binding of the constrained FKBP ligands in detail.

The final goal was to provide efficient and well understood scaffold for the further optimization of FKBP51 ligands.

4. Results and discussion

4.1 Design of conformationally defined FKBP ligands

The multiple interactions of **3a** with the protein made the direct assessment of the contribution of the C^1-C^6 cyclization difficult. We therefore decided to synthesize bicyclic [3.3.1] aza-amides derivatives **4** (Figure 12). This rigidified aza-amid nucleus is a simplified mimic of the **3a** core with the idea of limiting the flexibility of these monocyclic ligands which may decrease the entropic costs upon binding meanwhile increasing the flexibility of the R_1 and R_2 substituents to allow them to increase the interactions with the protein. The unrestricted substituents could be better suited to mimic the active conformation of monocyclic pipecolate-based FKBP ligands like **2**. In such a constrained bicycle, the C^1-carbonyl oxygen is preoriented for interaction with Ile[87]. A hydrogen bond with the backbone amide of this residue is a hallmark of most FKBP ligands known so far. In addition, the important hydrophobic interaction between the piperidine ring and the indole of Trp[90] together with the hydrogen bond between the C^8-amide carbonyl and Tyr[113]-OH would be highly conserved. Further optimization of R_1 could more closely resemble those present in the monocyclic ligands like **1** to help to improve the binding affinity. The bicyclic [4.3.1] aza-amide derivatives **5** (Figure 12) with a similar structure as **4** and a two-atom linker between C^1- C^6 was also proposed. It could adopt to a similar conformation as **4** and with the possiblity of further modification at C^8 and C^9 position.

Figure 12: Proposed bicyclic [3.3.1] aza-amide derivatives **4**, bicyclic [4.3.1] aza-amide derivatives **5** and the corresponding monocyclic derivatives **6** derived from **1** (FK506), prototypic synthetic FKBP ligand **2** (SLF) and polycyclic ligand **3a**.

4.2 Computer modelling

Computer modelling of the bicyclic [3.3.1] aza-amide nucleus **7** and the bicyclic [4.3.1] aza-amide nucleus **8** into the binding pocket of FKBP51 indicated no obvious sterical hindrance between the protein and the bicyclic aza-amide nucleus **7** and **8** (Figure 13). The C^1-C^6, N^7, O^1 and O^{10} of the bicyclic [3.3.1] aza-amide nucleus **7** and C^1-C^6, N^7, O^1 and O^{11} of the bicyclic [4.3.1] aza-amide nucleus **8** were overlaid with the corresponding atoms of **2** (SLF) in the cocrystal structure of **2** and FKBP51 FK1 domain. The binding mode of the bicyclic [3.3.1] aza-amide nucleus **7** and the bicyclic [4.3.1] aza-amide nucleus **8** was nearly superimposable with the common elements of the pipecolate and α-keto amide region (Figure 1 and 4). Small deviations were observed which may be due to the bicyclic ring strains in **7** and **8**. The geometry of the important hydrogen bond acceptor C^1=O was quantified by the O^1-C^1-C^2-N^7 dihedral angle which varied from 153° to 193° among known cocrystallized FKBP51 ligands (Table 2) while the O^1-C^1-C^2-N^7 dihedral angle in **7** is locked to 157° and 175° for **8**.
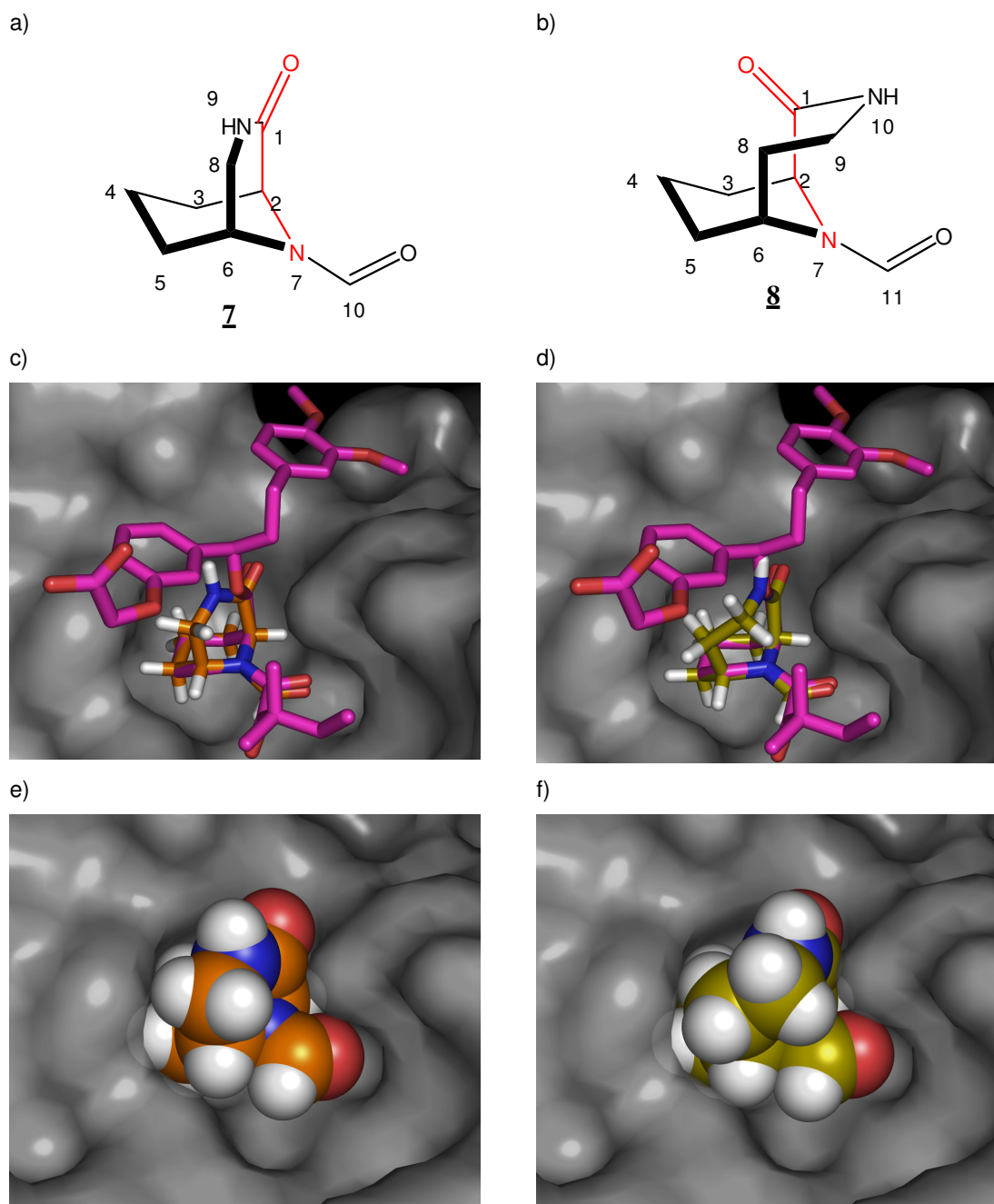
Figure 13: (a).The structure of the bicyclic [3.3.1] aza-amide nucleus **7** (b) The bicyclic [4.3.1] aza-amide nucleus **8** used for computer modeling. (c) Superimposition of **7** (orange) with **2**(magenta) modelled into the FKBP51 FK1 domain. (d) Superimposition of **8** (yellow) with **2**(magenta) modelled into the FKBP51 FK1 domain. (e) A space filling mode of **7** positioned into the pocket of FKBP51 FK1 domain. f) A space filling mode of **8** positioned into the pocket of FKBP51 FK1 domain.

Based on this parameter, the geometry of the bicyclic [4.3.1] aza-amide nucleus **8** along the C^1-C^2 bond is predicted to be preorganized nearly identical as the experimentally observed conformation in the unconstrained FKBP ligands, while the predicted dihedral angle in the bicyclic [3.3.1] aza-amide nucleus **7** deviates more. The similar geometry shared by the bicyclic [3.3.1] aza-amide nucleus **7** and the bicyclic [4.3.1] aza-amide nucleus **8** with the most unconstrained FKBP ligands might enhance the affinity of the bicyclic [3.3.1] aza-amide and bicyclic [4.3.1] aza-amide derivatives for the FK1 domain of FKBP51 and 52. We therefore decided to prepare the corresponding bicyclic [3.3.1] aza-amide derivatives **4** and bicyclic [4.3.1] aza-amide derivatives **5** to address the contribution of the bicyclization.

Compound (PDB number)	**3a**	**FK506 (1)** (3O5R)	**C2a** (4DRN)	**C2b** (4DRP)	**C3** (4DRQ)	**SLF(2)** (4DRK)	**7**	**8**
O^1-C^1-C^2-N' dihedral angle	153°	179°	193°	191°	185°	185°	157°	175°

Table 2: The O^1-C^1-C^2-N^7 dihedral angle for all known cocrystallized FKBP51 ligands and the computer modelling bicyclic [3.3.1] aza-amide nucleus **7** and the bicyclic [4.3.1] aza-amide nucleus **8**.

4.3 Synthesis

4.3.1 Synthesis of the bicyclic [3.3.1] aza-amide derivatives **4** and the bicyclic [4.3.1] aza-amide derivatives **5**

4.3.1.1 Retrosynthetic analysis and strategy of the bicyclic [3.3.1] aza-amide derivatives **4**

The retrosynthesis of the bicyclic [3.3.1] aza-amide derivatives **4** is outlined in Scheme 4. The R_1 substructure in **4** was envisioned to be incorporated through alkylation from **9** followed by sequential deprotection and introduction of the α-ketone amide moiety or sulfonamide moiety as R_2. The bicyclic nucleus **9** was expected to be most expediently generated by cyclization of a cis-2, 6-disubstituted piperidine precursor **10**. The piperidine ring in **10** was thought to be obtained from **11** with reduction of a 2, 6-disubstituted pyridine and the amine group could be obtained from reduction of a cyano group. **11** could be easily prepared from **12** via aromatic nucleophilic substitution.
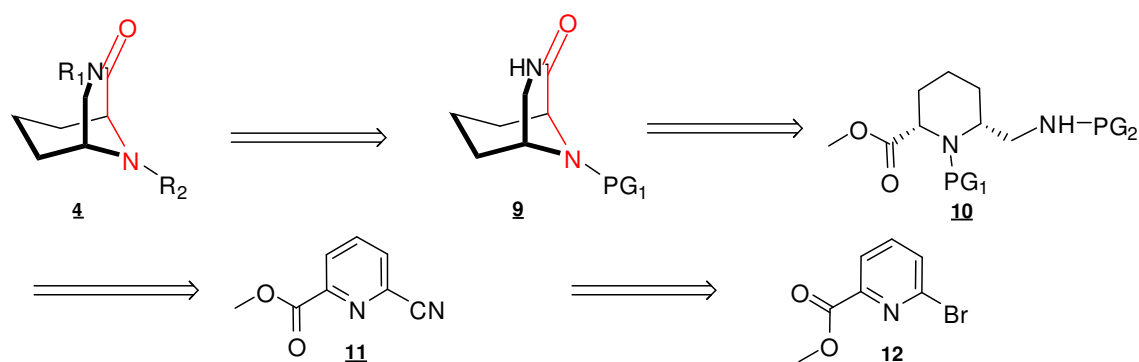
Scheme 4: Retrosynthesis of the bicyclic [3.3.1] aza-amide derivatives **4**

4.3.1.2 Synthesis of the bicyclic [3.3.1] aza-amide nucleus 17

The bicyclic [3.3.1] aza-amide nucleus **17** was prepared in a 6-step synthetic route as shown in Scheme 5. Aromatic nucleophilic substitution of commercially available ethyl 6-bromopicolinate **12** with copper(I) cyanide in presence of pyridine via a Rosenmund-von Braun reaction afforded the corresponding cyanylated compound **11**[189]. Selective hydrogenation of the cyano group with Raney-Ni with concomitant *in situ* protection of the produced primary amine group with the tert-butyloxycarbonyl (Boc) group was accomplished in a one-pot reaction to give the product **13**. Compound **13** was further reduced by platinum oxide in acetic acid at 50 bar H_2 from which the cis enantiomers **14** were seperated and used for the next step.[190] Incorporation of the carboxybenzyl (Cbz) group to protect the secondary amine group in **14** gave the product **15**. The Boc protection group was efficiently removed by 1:1 TFA in DCM to give the primary amine product **16.** Without isolation and purification, the crude product **16** was further subjected to ring closure in refluxing pyridine to yield the [3.3.1] core **17** in gram scale.
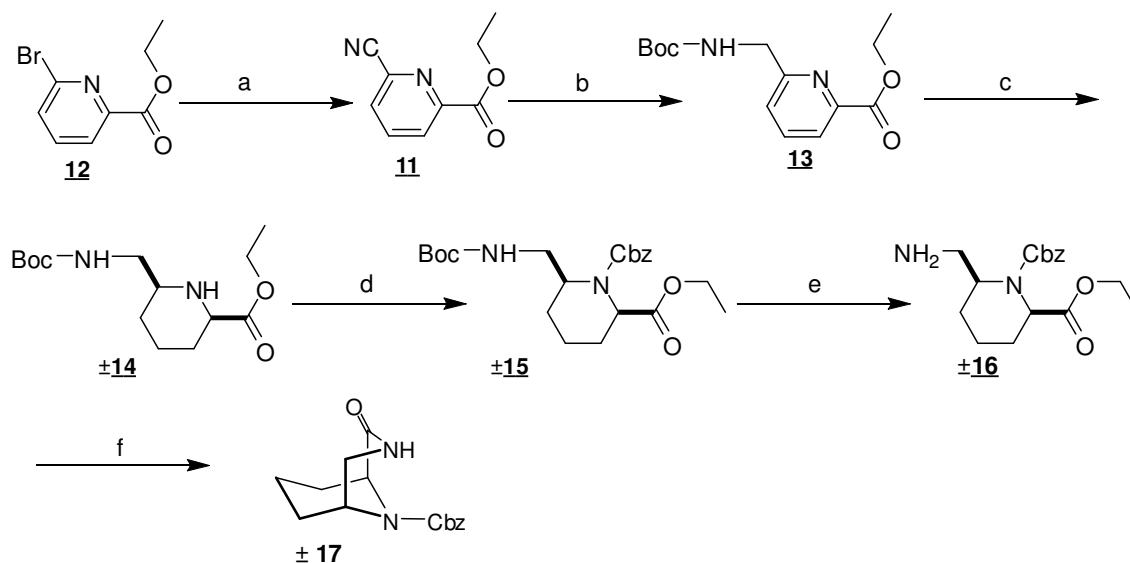
Scheme 5: Synthesis of bicyclic [3.3.1] aza-amide nucleus **17**: (a) CuCN, pyridine, reflux, 60%. (b) Raney-Ni, Boc$_2$O, H$_2$ 1 bar, RT, overnight, 68%. (c) PtO$_2$, AcOH, H$_2$ 50 bar, RT, 2 days, 49%. (d) Cbz-Cl, N,N-diisopropylethylamine RT, 6h, 96%. (e) 50% TFA in DCM, RT, 1h. (f) pyridine, reflux, 2h, 76% (2 steps).

Two products were observed by TLC and LCMS for the reduction of **13**. Theoretically, reducing the compound **13** could give four stereoisomers: two cis enantiomers **14a** and **14b** together with two trans enantiomers **14c** and **14d**. Only the cis enantiomers **14a** and **14b** (Scheme 6) could cyclize to afford compound **17**. The compound **17** and products thereof will be enantiomeric mixture, but only the final product from **14a** was expected to bind to the FKBPs due to the steric hindrance. **14a** and **14b** were seperated as racemic mixture and used for further reaction without stereochemical resolution. Compound **17** was characterized by HPLC, NMR and Mass spectroscopy, no diastereomers were observed.
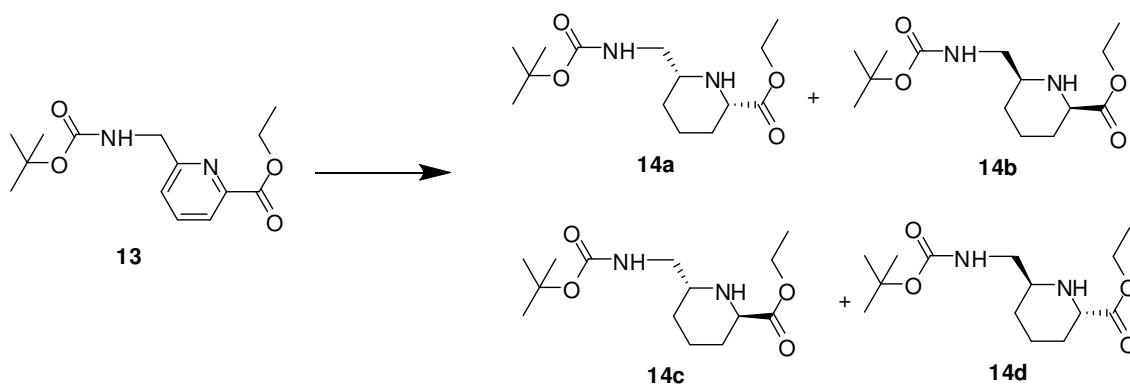
Scheme 6: The four stereoisomeric products **14a, 14b, 14c, 14d** from the reduction of **13**

Because of the high similarity between the bicyclic [3.3.1] aza-amide derivatives **4** and the bicyclic [4.3.1] aza-amide derivatives **5**, the following syntheses of **17** to afford **4** will be discussed later together with the synthesis of the bicyclic [4.3.1] aza-amide derivatives **5**.

4.3.1.3 Retrosynthetic analysis and strategy of the bicyclic [4.3.1] aza-amide derivatives 5

The retrosynthesis of the bicyclic [4.3.1] aza-amide derivatives **5** is outlined in Scheme 7. The analysis was based on the synthetic route of bicyclic [3.3.1] aza-amide derivatives described above. The R_1 substructure in **5** was envisioned to be incorporated through alkylation from **18** followed by sequential deprotection and introduction of the α-ketone amide moiety or the sulfonamide moiety as R_2. The bicyclic nucleus **18** was expected to be most expediently generated by cyclization of a cis-2, 6-disubstituted piperidine precursor **19**. The piperidine ring in **19** was thought to be obtained from **20** by reduction of a 2,6-disubstituted pyridine and the amine group could be obtained from reduction of a cyanomethyl group. **20** could be easily prepared from **21**.
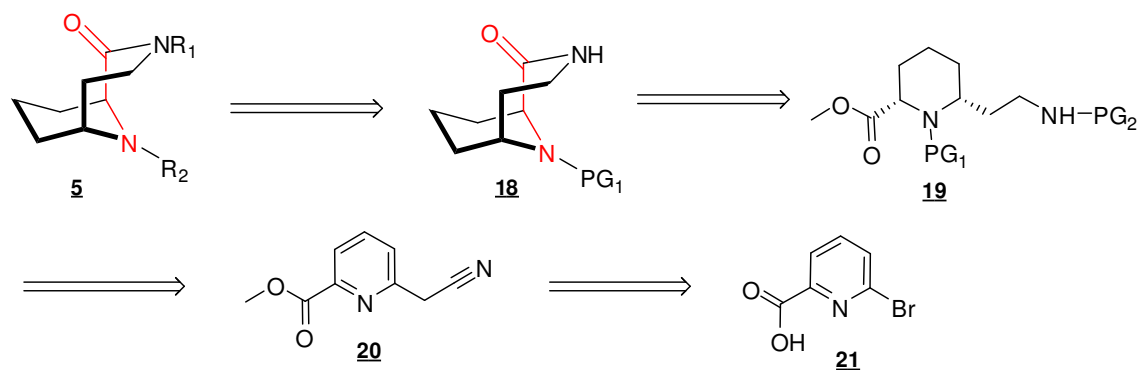
Scheme 7: Retrosynthesis of the bicyclic [4.3.1] aza-amide derivatives **5**

4.3.1.4 Synthesis of the bicyclic [4.3.1] aza-amide nucleus 27

The novel bicyclic [4.3.1] aza-amide nucleus **27** was prepared in a 7-step synthetic route as shown in Scheme 8. Aromatic nucleophilic substitution of commercially available 6-bromopicolinic acid **21** with acetonitrile in presence of n-butyl lithium

afforded the corresponding cyanomethylated product **22**[191]. The carboxylic acid group in **22** was further subjected to methylation under mild condition with trimethylsilyldiazomethane in MeOH at room temperature to give the product **20**[192]. Selective hydrogenation of the cyanomethyl group with Raney-Ni with concomitant *in situ* protection of the produced primary amine group with the tert-butyloxycarbonyl (Boc) group was accomplished in a one-pot reaction to give the product **23**. Compound **23** was further reduced by platinum oxide in acetic acid at 50 bar H_2 to afford a mixture of diastereomers which were used for the next step.[190] Incorporation of the carboxybenzyl (Cbz) group to protect the secondary amine group in **24** gave the product **25**. The Boc protection group was efficiently removed by 1:1 TFA in DCM to give the primary amine product **26.** Without isolation and purification, the crude product **29** was further subjected to ring closure to yield **27** in refluxing pyridine.
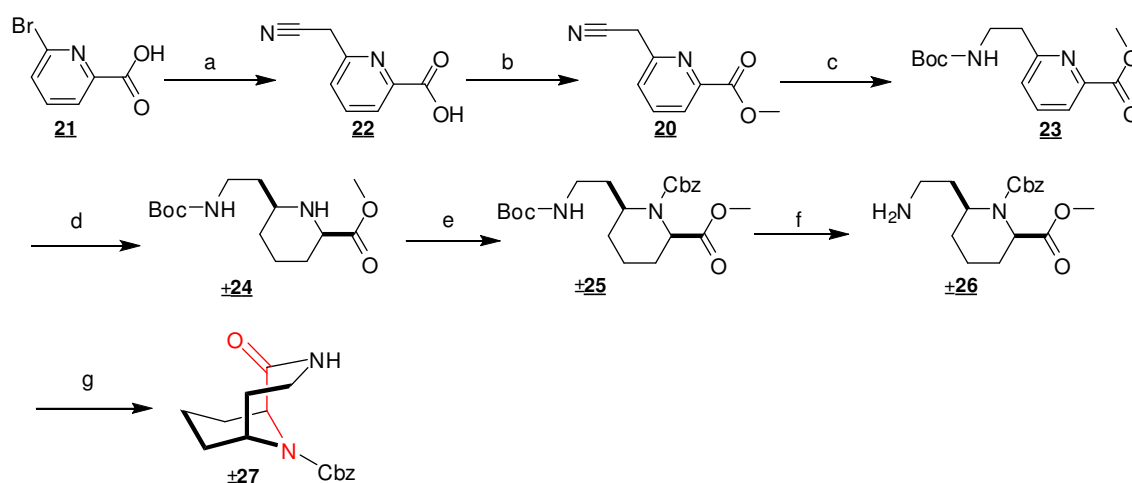
Scheme 8: Synthesis of the bicyclic [4.3.1] aza-amide nucleus **27**: (a) Acetonitrile, BuLi, -78°C, 3h, 87%. (b)Trimethylsilyldiazomethane, MeOH, RT, overnight, 46%. (c) Raney-Ni, Boc$_2$O, H$_2$ 1 bar, RT, overnight, 76%. (d) PtO$_2$, AcOH, H$_2$ 50 bar, RT, 2 days, 98%. (e) Cbz-Cl, N,N-diisopropylethylamine RT, 6h, 86%. (f) 50% TFA in DCM, RT, 1h. (g) Pyridine, reflux, 2h, 34% (2 steps).

Attempts to use **12** as starting material failed as **28** was found to be the main product under the condition of 1.1eq BuLi and 1.5eq acetonitrile at -78°C. (Scheme 9)
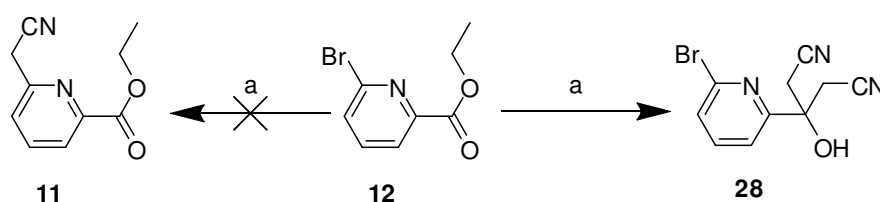
Scheme 9: Side reaction of cyanomethylation based on **12** (a) 1.5eq Acetonitrile, 1.1eq BuLi, -78℃, 3h, 75%.

Similar to the intermediate **14** described above, two products were observed for **24** by TLC and LCMS. Theoretically, reducing compound **23** would also give four stereoisomers: two cis-enantiomers and two trans-enantiomers. Only the cis-enantiomers **24a** and **24b** (Scheme 10) could cyclize to afford compound **27**. The compound **27** and product thereof will be two enantiomeric mixture, but only the final product from **24b** was expected to bind to the FKBPs due to the correct positioning of the C^1-carbonyl group. The diastereomeric mixture of compounds **24a, 24b**, **24c** and **24d** were used for further reaction without diastereomeric separation.
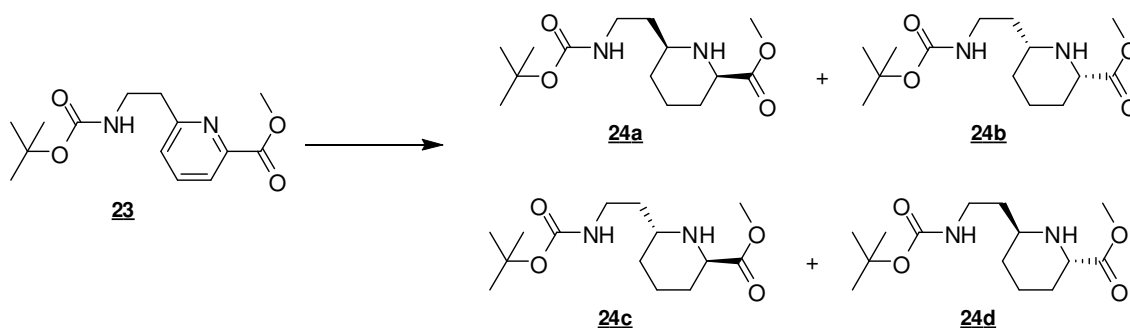
Scheme 10: The four stereoisomeric products **24a, 24b, 24c, 24d** from the reduction of **23**

Most of the synthetic steps carried out in Scheme 5 had good yield except the last two steps. The cyclization reaction in refluxing pyridine for two days to give the product **27** was accompanied by hydrolysis of ester in **26** and decomposition of **26**. The total yield for the final two steps was as low as 34%. One reason is that only two diastereomers of the four diastereomeric mixtures in **26** could cyclize to afford enantiomeric mixture of compound **27**. Furthermore, it might be due to the increased ring size that it becomes more difficult to construct the lactam ring through cyclization. Reactivity in cyclization reaction is influenced by the activation energy in the transition state. The activation energy is thought to reflect the strain energy of the ring to be formed and is markedly dependent on ring size. The higher strain energy makes the cyclization of **27** to form the 7-membered ring more difficult[193]. Compound **27** was characterized by HPLC, NMR and Mass spectroscopy, no diastereomers were observed.

4.3.1.5 Synthesis of the bicyclic [3.3.1] aza-amide derivatives 4 and bicyclic[4.3.1] aza-amide derivatives 5

Because of the high similarity between the bicyclic [3.3.1] aza-amide derivatives **4** and the bicyclic [4.3.1] aza-amide derivatives **5**, their following syntheses were carried out in the same way. The successful synthesis of bicyclic [4.3.1] aza-amide compound **17**/**27** makes further incorporation of different R_1 and R_2 substitutions into the scaffold **17**/**27** possible (Scheme 11).
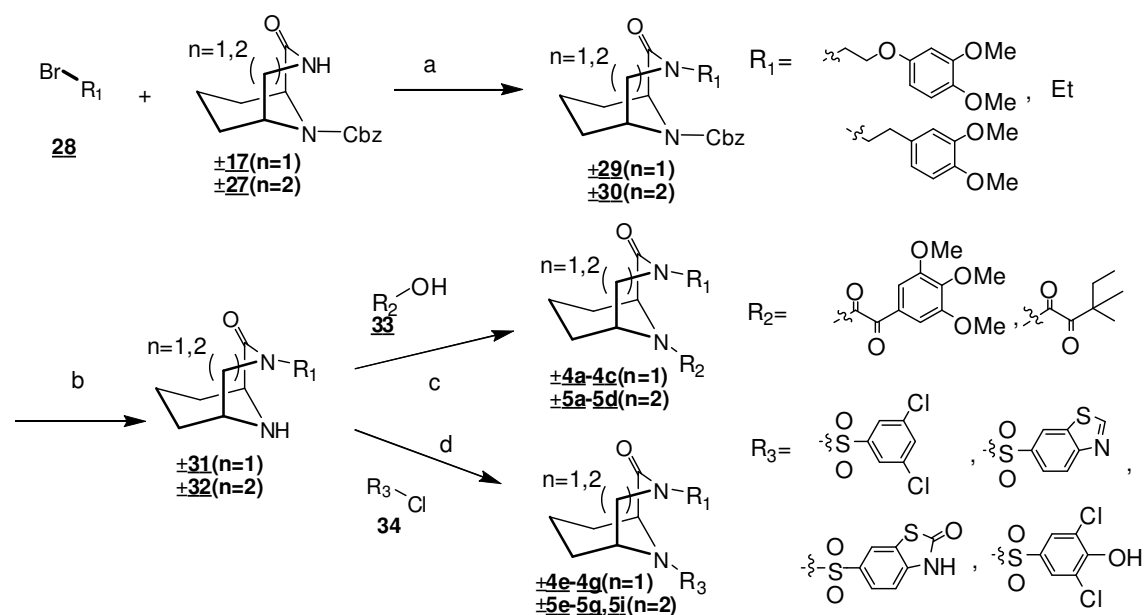
Scheme 11: Synthesis of bicyclic [3.3.1] aza-amide derivatives **4** and bicyclic [4.3.1] aza-amide derivatives **5**: (a) **28a**-**28c** (R_1-Br), NaH, THF, RT, 3 days (25% -95%). (b) Pd/C H_2 1 bar, RT, 1h (71% -100%). (c) **33a** or **33b** (R_2-OH) EDC-HCl, HOBT, TEA, RT, 6h (23% -76%). (d) **34a**-**34d** (R_3-Cl), DIPEA, DCM, RT, overnight (13% -53%).

The R_1 and R_2 substitutents were selected based on previous preliminary structure-activity relationships for FKBP51[143]. R_1 was intended to mimic the 3-[3,'4'-dimethoxyphenyl)propyl branch of the ester "top" group in the monocyclic ligand **2** or possibly the ring C of **3a**. The R_2 groups were chosen to resemble the α-keto amide and the pyranose moieties in FK506. Sulfonamides as R_3 were shown to be suitable surrogates for the α-keto amide substructure in monocyclic FKBP51/52 ligands[143].

The series of bicyclic [3.3.1] aza-amide ketoamide derivatives **4a**-**4c** and bicyclic [4.3.1] aza-amide ketoamide derivatives **5a**-**5d** were synthesized from **17**/**27** through a 3-step synthetic route as shown in scheme 8. **17**/**27** in dry THF was deprotonated

followed by addition of **28** to give the substituted products **29**/**30.** The Cbz-protected amine group was deprotected by catalytic hydrogenation using Pd/C in MeOH to give the free amine product **31**/**32**[194]. The secondary amine group in **31**/**32** was coupled with α-keto acid **33** to give the final product **4a**-**4c** and **5a**-**5d.**[139]

The series of bicyclic [3.3.1] aza-sulfonamide derivatives **4e**-**4g** and bicyclic [4.3.1] aza-sulfonamide derivatives **5e**-**5g** and **5i** were prepared by coupling the secondary amine group in **31**/**32** with commercial sulfonyl chloride **34a-d**.[139]

To further clarify the contribution of the R_1 group to the overall ligand efficiency, the bicyclic ligands **4h** and **5h** without R_1 were prepared by hydrogenation cleavage of the Cbz group in **17** and **27** followed by coupling of the secondary amines of **35** and **36** with 2-oxo-2,3-dihydro-benzothiazole-6-sulfonyl chloride **34c**. (Scheme 12).
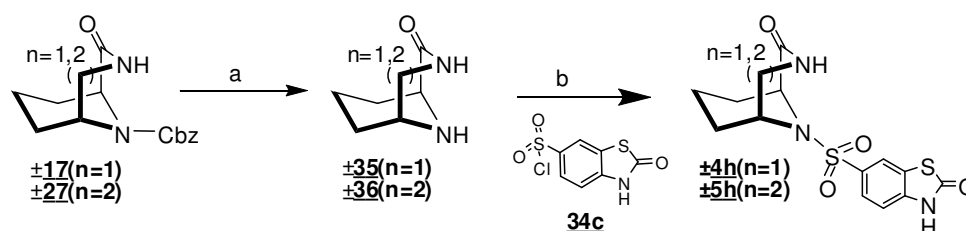
Scheme 12: Synthesis of bicyclic [3.3.1] aza-amide derivative **4h** and bicyclic [4.3.1] aza-amide derivative **5h**: (a) Pd/C H_2 1 bar, RT, 1h (82% for **35**,100% for **36**) (b) **34c**, DIPEA, DCM, RT, overnight (43% for **4h**, 12% for **5h**)

All of these two series of ligands were obtained as an enantiomers mixture, but only one of the enantiomers was expected to bind to the FKBPs due to the steric hindrance. Ligands were characterized by HPLC, NMR and Mass spectroscopy, no diastereomers were observed.

4.3.1.6 Synthesis of the monocyclic derivatives 6

To assess the role of the cyclization, the corresponding mononcyclic derivatives **6** as reference compounds bearing the same substituents as in **4** and **5** were prepared (Scheme 13). Nucleophilic substitution of commercially available Boc-pipecolic acid **37** with **28a** followed by cleavage of the Boc group afford **39**. This was then converted to corresponding α-keto amide **6a** and sulfonamides **6e**-**6g**. (scheme 10)

Scheme 13: Synthesis of monocyclic ligands **6a** and **6e**-**6g**: (a) K$_2$CO$_3$, acetone, reflux, overnight (100%) (b) 20%TFA in DCM, RT, 2h (100%) (c) **33a** (R$_2$-OH), TEA, HATU, DCM, RT, overnight (42% for **6a**) (d) **34a**-**34c** (R$_3$-Cl), DIPEA, DCM, RT, overnight (20%-48% for **6e** to **6g**)
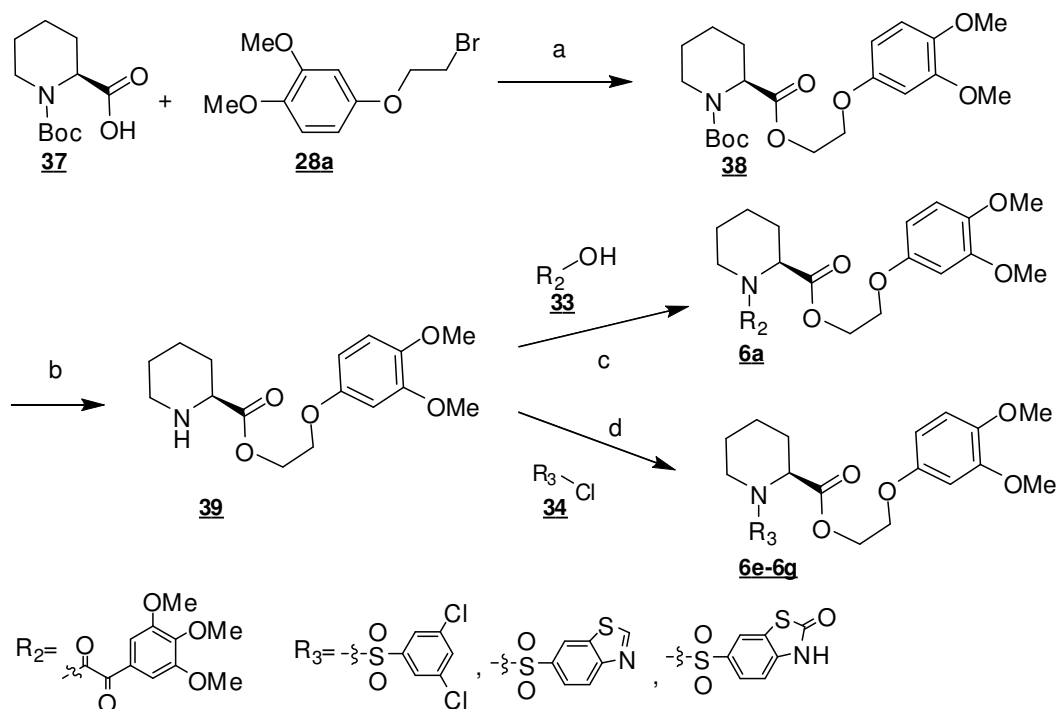
4.4 Competition binding fluorescence polarization assay

4.4.1 Binding affinity of the bicyclic aza-amide series.

A competition binding fluorescence polarization assay[141] was used to evaluate the binding of potential ligands to the FKBP12 and to the FK1 domain of FKBP51 and FKBP52. SLF **2** linked to a flurophore was used as a tracer. The affinity of any new synthesized ligand was assessed by its ability of competition with fluo-**2** for the FKBPs.

Among the α-keto amide series (Table 3), the tert-pentyl series compounds **4b**, **5b** and **6b** were all inactive for FKBP51/52. The higher affinities of **4a** compared to **4b** and **5a** compared to **5b** for FKBP51/52/12 indicated that the trimethoxyphenyl moiety is a better R2 substructure than tert-pentyl for the bicyclic scaffolds. The activity of **5c** for FKBP51/52/12 suggested the cyclohexyl analog which more closely mimics the pyranose group of the high affinity natural product ligands like FK506 is also effective

in the bicyclic context. The higher affinity of **5a** compared to **5d** for FKBP51/52/12 suggests that a three-atom spacer compared to a two-atom spacer is preferred for optimal positioning of the dimethoxyphenyl group in R_1. This is consistent with the SAR observed for monocyclic FKBP51/52 ligands.[134]

Compound	n	R_1	R_2	FKBP52 Ki (µM) (LE)	FKBP51 Ki (µM) (LE)	FKBP12 Ki(µM) (LE)
4a	1			**79.4±20** **(0.15)**	**51.1±7.6** **(0.15)**	**0.2±0.01** **(0.24)**
5a	2			**45.2±13.5** **(0.15)**	**23.7±3.1** **(0.16)**	**0.3±0.007** **(0.23)**
6a	-			>100	>100	**0.3±0.03** **(0.22)**
4b	1			>100	>100	**3.5±0.1** **(0.24)**
5b	2			>100	>100	**1.5±0.1** **(0.24)**
6b	-			>100	>100	**0.9±0.1** **(0.27)**
4c	1			>100	>100	**6.3±0.02** **(0.26)**
5c*	2			**27.2±0.2** **(0.17)**	**19.7±0.5** **(0.18)**	**0.6±0.1** **(0.23)**
6c*	-			>100	>100	**2.78** **(0.22)**
5d	2			>100	>100	**1.5±0.04** **(0.21)**

Table 3: Binding affinities of monocyclic or bicyclic ketoamide ligands for FKBP51, FKBP52 and FKBP12 determined by fluorescence polarization assay[141]. LE is indicated in parentheses. *Mixture of diasteromers.

With simplified R_1 in **4c**, the affinity for FKBP51/52/12 was abolished regardless of R_2 indicating the importance of binding contributions by suitable R_1 groups. The comparison of **4a**, **5a** and **6a** for FKBP51/52 indicates that the bicyclic [4.3.1] aza-

amide scaffold has a better degree of preorganization than the bicyclic [3.3.1] aza-amide scaffold which in turn is preferred over the monocyclic scaffold. The same trend was observed for FKBP51/52/12 in the cyclohexyl analog series (**5c** > **6c**). In terms of ligand efficiency,where the free energy is divided by the number of non-hydrogen atoms[147], the bicyclic [4.3.1] aza-amide scaffold and bicyclic [3.3.1] aza-amide scaffold both represented a clear improvement over the monocyclic scaffold.

4.4.2 Binding affinity of the bicyclic aza-sulfonamide series.

A library of sulfonamide ligands was first described for FKBP12[195]. Recently, sulfonamides were identified as suitable surrogates for the α-keto amide substructure in monocyclic FKBP51 ligands[143]. To test whether this SAR would be extended to the constrained bicyclic scaffolds, selected phenyl sulfonamides were introduced at the N^7 position of the bicycles. All the bicyclic [3.3.1] aza-sulfonamides and bicyclic [4.3.1] aza-sulfonamides have low mircomolar binding affinities for FKBP51/52. **5g** even displayed submicromolar affinity for FKBP51 while all bicyclic sulfonamides have submicromolar or even low nanomolar level binding affinities for FKBP12. All sulfonamides had better binding affinities than the corresponding a-keto-amide series compounds for FKBP51/52/12. For the sulfonamide series, the bicyclic [4.3.1] scaffod provides better binding affinity than the bicyclic [3.3.1] scaffod than the monocyclic scaffod. The same trend was also observed for the α-keto amide series before (Table 4).

For the first three sulfonyl aza-sulfonamide series (Table 4), the preferred 2-(3',4'-dimethoxyphenyl)oxy ethyl substituent identified above was kept constant as R_1 group. With the m,m-dichlorophenyl substructure as R_2, for FKBP51/52/12 both the [3.3.1] aza-sulfonamide **4e** and the bicyclic [4.3.1] aza-sulfonamide **5e** have better binding affinity than monocyclic sulfonamide **6e** while **5e** is slightly worse than **4e**. With the benzothiazole substructure as R_2, for FKBP51/52 both the [3.3.1] aza-sulfonamide **4f** and the bicyclic [4.3.1] aza-sulfonamide **5f** have better binding affinity than monocyclic sulfonamide **6f**. For FKBP12, **5f** is better than **6f** than **4f**.

Compound	n	R_1	R_2	FKBP52 K_i [µM] (LE)	FKBP51 K_i [µM] (LE)	FKBP12 K_i [µM] (LE)
4e	1	*(structure, OMe)*	*(structure, Cl)*	12.2±3.7 (0.20)	8.8±1.1 (0.21)	0.14±0.01 (0.28)
5e	2	*(structure, OMe)*	*(structure, Cl)*	1.6±0.3 (0.23)	1.2±0.2 (0.23)	0.01±0.002 (0.32)
5i	2	*(structure, OMe)*	*(structure, Cl, OH)*	3.5±0.4 (0.21)	1±0.1 (0.23)	0.4±0.04 (0.24)
6e	-	*(structure, OMe)*	*(structure, Cl)*	>100	>100	0.4±0.006 (0.27)
4f	1	*(structure, OMe)*	*(benzothiazole)*	>100	64.8± 12.3 (0.17)	0.9±0.2 (0.24)
5f	2	*(structure, OMe)*	*(benzothiazole)*	3.6±0.5 (0.21)	2.1±0.2 (0.22)	0.03±0.007 (0.29)
6f	-	*(structure, OMe)*	*(benzothiazole)*	>100	>100	0.1±0.00003 (0.28)
4g	1	*(structure, OMe)*	*(benzothiazolone)*	>100	13.9±0.9 (0.19)	0.07±0.0004 (0.28)
5g	2	*(structure, OMe)*	*(benzothiazolone)*	1.2±0.2 (0.22)	0.3±0.02 (0.24)	0.001±0.0003 (0.34)
6g	-	*(structure, OMe)*	*(benzothiazolone)*	12.4±1.3 (0.19)	7.6±0.5 (0.20)	0.002±0.0001 (0.35)
4h	1	H	*(benzothiazolone)*	46.4±3.8 (0.26)	27±1.7 (0.27)	0.1±0.0005 (0.42)
5h	2	H	*(benzothiazolone)*	22.6±1 (0.27)	9.8±0.5 (0.29)	0.06±0.002 (0.41)
6h	-	ethyl	*(benzothiazolone)*	>100	>100	0.2±0.004 (0.38)

Table 4: Binding affinities of monocyclic or bicyclic sulfonamide ligands for FKBP51, FKBP52 and FKBP12 determined by fluorescence polarization assay[141]. LE is indicated in parentheses.

With the benzothiazolone substructure as R_2, for FKBP51/52/12 the bicyclic [4.3.1] aza-sulfonamide **5g** has better binding affinity than monocyclic sulfonamide **6g**, but the [3.3.1] aza-sulfonamide **4g** is worse than **6g**. The p-hydroxyl m,m-dichlorophenyl substructure as R_2, the bicyclic [4.3.1] aza-sulfonamide **5i** showed higher binding

affinity compared to the similar analog **5e** for FKBP51/52 but not for FKBP12. When R_1^A substituent was minimized or deleted, (the series of **4h**, **5h** and **6h**), as expected this reduced the affinity to FKBP51/52/12 but only to a rather small extent, at least in the context of the high-affinity benzothiazolone substituent as R_2. As observed before, the cyclization improved affinity (**5h** > **4h** > **6h**) and the same trend was observed for the smaller homolog FKBP12. For these sulfonamide series, the bicyclic [4.3.1] aza-amide scaffold and the bicyclic [3.3.1] aza-amide scaffold also showed a clear improvement over the monocyclic scaffold with the constantly highest ligand efficiency value of the bicyclic [4.3.1] aza-amide scaffold. Importantly, however, removal of the R_1^A substituent increased ligand efficiency in all cases. Ligand **5h** is much more efficient than the natural products FK506 or rapamycin and represents the most efficient FKBP ligand known today. It is the first lead-like ligand (MW= 367Da, LE= 0.29, clogP= 0.95) for the clinically relevant FKBP51 and offers three rigidly defined attachment points (R^1, R^2 and C^8) for further lead optimization.

The assay results of the α-keto amide series and the sulfonamide series strongly suggests that the higher affinities of the [4.3.1] aza-amide series are indeed an inherent property of the seven-membered bicycle. Importantly, for all four sulfonyl [4.3.1] aza-amides **5** prepared low micromolar affinities were obtained which is almost a factor of ten better than the corresponding sulfonamide analogs of **2**, i.e., in an optimized monocyclic scaffold[143].

4.5 Cocrystal structure of **4g**, **5f** and **5g** with FKBP51 FK1

To better understand the enhanced binding of the [4.3.1] aza-amide bicycles, the ligands **4g**, **5f** and **5g** were cocrystallized with the FK506-binding domain of FKBP51 with resolution of 1.08Å, 1.1Å and 1.15Å respectively (Figure 14). The overall binding modes of **4g**, **5f** and **5g** were similar to those observed for compound **2**[134] or for a sulfonamide-based analog[143] in complex with FKBP51. Importantly, the positioning of the C^1-carbonyl oxygen of **5f** and **5g** and the geometry of the hydrogen bond to Ile[87]-NH was more similar to those observed for FK506 or to **2** than those of the [3.3.1] bicycles **4g** or **3a** compared to the latter two.

The dihedral angle formed by O^1-C^1-C^2-N^7 of **5f** and **5g** were between 173° and 175°. This is very similar to unconstrained FKBP ligands when bound to FKBP51

(167°-179°, Table 5). In contrast, the O^1-C^1-C^2-N^7 dihedral angle of the [3.3.1] bicycle **4g** was substantially smaller (148°). This translated into an altered orientation of the C^1-carboyl group towards the Ile^{87}-NH donor (quantified by the C^1-O^1-Ile^{87}N-Val^{86}C dihedral angle and the O^1-C^1-Tyr^{113}O angle). The C^1-O^1-Ile^{87}N-Val^{86}C dihedral angle was substantially smaller for the [3.3.1] bicycles (122° for **4g**, 97° for **3a**) compared to the [4.3.1] bicycles (147°-167°, Table 5), which resembled much closer the unconstrained FKBP ligands (144°-196°, Table 5). Likewise, the O^1-C^1-Tyr^{113}O angle, which defines the C^1-Tyr^{113}O dioplar contact, is much more similar between the [4.3.1] bicycles (100°-102°) those and the unconstrained FKBP ligands(99°-114°) than those observed for the [3.3.1] bicycles (90° for **4g**, 86° for **3a**).

Similar to **3a** the C^8-methylenes of the bicyclic linker in **4g**, **5f** and **5g** form van-der-Waals contacts with Phe^{77} while the C^9-methylene of **5f** and **5g** do not seem to engage in any contacts with the protein nor intramolecularly with other parts of the ligand. The benzothiazole substituent and benzothiazolone substituent as R_2 sit in a pocket below the 80s loop (Ser^{118}-Ile^{122}) which is known to be functionally relevant for the modulation of the steroid hormone receptors by the large FKBPs [31]. Here, two orientations for the benzothiazole/benzothiazolone substituents seem to be possible, each rotated vs. each other by 180°. In one conformation of the thiazolones, the sulfur is within hydrogen bond distance to Ser^{118}. The C^{15}-H of **5f** engages the backbone carbonyl of Leu^{119} below van-der-Waals distance (2.9Å).

Compound (PDB number)	C^1-Tyr-O dipolar distance (Å)	angle O^1-C^1-Tyr^{113}-O	O^1-Ile^{87}N bond distance (Å)	dihedral angle O^1-C^1-C^2-N^7	dihedral angle Val^{86}C-Ile^{87}N- O^1-C^1
3a	3.4	86°	2.8	153°	96°
FK506 (**1**) (3O5R)	3.2	101°	2.9	179°	144°
C2a (4DRN)[134]	3.5	114°	2.9	193°	197°
C2b[134] (4DRP)	3.5	111°	2.8	191°	164°
C3[143] (4DRQ)	3.1	99°	3.0	185°	158°
SLF(**2**)[134] (4DRK)	3.2	107°	2.9	185°	144°
5f in conformation1	3.0	102°	2.8	173°	142°
5f in conformation2	3.0	102°	2.9	172°	144°
5g in conformation1	3.0	100°	2.8	175°	152°
5g in conformation2	3.0	102°	2.8	175°	158°
4g in conformation1	3.1	90°	2.8	147°	128°
4g in conformation2	3.1	90°	2.8	148°	122°

Table 5 Quantification of structual parameters for known cocrystallized FKBP51 ligands and the cocrystallized FKBP51 ligands **4g**, **5f** and **5g**.
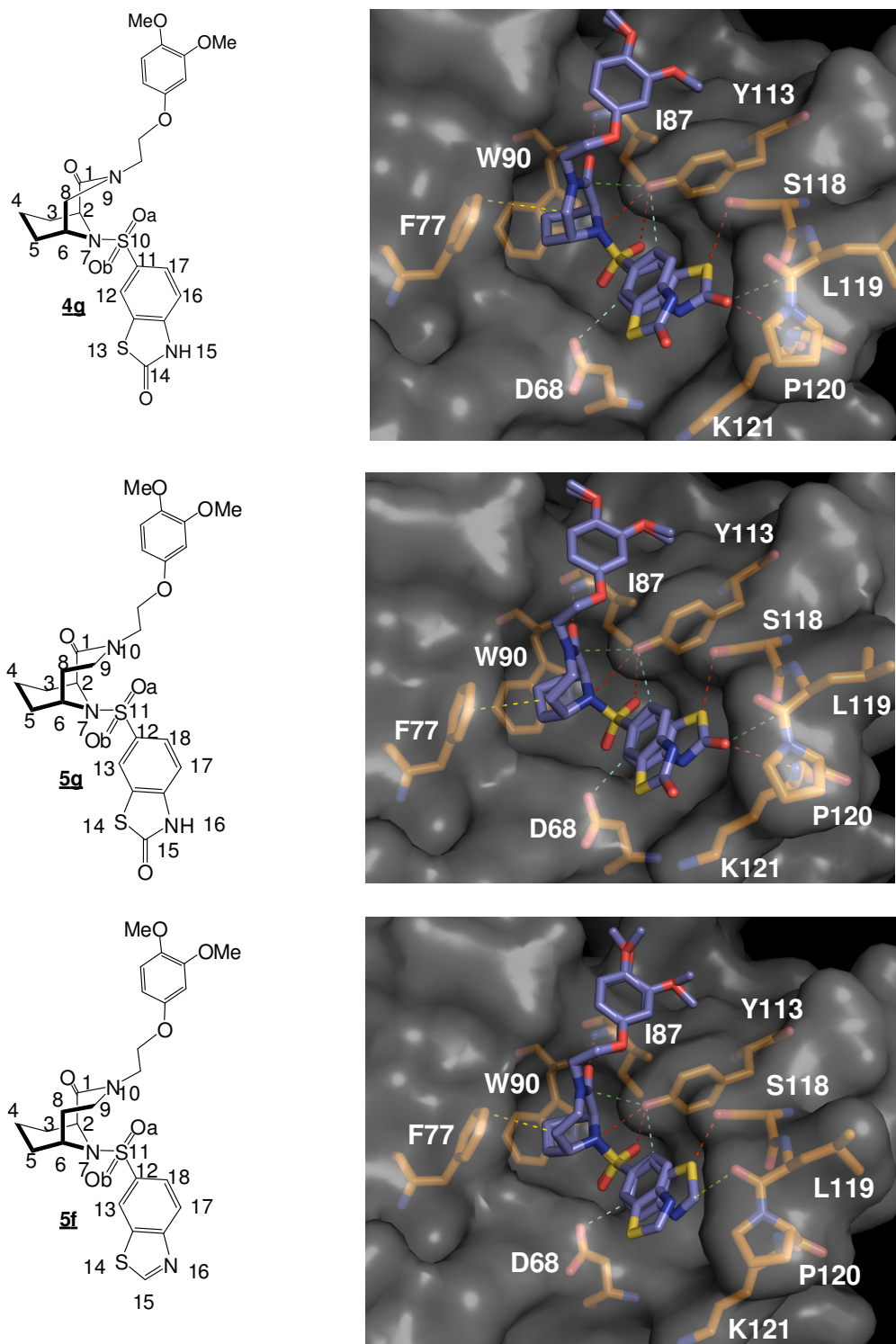
Figure 14: The bicyclic sulfonyl [3.3.1] aza-amide derivative **4g**, the bicyclic sulfonyl [4.3.1] aza-amide derivative **5f** and **5g** and their cocrystal structures with the FK506-binding domain of FKBP51, resolved to a resolution of 1.08Å, 1.1Å and 1.15Å respectively[146]. Color code is as in Figure 2, putative hydrogen bonds are dashed in orange, aromatic hydrogen bonds are dashed in cyan. Lys[121] is removed for clarity.

In the homologous cocrystal structure of **5g**, Leu[119] moves outward and the O^{14}-thiazolone engages the carbonyl of L^{119} in a dipolar interaction. Almost identical contacts are observed for the thiazolone in the corresponding [3.3.1] analog **4g**. For both conformations of **4g, 5f** and **5g**, the ortho-hydrogens of the aryl sulfonamide form aromatic hydrogen bonds with Tyr[113] and Asp[68], respectively, similar to those previously observed for monocyclic pipecolate sulfonamide ligands[143]. Importantly, only minimal interactions of the benzothiazole or the benzothiazolone ring are present for **5f, 5g** and **4g**. Indirectly the C^9 stabilized the observed conformation. The 2-(3',4'-dimethoxyphenyl)oxy ethyl substituent R_1 overlays almost perfectly with the 3-(3',4'-dimethoxyphenyl)propyl moiety in the complex of **2**, sitting in a cradle formed by Gly^{84}-Ile^{87} and Tyr[113].

Compound	Scaffold	N^7-Tyr[113]-O distance (Å)	O^a- Tyr[113]-O distance (Å)	pyramidalization[a]
FK506		3.6	2.6	176°
C2a (comp **3f-1**[196])		3.9	2.7	180°
C2b (comp **3f-2**[196])		3.7	2.6	-178°
SLF (2) (comp **2a**[196])		3.6	2.6	-179°
C3 (comp **20**[197])		3.8	3.4	146°
3a		3.5	2.6	-178°
4g (conformation1)		3.3	3.6	139°
4g (conformation2)		3.2	3.6	140°
5f (conformation1)		3.1	2.8	136°
5f (conformation2)		3.0	2.7	132°
5g (conformation1)		3.3	3.2	136°
5g (conformation2)		3.3	3.2	139°
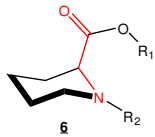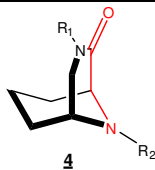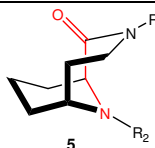
Table 6: Quantification of the N^7 and $S=O^a$ interactions with Tyr[113] of FKBP51 for the known cocrystallized FKBP51 ligands and for bicycles of this work. [a] The pyramidal is quantified by the angle of $S-N^7$ vs the $C^2-N^7-C^6$ plane.

A strong tendency for pyramidalization of N^7 of the sulfonamides was also observed which indicated a substantial degree of sp^3 hybridization (Table 6). For all bicylcic sulfonamides a distance below 3.3 Å was observed between Tyr[113]-OH and N^7 accompanied by an increased distance between Tyr[113]-OH···O^A=S. The Tyr[113]-OH···O^A=S contact in **5f, 5g** and **4g** is substantially longer than the corresponding bond distance in α-keto amide ligands like **5a** and **2** (Table 6). In the cocrystal structure of **5f**, Tyr[113]-OH clearly approaches the O^A=S and N^7 within a distance of a

bifurcated hydrogen bond. Both sulfonamide oxygens in **5f**, **5g** and **4g** are involved in several close edge-on aromatic CH···O contacts. The strong tendency for pyramidalization and the shifting from a hydrogen bond to a bifurcated hydrogen bond (to O^A=S and N^7) together with the higher binding affinity of the bicyclic aza-sulfonamides than the corresponding α-keto amides indicated that the bicyclic aza-sulfonamide might better represent the active conformation for FKBP51.

4.6 GR hormone radioactive binding assay

The main physiological role of FKBP51 is believed to be the inhibition of glucocorticoid receptor signalling, especially in stressful situations[113]. The FKBP51-GR interplay has been difficult to assess pharmacologically, however, largely due to lack of appropriate chemical probes. With the optimized FKBP51 ligands in hand we therefore set out to investigate the functional consequences of FKBP51 inhibition in a GR hormone radioactive binding assay, a defined reconstituted biochemical model of GR activity that obviates many of the pitfalls of the assays used earlier[113, 198]. The functional effects of the ligands were assessed by their ability to block the inhibitory effect of FKBP51 on GR activity. Gratifyingly, we observed a clear dose-dependent recovery of GR binding by **4g**, **5g** and **6g** (Figure 15), which showed functional activity on an important downstream FKBP51 target and mirrored their affinities to FKBP51 in the fluorescence polarization assay results (Table 4).
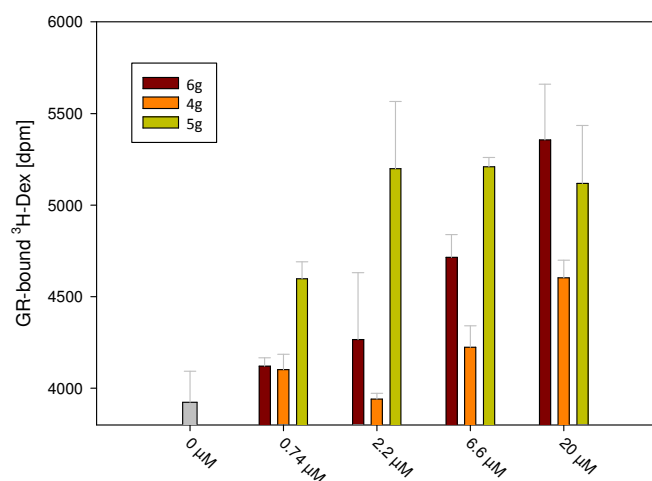
Figure 15: Relieve of FKBP51-mediated suppression of the glucocorticoid receptor hormone binding affinity by **4g**, **5g** and **6g**.

4.7 Thermodynamic analysis

The [4.3.1] bicyclization contributed $\Delta\Delta G > 2$kcal/mol to the binding energy compared to the monocycles. This is more than could have been achieved by van-der-Waals contacts of the bridging C^8-methylene [199]. Towards elucidating the origin of the additional binding energy in more detail, the thermodynamic parameters for complex formation of the most advanced compounds **4g**, **5g** and **6g** with FK506-binding domain of FKBP51 were determined by isothermal titration calorimetry (ITC) (Figure 16). The binding affinities (K_d) of **4g**, **5g** and **6g** were obtained by ITC were 10.5μM, 0.36μM and 3.3μM respectively which is in excellent agreement with the fluorescence polarization assay results (Table 4).

The binding of **6g** and **4g** was driven both enthaplically and entropically. Surprisingly, however, we observed a strong increase in binding enthalpy ΔH for the [4.3.1] bicycle **5g** compared to **6g** and **4g** (-13.5kcal/mol *vs* -3.0 and -4.5kcal/mol, respectively) which was largely compensated by a substantial entropic offset. Similar, on first sight counter-intuitive negative changes of binding entropy upon ligand rigidification have recently been observed by several groups[200-203]. In one case the counterproductive entropic change was shown to be caused by a stronger ordering of the protein by the more rigid ligands[203]. The large increase in binding enthalpy of **5g** vs **6g** is probably due to (i) the better hydrogen bond acceptor properties of the C^1-amide compared to the C^1-ester, (ii) stabilization of the conformation of O^1-C^1-C^2-N^7, (iii) additional van-der-Waals contacts by the C^8-methylene. (iv) stabilization of the N^7 pyramidalization. The direct comparison of **5g** and **4g** reveals the strong orientation dependence of the hydrogen bond and dipolar contact network around the C^1=O carbonyl which could account for a substantial amout of the additional binding entropy of **5g**. Importantly, amide *vs* ester replacements had previously been shown to be inactive in the monocyclic scaffolds[134, 143] .
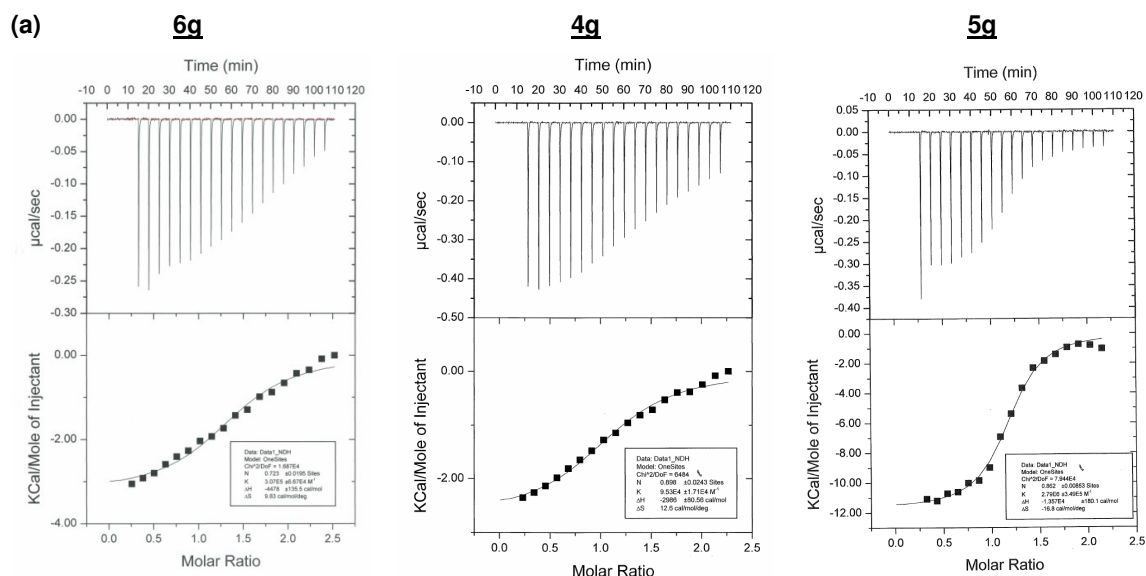
Compound	ΔH (KCal/mol)	ΔS (KCal/mole/K)	TΔS (KCal/mol)	ΔG (KCal/mol)	K_d (µM)
6g	-4,47800	0,00983	2,88166	-7,35966	3,25733
4g	-2,98600	0,01260	3,69369	-6,67969	10,49318
5g	-13,57000	-0,01680	-4,92492	-8,64508	0,35842

(b)
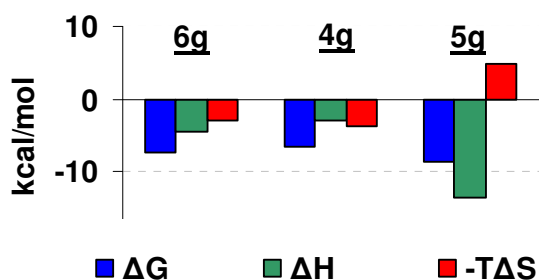
Figure 16: (a). Thermodynamic parameters for binding of **4g**, **5g** and **6g** to FK506 binding domain of FKBP51. (b) Thermodynamic signatures of **4g**, **5g** and **6g** upon binding to the FK506-binding domain of FKBP51.

4.8 Synthesis of the C^8-derivatized bicyclic [4.3.1] aza-amides 57

From the above results, the bicyclic [4.3.1] aza-amide scaffold was identified as a priviledged substructure for FK506-binding proteins (FKBPs). The cocrystal structures of the bicyclic [4.3.1] aza-amide derivatives **5f** and **5g** in complex with FKBP51 FK1 revealed the possibility to further introduce additional substituents into

the bicyclic [4.3.1] aza-amide nucleus at C^8 which would increase the contact surface with the FKBP51/52 and may help to increase the binding affinity. Therefore we designed and synthesized a new series of C^8-derivative bicyclic [4.3.1] aza-amide derivatives **41** (Figure 17).
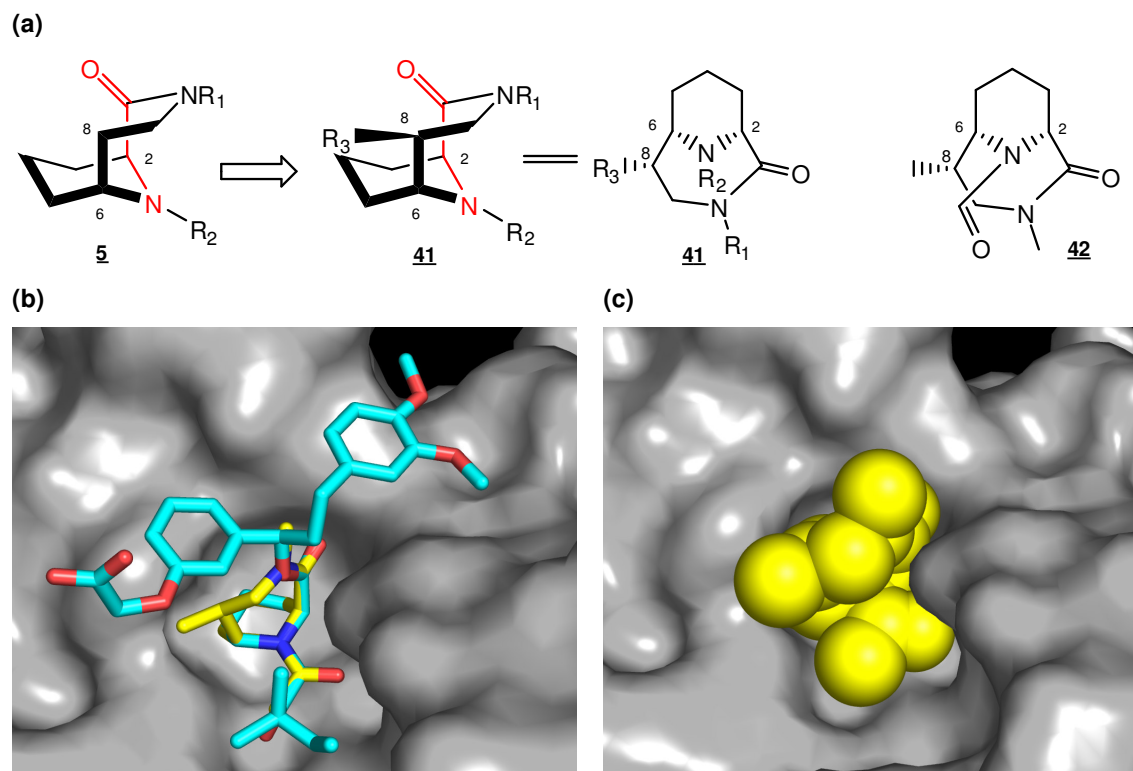
Figure 17: (a) Proposed C^8-derivatized bicyclic [4.3.1] aza-amide derivatives **41** based on the bicyclic [4.3.1] aza-amide derivatives **5** and the C^8-substituted bicyclic [4.3.1] aza-amide nucleus **42** used for the computer modelling study. (b) The superimposition of the energy-minimized C^8-derivative bicyclic [4.3.1] aza-amide nucleus **42** (yellow) with compound **2** (blue) bound to the FKBP51 FK1 domain [134]. (c) Space filling model of the energy-minimized C^8-derivative bicyclic [4.3.1] aza-amide nucleus **42** positioned into the FKBP51 FK1 domain as in b.

The C^8-derivatized bicyclic [4.3.1] aza-amide nucleus **42** was modelled into the binding pocket of FKBP51 (Figure 17b, 17c). The C^1-C^6, N^7, O^1 and O^{11} of the **42** were overlaid with the corresponding atoms of **2** (SLF) in the cocrystal structure of **2** and FKBP51 FK1 domain. A conserved binding mode of C^8-derivative bicyclic [4.3.1] aza-amide nucleus **42** was enforced with the common elements of the pipecolate and α-keto amide region (Figure 9) being nearly superimposable in the two structures. It indicated no obvious sterically hindrance between the protein and the bicyclic aza-amide nucleus **42**.

4.8.1 Retrosynthetic analysis and strategy

To control the stereochemistry at C^2, C^6 and C^8 a new synthetic strategy was devised as outlined in Scheme 14. The bicyclic nucleus **43** was envisioned to be prepared from **44** through carbon-carbon bond formation between C^6 and C^8 by N-acyliminium cyclization. The stereochemistry of C^6 would be dictated by the stereochemistry at C^2 whereas the stereochemistry at C^8 was envisioned to be substrate-controlled by steric interference with C^4 of the piperidine ring. An electron-donating group at the vinyl group of C^8 was thought to facilitate the intramolecular cyclization as well as to subsequently provide a functional group for further diversification. The amide moiety in **44** could be incorporated by coupling between **45** and **46**.
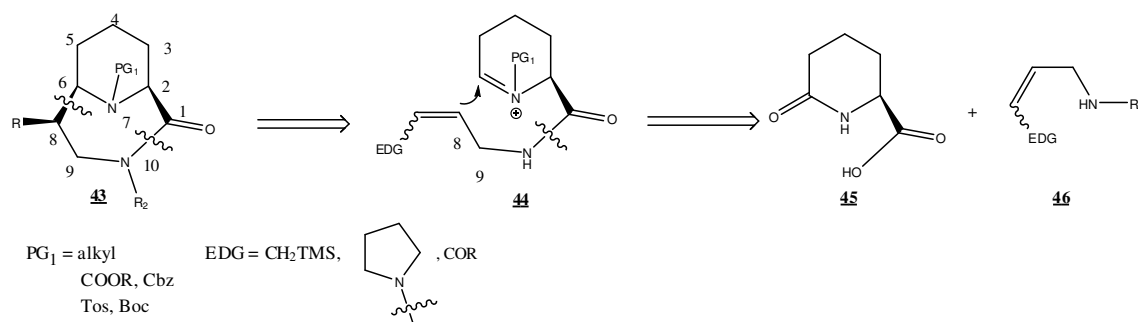
Scheme 14: Retrosynthsis of the C^8-substituted bicyclic [4.3.1] aza-amide nucleus **43**.

4.8.2 Synthesis of the bicyclic [4.3.1] aza-amide nucleus 57

The commercially available **44** was alkylated with **45** to afford compound **28a**, which was reacted with commercially available **47** to yield compound **48**. The allyltrimethylsilyl group was introduced by a metathesis reaction with Grubbs catalyst I in DCM as a cis/trans isomeric mixture **50** (1:1 based on NMR) followed by deprotection of the Boc-protection group with silica to give the N^{10}-building block **51**. The secondary amine group in **51** was coupled with commercial (S)-6-oxopiperidine-2-carboxylic acid **52** in presence of HOAt, EDC-HCl and DIPEA in DCM at room temperature to give **53** followed by Boc-protection of the N^7-position in **53** to give the compound **54. 54** was regioselectively reduced with DIBAL-H followed by cyclization within 30% TFA in DCM and cleavage of Boc protection group to afford **57** in a one-

pot reaction with 76% yield and excellent diastereoselectivity (dr>99:1 determined by NMR) (Scheme 15).
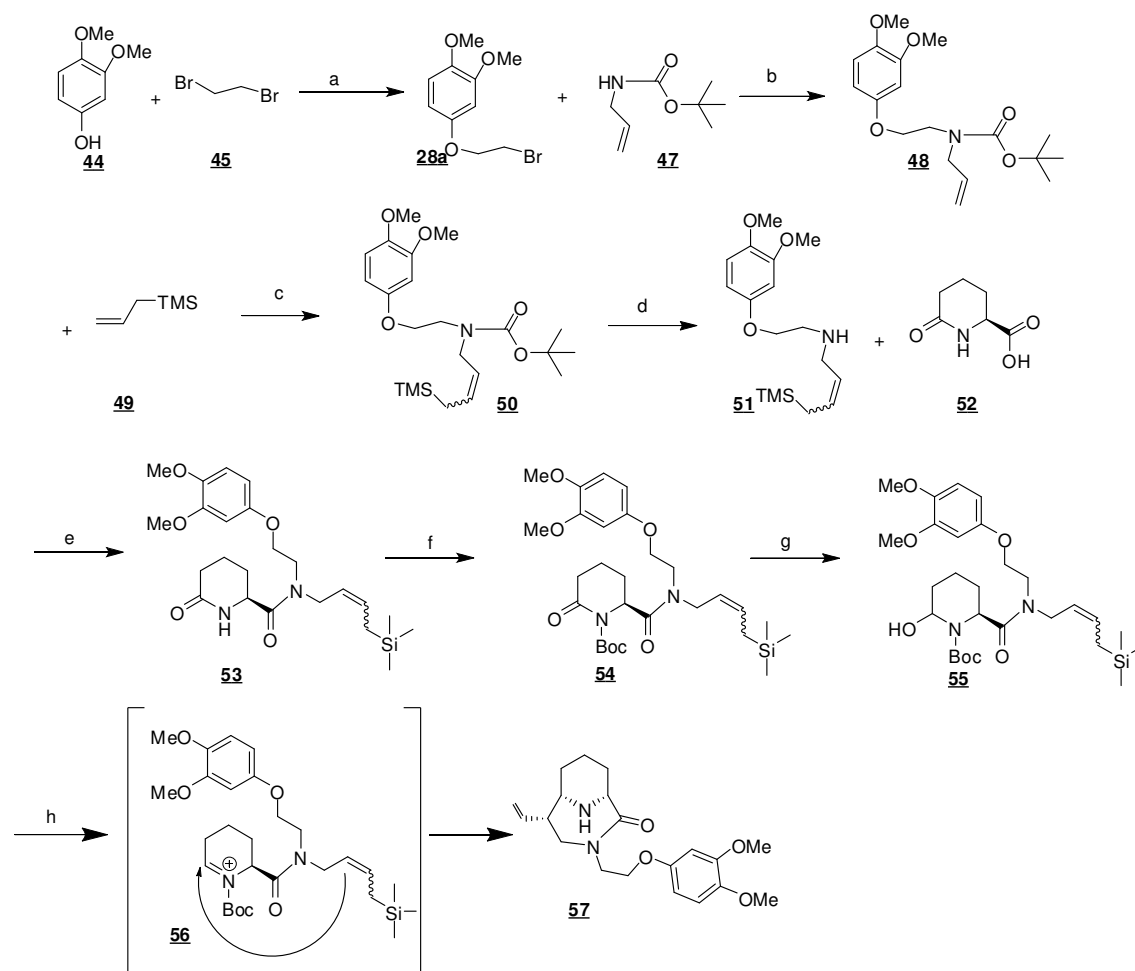
Scheme 15: Synthesis of **57** (a) K_2CO_3 in acetone, reflux, overnight, 46% (b) NaH in DMF, 0°C, 2h, 69% (c) Grubbs catalyst I in DCM, reflux, 67% (d) SiO_2, 150°C, vacuo, 85% (e) HOAt, EDC, DIPEA in DCM, RT, 24h, 90% (f) BuLi, (Boc)$_2$O in THF, -78°C, overnight, 72% (g) 3eq DIBAL-H, THF, -78°C (h) 30% TFA in DCM at 0°C (76% for two steps)

The C^2 position is particularly prone to racemization. To support the absence of racemization, simplified model reactions were carried out (Scheme 16). The Boc-protection group in **48** was cleaved with 50% TFA in DCM at room temperature followed by coupling with commercial (S)-6-oxopiperidine-2-carboxylic acid **52** to afford **59**. The N^7-position in **59** was protected with Cbz group to give the compound **60** which had excellent enantiomeric excess (ee >99:1) based on chiral HPLC analysis.

a)
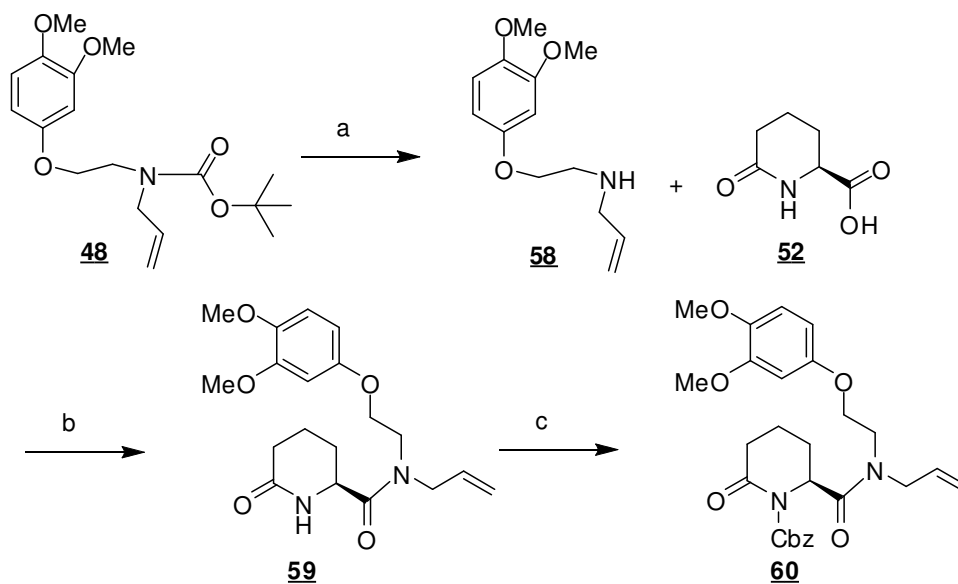
b)
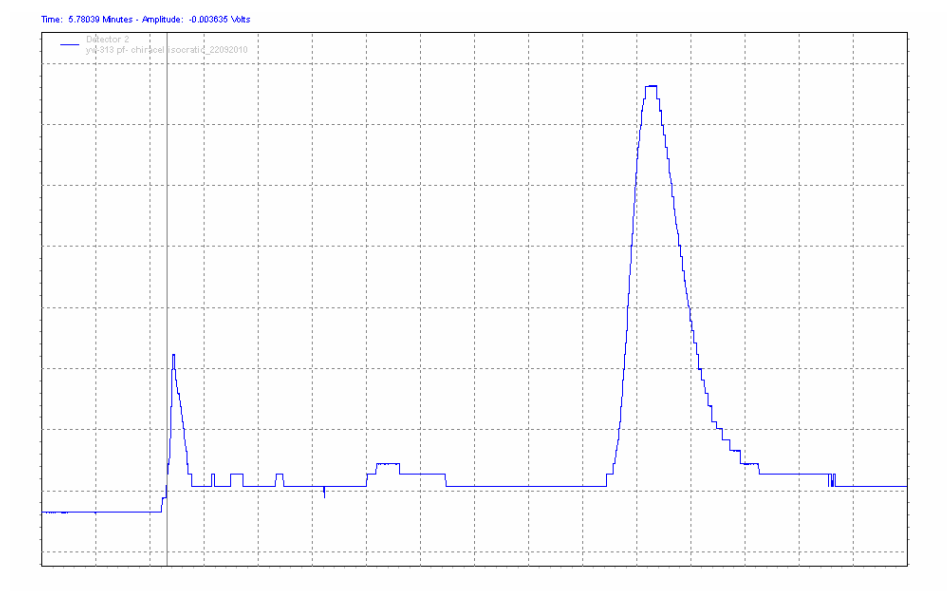
Scheme 16: a).Synthesis of a model compound **60** to check the racemization at C^2 position.(a) 50% TFA in DCM, RT, 2h (b) HBTU, DIPEA in DCM, RT, 24h, 95% (c) BuLi, Cbz-Cl in THF, -78°C, 5h, 60%. b) Chiral HPLC spectroscopic data of **60**.

4.8.3 Systematic study of the cyclization reaction.

A mechanism study showed that when **55** was treated with 10% TFA in DCM at -78°C and stirred at -20°C for 2h, **55** was converted to **61** as the only product

51

observed in LCMS. With further addition of TFA to 50% at 0℃, **61** was converted to **57** as the only product which supported that the cyclization was through intramolecular N-acyliminium cyclization but not intramolecular iminium cyclization (Scheme 17).
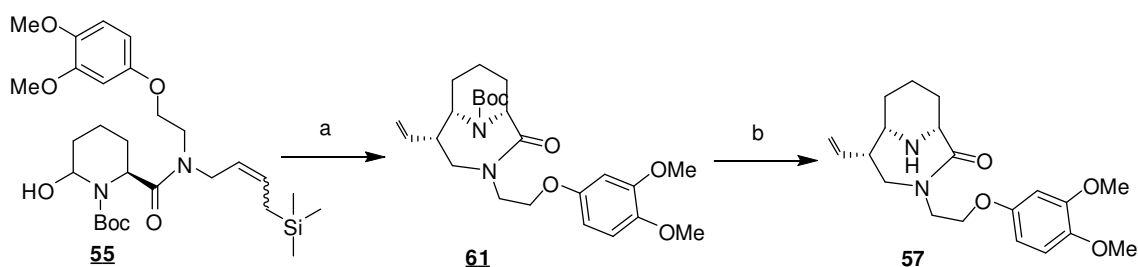
Scheme 17: Mechanism study for the cyclization step based on **55**. (a) 10% TFA in DCM, -78℃, 2h (b) 50% TFA in DCM, 0℃ , 2h, (76% for two steps)

Before the establishment of the crucial intramolecular N-acyliminium cyclization, different cyclization conditions were tested. As the N-acyliminium cyclization was planned to be carried out under acid condition, the N^7-position in **53** was first protected with Cbz-protection group instead of the acid sensitive Boc-protection group to afford **62**. Different reduction conditions were then carried out to selectively reduce **62** (Scheme 18).

Under condition b [204, 205] only trace amounts of **63** were produced but the cleavage of Cbz group to afford **53** (based on NMR and Mass spectroscopy) as the main product. Condition c could afford the production of **63** but with low conversion rate while excessive amounts of $NaBH_4$ in MeOH afford **63** with **64** as a side product. The side reaction could be reduced to a smaller extent by using excessive amounts of $NaBH_4$ under mild acidic condition (pH= 6) in MeOH (condition d)[206]. No reaction was observed when THF or DMF was used as solvent instead of MeOH. Condition e was found to be the best to convert **62** to **63** without any side reaction. Unfortunatly, **63** is very labile and attempts to purify **58** by chromatography were unsuccessful and the production of **63** was deduced from LCMS results.

	Condition	Product
b	1.2eq LiEt$_3$BH,THF,-78℃	**53**
c	1.2eq NaBH$_4$,MeOH,0℃	**63**+**64**
d	excessive NaBH$_4$,MeOH,0℃ under acidic condition by adding 10%TFA	**63**+**64**
e	3eq DIBAL-H, THF, -78℃	**63**
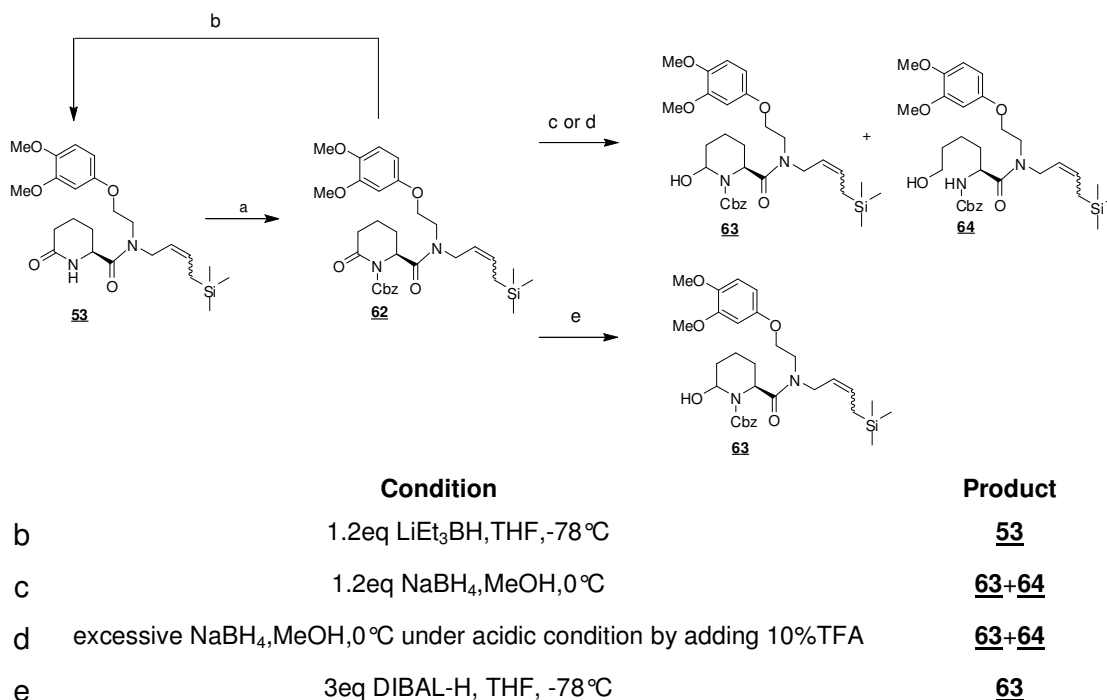
Scheme 18: Different reduction conditions and possible products from the reduction of **62**. a) BuLi, Cbz-Cl in THF, -78℃, overnight, 60%

To better understand this reduction reaction, a model reaction was carried out to check the reduction condition and stability of the hemiaminal product. When **65** was treated with NaBH$_4$ in MeOH at 0℃, **66** and **67** were produced. Both of them were purified with chromatography and characterized with NMR (Scheme 19). The low yields might be due to other side reactions such as Cbz group cleavage of **65**, but further efforts to elucidate the side reactions were not put forth.
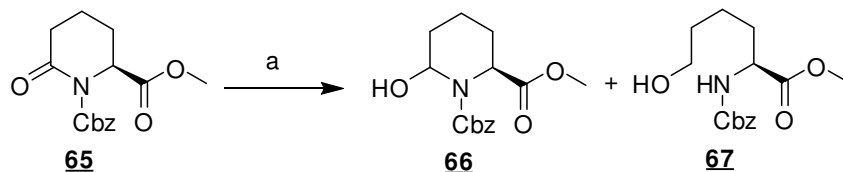
Scheme 19: A simplified model study of the selective reduction step based on **65**. (a) 2.2 eq NaBH4 in MeOH, RT, 2h, (26% for **64**, 21% for **65**)

The lability of **63** might be due to the coexistence of the electron-rich substructure and hemiaminal in one molecule. Thus, **63** was used for the next step without purification.
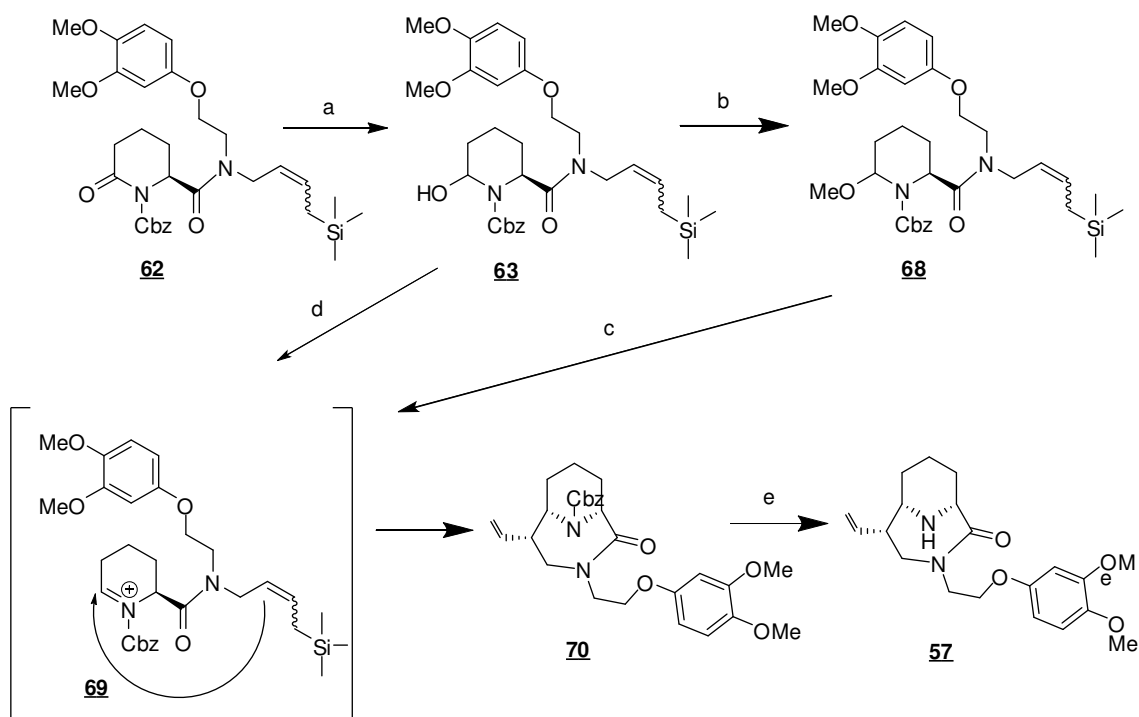
Scheme 20: Three conditions for the synthesis of **62** based on **57**.

Condition 1: (a) excessive NaBH4, MeOH,0℃, (b) 20% TFA in DCM at 0℃, (c) 60% TFA in DCM at 0℃, (34% for three steps)

Condition 2: (a) excessive NaBH4, MeOH,0℃ (d) 10% TFA in DCM at 0℃, (51% for two steps)

Condition 3: (a) 3eq DIBAL-H, THF,-78℃ (d) 20% TFA in DCM at 0℃, (83% for two steps)

(e) 33% HBr in acetic acid at 0℃, 69%

When NaBH$_4$ was used as a reducing reagent, 20% TFA was added to the reaction mixture of **63** at 0℃ to afford the methoxylated compound **68** *in situ* followed by cyclization in the presence of 60% TFA in DCM at 0℃ to afford **70** with 34% yield in all three steps and excellent diastereoselectivity (dr>99:1 determined by HPLC) (Scheme 20 condition 1). Later it was found that the methoxylation step was not a prerequisite and that **63** could be converted to **70** directly by cyclization with 10% TFA in DCM at 0℃ with 51% yield for all two steps and excellent diastereoselectivity (dr>99:1 determined by NMR) (Scheme 20 condition 2). Different acidic conditions like SnCl$_4$[207, 208], TiCl$_4$ or formic acid[161, 208] instead of TFA were tried for the cyclization process. Rapidly decomposition of **63** was observed in the presence of the lewis acid SnCl$_4$ or TiCl$_4$ at -78℃ while slow conversion and many side reactions were observed when formic acid was used at -20℃ . When DIBAL-H was used as a reducing reagent, the reaction mixture of **63** was evaporated *in vacuo* followed by cyclization within 20% TFA in DCM at 0℃ with 83% yield for two steps and excellent

diastereoselectivity (dr>99:1 determined by NMR) (Scheme 20 condition 3). The Cbz group in **70** was then cleaved by 33% HBr in acetic acid at 0°C to afford **57** with 69% yield.

4.8.4 Functionalization of bicyclic [4.3.1] aza-amides nucelus **57**

At this point a m,m-dichlorophenylsulfonyl group as a preferred substructure for FKBPs was installed at the N^7 of **57** in presence of DIPEA to afford **71** with moderate yield and conversion ratio which might be due to the steric hindrance of the secondary amine. The terminal vinyl group at C^8 in **71** was further submitted to dihydroxylation. The attempts to stereoselective dihydroxylate the vinyl group in **71** was conducted with AD-Mix-Alpha or AD-Mix-Beta at room temperature. Unfortunately, the dihydroxylation with 7 eq AD-Mix-Alpha affored **72** as a 6:1 diasteremeric mixture of C^{11} epimers with only 60% conversion, while with 2 eq AD-Mix-Beta, **73** was obtained with 100% conversion but still as a 2:1 diasteremeric mixture of C^{11} epimers (Scheme 21). Diastereomers were observed by NMR for both **72** and **73** which could not be separated by HPLC.
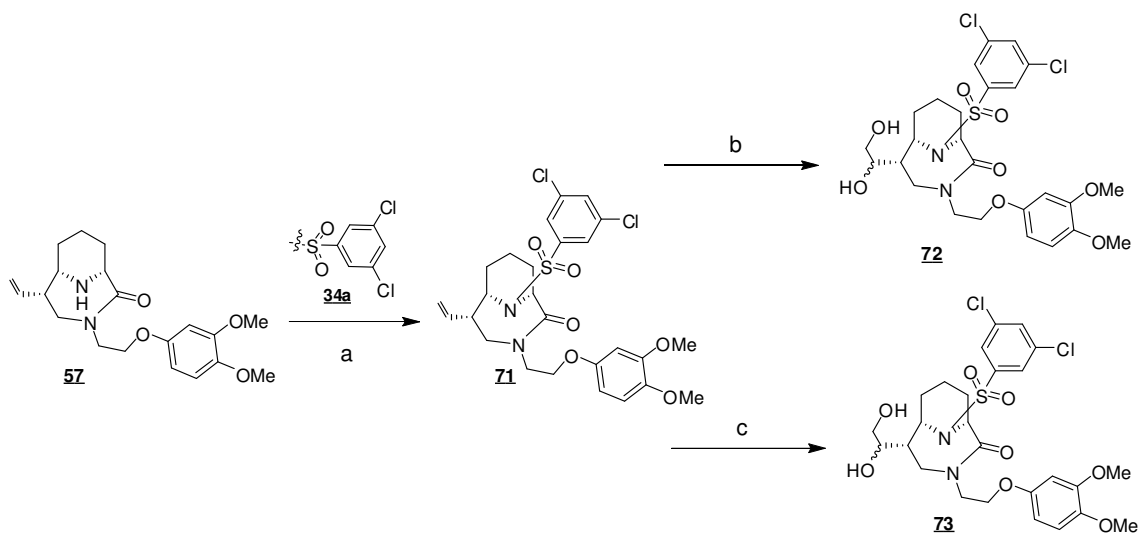
Scheme 21: Synthesis of **71**, **72** and **73** (a) **34a**, DIPEA, DCM, RT, overnight, 48%, (b) 7eq AD-Mix-Alpha, water, t-BuOH, RT,57%, (c) 2eq AD-Mix-Beta, water, t-BuOH, RT,94%.

a)
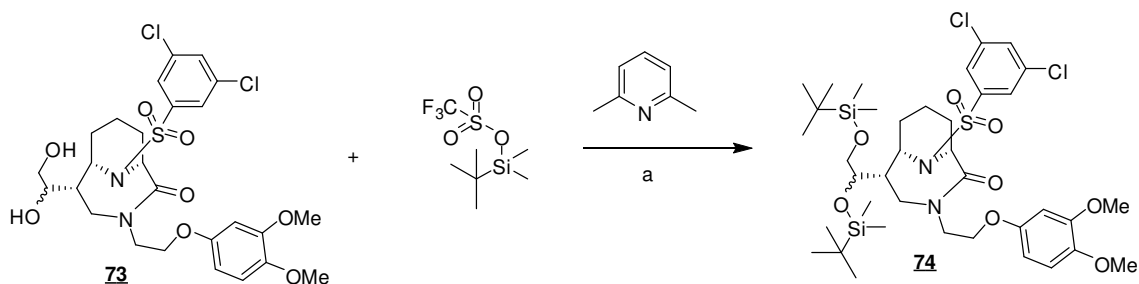
b)
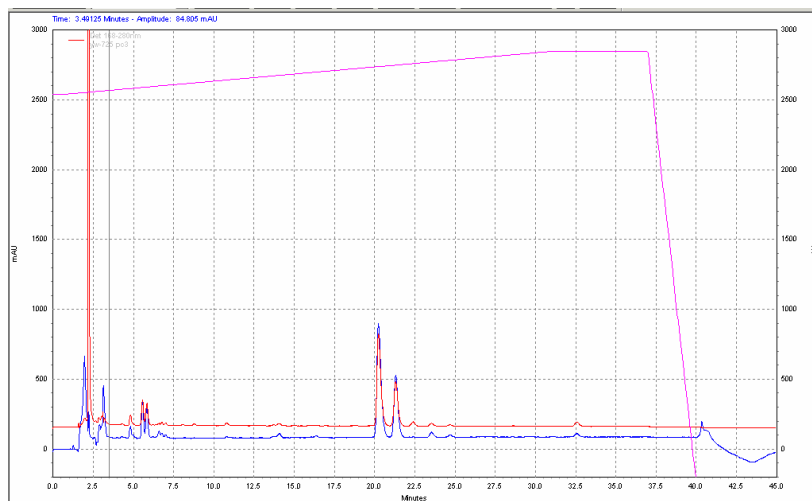
Scheme 22: a) Synthesis of 65 (a) 6eq tert-Butyldimethylsilyl trifluoromethanesulfonate, 2,6-lutidine, DCM, 0 °C. b) HPLC spectroscopic data of the crude 74.

In a small test reaction, the double silylation of **73** resulted in two separable peaks with the same mass identified by LCMS. These two peaks have a ratio of 2:1 by HPLC analysis (Scheme 22). Further purification of these two peaks was to be carried out in the future.

Although the attempt to stereoselective dihydroxylate the vinyl group in **71** was unsuccessful, the terminal vinyl group at C^8 allows for a versatile and straightforward derivatization to further improve the interaction with FKBPs. An overview for future SAR study is outlined in Scheme 23.
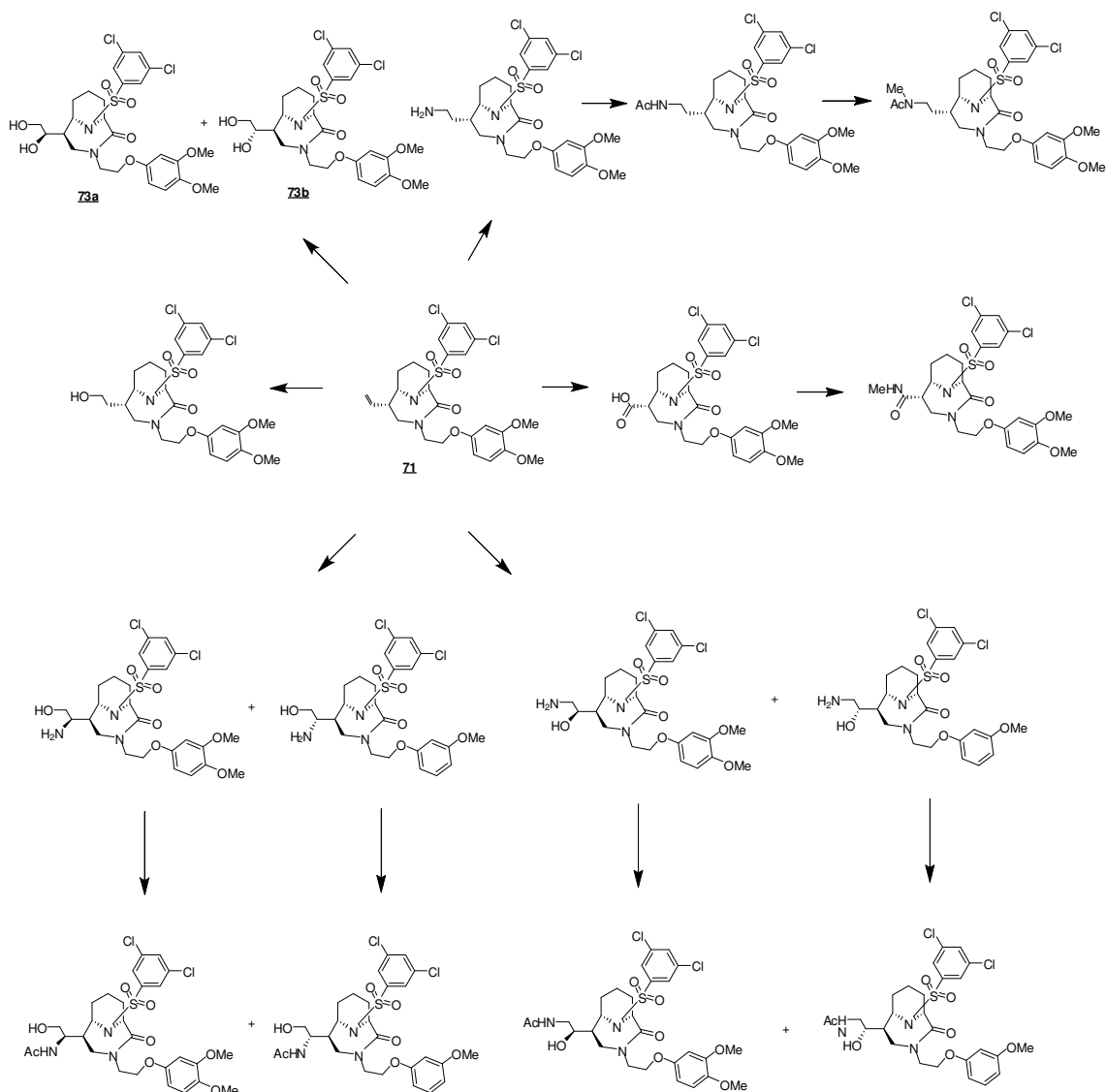
Scheme 23: Possible derivatization of the terminal vinyl group at C[8] for compound **71**

4.9 Competition binding fluorescence polarization assay

The affinities of the C[8]-derivatized ligands **71** and **73** for FKBPs were measured by a fluorescence polarization assay using purified human FKBP12 or the purified FK506-binding domain of FKBP51 and FKBP52 expressed in *E.coli* (Table 7)[141]. As SLF (**2**) has a comparable higher binding affinity than other simplified synthetic ligands, it was linked to a flurophore to be used as a fluorescence-labelled ligand. The affinity of **71** and **73** were assessed by its ability of competition with the fluo-**2** for the FK1 domain of FKBP.

57

Compound **71** retained slightly improved binding affinity and similar ligand efficiency compared to the corresponding C^8-unmodified control **5e** demonstrating that substituents can be accommodated in the C^8-position. The approximately 5 times better binding affinity of **73** compared to **5e** might result from the increased contact surface between ligand and protein. The introduction of additional hydroxyl groups at C^{11} and C^{12} substantially improved the ligand affinity and efficiency for all FKBPs yielding ligands with low nanomolar potencies. **73** is 175 times (for FKBP51) and 75 times (for FKBP52) better than **63** and rivalls the affinity of the natural product FK506.

Compound	FKBP51		FKBP52		FKBP12	
	Ki(µM)	LE	Ki(µM)	LE	Ki(µM)	LE
71	1.4 ±0.2	0.22	2.1±0.4	0.21	0.03±0.003	0.28
73	0.008 ± 0.02[a]	0.29	0.03 ± 0.08	0.27	<0.001[b]	
5e	8.8±1.0	0.21	12.3±3.7	0.2	0.14±0.01	0.28
FK506	0.09±0.02[a]	0.17	0.23±0.07	0.16	0.0006±0.0001	0.22

Table 7: Binding affinities **71**, **73** and **5e** for FKBP51, FKBP52 and FKBP12. (a) With sg586 as tracer. (b) This the detection limit of tracer fluo-**2**.

4.10 Cocrystal structure of **71** and FKBP51

The X-ray crystal structure of the FKBP51 FK1 domain complexed with ligand **71** was solved to 1.08 Å resolution. In this complex, FKBP51 adopts the same folding topology as observed in FKBP51 complexed with **5f** and **5g**. The ligand adopts a similar binding mode compared to that of **5f** or **5g** with the common pipecolate ring being nearly superimposable (Figure 18). The pipecolyl ring of the ligand sits atop the indole of Trp^{90}, which forms the floor of the FKBP binding pocket. Similar to FK506 the C^1-carbonyl of the pipecolate forms a hydrogen bond with the backbone amide of Ile^{87} with a distance of 2.8Å, almost the same as the [4.3.1] bicycles **5f** and **5g** (2.8-2.9 Å). The C^1-O^1-Ile^{87}N-Val^{86}C dihedral angle was 167° (Table 8). This is very similar to **5f** and **5g** (142°-158°, Table 5) and resembled the unconstrained FKBP ligands (144°-196°, Table 5). The dihedral angle formed by O^1-C^1-C^2-N^7 of **71** was 175° which is the same as in **5g**, only marginally different from **5f**, and very similar to

unconstrained FKBP ligands when bound to FKBP51 (167°-179°, Table 5). Likewise, the O^1-C^1-$Tyr^{113}O$ angle and C^1-$Tyr^{113}O$ dipolar distance which define the C^1-$Tyr^{113}O$ dioplar contact, are 101° and 3.1Å respectively. Both values are similar to the [4.3.1] bicycles **5f** and **5g** (100°-102°, 3.0 Å).

71
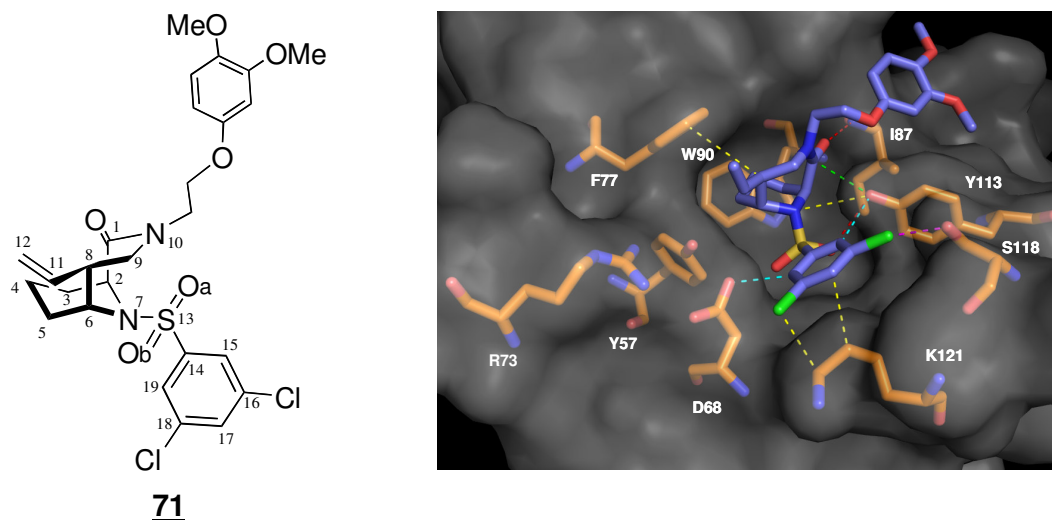
Figure 18: The C^8-substituted bicyclic [4.3.1] aza-amide derivative **71** and cocrystal structures with the FK506-binding domain of FKBP51, resolved at a resolution of 1.08 Å. **71** bound to the FK1 domain of FKBP51. Key residues of FKBP51 are show in orange, the two hydrogen bonds between O^1 and HN-Ile^{87} and between O^{13a} and HO-Tyr^{113} are shown dashed red. The dipolar interaction between the C^1-carbonyl and HO-Tyr^{113} is dashed in green. Aromatic hydrogen bonds between C^{15}-H and OH-Tyr^{113}, C^{19}-H and OH-Asp^{68} are dashed in cyan. van-der-Waals interactions between Cl^{18} and C-Lys^{118} are dashed yellow. The halogen bond between Cl^{16} and O-Ser^{118} is dashed magneta.

One oxygen of the sulfonamide (S=O_a) forms a rather weak hydrogen bond with the hydroxyl group of Tyr^{113} with a distance of 3.2Å which is longer than the corresponding bond distance in α-keto amides like **FK506**, **5a** and **2**. FKBP51 and **71** engage in a number of aromatic CH···O-acceptor interactions, e.g., the oxygen of the sulfonamide (S=O_b) and the ε-hydrogens of Tyr^{57}, Phe^{67} and Phe^{130}. As expected, the dichloro aryl ring sits below the 80s loop and packs on Ile^{122}. The two ortho-hydrogens of the sulfonylphenyl ring form close contacts (2.9 Å) with the p-oxygen of Tyr^{113} and with carboxylate of Asp^{68} (2.8 Å), respectively. These two contacts are much shorter than normal aromatic hydrogen bonds. One of the aromatic chlorines might form a van-der-Waals contact with Lys^{121} (3.3 Å). The other chlorine approaches Ser^{118} to form a halogen bond (2.5 Å) with the C^{16}-Cl-Ser^{118}-O angle of

166°. The Ser[118] Such short distance is rather uncommon for halogen bonds. Like **4g**, **5f** and **5g** (Table 6), **71** also has a similar N^7 pyramidalization (Table 8) and a short distance of 3.4 Å between N^7 and Tyr^{113}-OH. The C^{11} approaches Tyr^{57} with a distance of 3.7 Å and the C^{12}- C^{11}- Tyr^{113}-O angle of 125°. The C^8-vinyl substitution points out of the pocket which clearly confirmed the desired conformation obtained from our stereoselective synthesis and also indicated the possibility of introducing more potential ligand-protein interaction with further allyl functionalization.

Compound (PDB number)	C^1-Tyr^{113}-O dipolar distance (Å)	angle O^1-C^1-Tyr^{113}-O	O^1-$Ile^{87}N$ distance (Å)	dihedral angle O^1-C^1-C^2-N^7	dihedral angle $Val^{86}C$-$Ile^{87}N$-O^1-C^1	$O^8/S=O^a$ Tyr^{113}-O distance (Å)	N^7-Tyr^{113}-O distance (Å)	Pyramidalization (a)
Fk506 (**1**) (3O5R)	3.2	101°	2.9	179°	144°	2.6	3.6	176°
71	3.1	101°	2.8	175°	167°	3.2	3.4	134°

Table 8: Quantification of structual parameters for cocrystallized **71** with FKBP51 FK1 and compared with the cocrystal structure of FK506. (a) The pyramidalization is quantified by the angle of S-N^7 vs the C^2-N^7-C^6 plane.

4.11 Hypothetical binding mode of **73a** and **73b**

The low nanomolar potency of **73** based on the dihydroxylation of **71** showed the importance of these two hydroxy groups. Due to the difficulties of stereoselective dihyroxylation and purification, their cocrystal strucutures with FKBP51 FK1 domain were not available. Based on the cocrystal strucuture of **71** with FKBP51 FK1 domain, the hypothetical binding mode of **73a** and **73b** were proposed by computer modelling which was carried out by Dr. Uwe Koch from Lead Discovery Center GmbH (Figure 19). **73a** and **73b** bind to the FKBP51 FK1 domain with the conserved binding mode as **71**. The only difference between **73a** and **73b** is at the C^{11} position with a R-conformation for **73a** and a S-conformation for **73b**. In **73a**, the C^{11}-OH approaches Tyr^{57} and Asp^{68} with a distance of 4.2Å and 3.8Å respectively which would be too far to form hydrogen bonds. In **73b**, the C^{11}-OH approaches Asp^{68} with a distance of 3.8Å which is still above the threshold of hydrogen bond while it might engage in a hydrogen bond with Tyr^{57} with a proposed distance of 2.9 Å. This could

explain the higher binding affinity of the **71**. The angle formed by C^{11}- O^{11}-Tyr^{57}- O of **73b** was 133° and the dihedral angle C^8- C^{11}- O-Tyr^{57} was 62°. While the angle formed by O^{11}- Tyr^{57}- O- Tyr^{57}-C^4 angle was 147° and the dihedral angle O^{11}- Tyr^{57}- O- Tyr^{57}- C^4- Tyr^{57}-C^3 was 117° (Table 9). This hypothesis has to be confirmed in the future by experimental cocrystal structures.

(a)

(b)

(c)

(d)
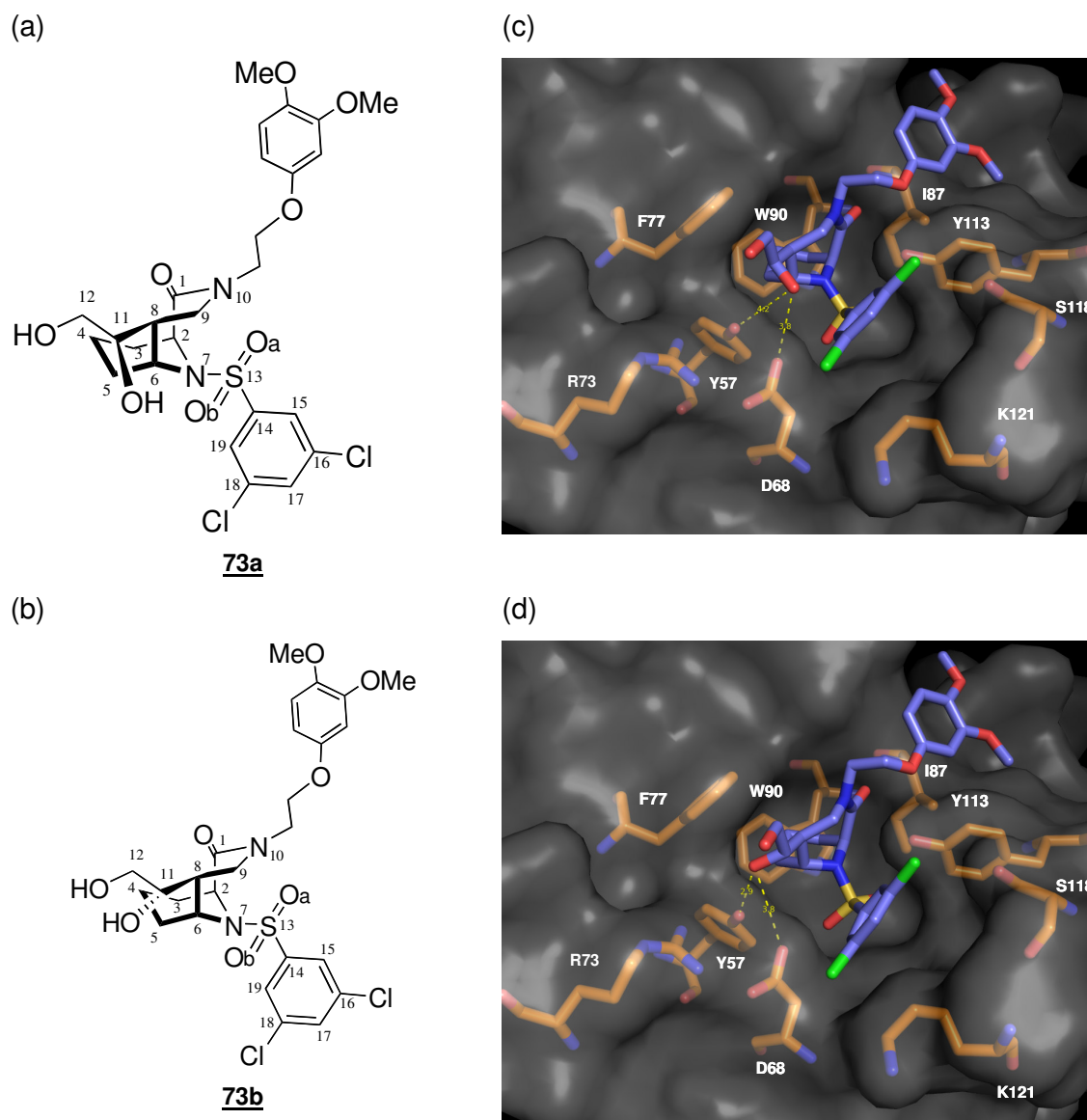
Figure 19: a, b) The structure of **73a** and **73b** used for computer modelling study. c). Computer modelling of **73a** (blue) bound into the FKBP51 FK1 domain with the distances measured between C^{11} hydroxy group and Tyr^{57} and Asp^{68}. d) Computer modelling of **73b** (blue) bound into the FKBP51 FK1 domain with the distances measured between C^{11} hydroxy group and Tyr^{57} and Asp^{68}. The distance measurement between C^{11} hydroxy group and Tyr^{57} and Asp^{68} are dashed yellow.

61

Compound	C^{11}- O^{11}- Tyr^{57}- O angle	dihedral angle C^8- C^{11}- O-Tyr^{57}	O^{11}- Tyr^{57}- O- Tyr^{57}- C^4 angle	dihedral angle O^{11}- Tyr^{57}- O- Tyr^{57}- C^4- Tyr^{57}-C^3
73b	133°	62°	147°	117°

Table 9: Quantification of structual parameters for the proposed hydrogen bond between Tyr^{57}–OH and C^{11}-OH.

5. Conclusion

In order to improve the ligand affinities and efficiencies of the the FKBPs ligands, new scaffolds were proposed to preorganize the ligands to limit the flexibility and mimic the active conformation. The bicyclic [3.3.1] aza-amide and bicyclic [4.3.1] aza-amide core structures were designed as rigid replacements for the pipecolyl-monocyclic scaffold and their potential binding modes were analyzed *in silico.* With the synthetic route established in this study, a series of bicyclic [3.3.1] aza-amide derivatives **4** and bicyclic [4.3.1] aza-amide derivatives **5** were prepared. Their binding affinities for FKBP51, 52 and 12 were measured with a competition binding fluorescence polarization assay. Among the α-keto amide series, the trimethoxyphenyl moiety is shown to be a better R_2 substructure than tert-pentyl for the bicyclic scaffold, while the cyclohexyl analog which more closely mimic the pyranose group in the high affinity natural product ligands is also effective in the bicyclic context. A three-atom spacer compared to a two-atom spacer is preferred for optimal positioning of the dimethoxyphenyl group in R_1. For the sulfonyl aza-amides series, the benzothiazolone substituent was found to be the best R_2 to afford **5g** with nanomolar affinities for FKBP51/52/12. When R_1 substituent was minimized or lacking, the affinities of the bicyclic compounds to FKBP51/52/12 were only reduced to a rather small extent with the benzothiazolone substituent as R_2. Ligand **5h** is much more efficient that the natural products FK506 or rapamycin and represents the most efficient FKBP ligand known today. It is the first lead-like ligand (MW= 367Da, LE= 0.29, clogP= 0.95) for the clinically relevant FKBP51 and offers three rigidly defined attachment points (R^1, R^2 and C^8) for further lead optimization. Both compound series indicate that the bicyclic [4.3.1] aza-amide scaffold has a better degree of preorganization than the bicyclic [3.3.1] aza-amide scaffold which in turn is preferred over the monocyclic scaffold. The higher affinities of the [4.3.1] aza-amide series are an inherent property of the seven-membered bicycle. Such a trend was also observed in a GR hormone radioactive binding assay and isothermal titration calorimetry (ITC) measurements of **4g**, **5g** and **6g**. The higher binding affinity of **5g** compared to **4g** and **6g** was dissected to be a strong increase in binding enthalpy with a substantial entropic offset compensation. The cocrystal structures of **4d**, **5c** and **5d** with the FKBP51 FK1 domain showed that their binding modes are similar to

those observed for compound **2** in complex with FKBP51 FK1. This confirmed the rational design of the ligands and also provided valuable information for future SAR studies.

Based on the cocrystal structure of **5c** and **5d**, a C^8 substitution was proposed to be introduced into the bicyclic [4.3.1] aza-amide scaffold which was identified as a priviledged scaffold for FK506-binding proteins (FKBPs). The C^8 substitution was predicted to increase the contact surface between ligand and protein to further enhance the binding affinity for FKBP51 and 52. The idea was supported by computer modelling which showed the steric possibility for further incorporating substituents at the C^8 position. A new stereoselective synthetic route was established and optimised in which a stereoselective carbon-carbon bond formation by N-aciliminium cyclization was the key step with 76% yield and excellent diastereoselectivity (dr>99:1 determined by NMR). In the cocrystal structure of **63** with FKBP51 FK1, the retained binding mode of **63** compared to the corresponding C^8-unmodified control **5e** demonstrates that substituents can be accommodated in the C^8-position. It confirmed the desired conformation obtained from the stereoselective synthesis and also indicated the possibility of introducing more potential ligand-protein interaction by further functionalization of the vinyl group. The racemic dihydroxylation of the C^8 vinyl group substantially improved the affinity for all FKBPs yielding ligands with low nanomolar potencies that rivalled those of the natural product FK506. The higher binding affinity was proposed to be obtained from a putative hydrogen bond between the C^{11}-OH of **64b** and Tyr^{57}. This will be confirmed in the future by a corresponding cocrystal strucuture. A more detailed and systematic SAR study of the terminal vinyl group at C^8 will be carried out.

6. Materials and Methods

6.1 Biological analytical methods

6.1.1 Molecular modelling

The co-crystal structure of SLF, FKBP51 or Compound **3a** with the FK1 domain of FKBP51 were obtained from Dr. Andreas Bracher in Prof. Ulich Hartl `s group at Max Planck Institute of Biochemistry. Two of these structures were later published (4DRK and 3O5R) [134, 209].

All computer simulations were performed on Dell computer AMD athlon™64x2 dual core processor 3800+ 2.00GHz, 960MB RAM. Microsoft windows XP professional version 2002 service pack 2.

6.1.2 Molecular modelling of FKBP51 with bicyclic derivatives 7, 8, 42

The bicyclic [3.3.1] aza-amide nucleus **7**, the bicyclic [4.3.1] aza-amide nucleus **8** and the C^8-derivative bicyclic [4.3.1] aza-amide derivatives **42** were constructed with Chemdraw 3D ultra 10.1. The structures were first drawn and cleaned up followed by energy calculation and minimization by MM2 computations with the minimum RMS gradient value at 0.1. Then, the C^1-C^6, N^7, O^1 and O^{10} of the bicyclic [3.3.1] aza-amide nucleus or the C^1-C^6, N^7, O^1 and O^{11} of the bicyclic [4.3.1] aza-amide nucleus was aligned and overlaid with corresponding atoms of **2** in the cocrystal structure of **2** and FKBP51. The resulting structures were saved as pdb files and visualized in PyMol.

6.1.3 Competition Binding Fluorescence Polarization Assay

The competition binding fluorescence polarization assay was performed as described[141] under the guidance of Dr. Christian Kozany and Bastiaan Hoogeland. Fluorescence polarization (FP) assays are widely used in high throughput screening in drug discovery. The flurophore-labeled ligand with size less than 5000 Da[210] is

excited by polarized light and emit depolarized light due to the rapid molecular motion of the flurophore during its fluorescence lifetime. This is usually in the nanosecond range and defined as the period between absorption of an excitation photon and the emission of a photon through fluorescence (Figure 14). If the flurophore-labeled ligand binds to a receptor of significantly greater size, the rotation of flurophore compared to the fluorescence lifetime is severely slowed down which causes less depolarization of the original plane of polarization. The extent of binding can be quantified by measuring the extent of depolarization.
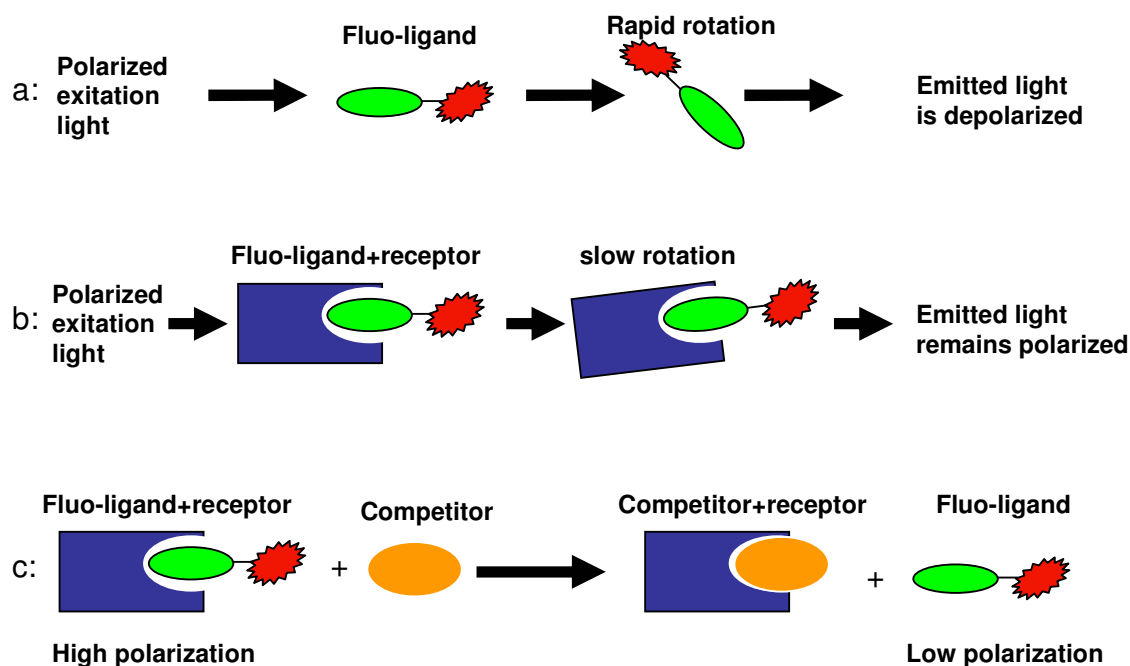
Figure 14: (a) and (b) Scheme of FP assay mechanism. (c) Scheme of a competition binding FP assays.

In competition binding FP assays, an inhibitor competes with flurophore-labeled ligand in binding for a receptor which results in the increase of free flurophore-labeled ligand in solution. Thereby relatively less polarized light is emitted. Titration of the flurophore-labeled ligand and receptor complex with the inhibitor gives the relative binding affinity (IC_{50}) of the inhibitor. The competition binding FP assay allows the determination of binding affinity of inhibitors from low nanomolar to high micromole range quickly and reproducibly.

6.1.4 Isothermal Titration Calorimetry experiments

The Isothermal Titration Calorimetry experiments were performed by Anne-Katrin Fabian.

Bacterially expressed, affinity purified human HisFKBP51FK1 (aa 1-140)[141] was dialysed against ITC buffer (20mM HEPES pH=8, 150mM NaCl, 5% DMSO). The activity was confirmed by active site titration in an FP Assay as described before[141]. The pH of protein was determined and ligand solutions were degassed and matched within 0.02 pH units.

ITC experiments were performed with a MicroCal iTC200 titration microcalorimeter (GE Healthcare). All experiments were conducted at 20°C. Compound **3d** (1mM) was measured by injection into the measurement cell containing the protein (89µM). Due to the limiting solubility compounds **2d** and **4d** were measured in a reverse setup injecting the protein (0.5mM and 0.16mM, respectively) into a solution of the ligand (40µM for **2d**, 15µM for **4d**). Heats of dilution were measured in blank titrations and subtracted from the binding heat values. ORIGIN software (version 7.0 Microcal) was used for data collection and analysis.

6.1.5 GR hormone binding assay.

The GR hormone binding assay was performed by Alexander Kirschner.

6.1.6 Crystallography

The crystallography was performed by Dr. Andreas Bracher as described[209].

6.1.7 Reference compounds 5, 6b , 6c and 6h

The polycyclic compounds **5** and monocyclic compounds **6b** , **6c** and **6h** were prepared by Christoph Kress and Ranganath Gopalakrishnan.

7. Experimental Section

7.1 General chemical methods

All reactions were preformed in flame-dried glassware fitted with rubber septa under argon unless otherwise noted. Air- and moisture-sensitive liquids were transferred via syringe. Organic solvents were dried over $MgSO_4$ and concentrated by rotary evaporation.

7.1.1 Nuclear Magnetic Resonance (NMR)

The NMR measurements were performed by Claudia Dubler and Dr. David S. Stephenson.

The ^1H, ^{13}C-NMR-spectra, 2D HSQC, HMBC, COSY and NOESY were recorded on a Bruker AC 300, Bruker XL 400 or Bruker AMX 600 at room temperature at the NMR-facility, Department of Chemistry and Pharmacy, Ludwig-Maximilians-Universitaet Muenchen. Chemical shifts were reported in δ values (ppm); the hydrogenated residues of deuterated solvent were used as internal standard ($CDCl_3$: δ = 7.26 ppm in 1H NMR and δ = 77 ppm in 13C NMR). Signals were described as s, d, t, and m for singlet, doublet, triplet and multiplet respectively. All coupling constants (J) were given in Hz.

7.1.2 Mass Spectrometry

The Mass spectra (m/z) were obtained on a Thermo Finnigan LCQ DECA XP Plus mass spectrometer (ESI) at the Max Planck Institute of Psychiatry while the high resolution mass spectrometry was carried out by Elisabeth Weyher at MPI for Biochemistry (Microchemistry Core facility) on Varian Mat711 mass spectrometer (ESI) or on a JMS GCmate II JEOL mass spectrometer (EI) by Dr. Lars Allmendinger at the Department of Chemistry and Pharmacy, Ludwig-Maximilians-University Munich.

7.1.3 Flash Chromatography

Flash chromatography was performed using thick-walled glass columns and silica gel 60 (0.04 – 0.063 mm) from Roth. The relative proportion of solvents in mixed chromatography solvents refers to the volume: volume ratio.

Interchim Puriflash 430 with an UV detector was used as automated flash chromatography.

7.1.4 Thin Layer Chromatography

Thin layer chromatography (TLC) was performed on alumina plates coated with silica gel (Merck silica gel 60 F254, layer thickness 0.25mm) using the indicated solvent ratio (volume: volume). UV- active compounds were detected by UV- light determination (λ = 254 nm and λ = 366 nm), non-UV-active compounds were detected with different TLC staining solutions:

Hanessian's Staining Solution:

$$5 \text{ g CeSO}_4,$$
$$25 \text{ g NH}_4\text{MO}_7\text{O}_{24} \cdot 4 \text{ H}_2\text{O},$$
$$450 \text{ mL H}_2\text{O},$$
$$50 \text{ mL, H}_2\text{SO}_4$$

Ninhydrin Staining Solution:

$$0.5 \text{ g Ninhydrin},$$
$$100 \text{ mL EtOH},$$
$$5\text{mL AcOH}$$

Potassium Permanganate Staining Solution:

$$1.5 \text{ g KMnO}_4,$$
$$10 \text{ g K}_2\text{CO}_3,$$
$$1.25 \text{ mL 10\% NaOH}$$

$$200 \text{ mL } H_2O$$

The TLC plates were dipped in one of the reagents listed above and then heated to stain the spots.

7.1.5 High performance liquid chromatography (HPLC)

Analytical HPLC: Beckman System Gold 125S Solvent Module, System Gold
                     Diode Array Detector Module 168

Column: Jupiter 4 µm Proteo 90 A, 250 x 4.6 mm, Phenomenex,
                     Torrance, USA,

Wavelength: 224nm, 280nm, Diode Array

Mobile phase:

Solvent A: 95% H_2O
                     5% AcCN
                     0.1% TFA

Solvent B: 95% AcCN
                     5% H_2O
                     0.1% TFA

Flow rate: 1ml/min

Standard Gradient: 0-100% B in 20min, 1 ml/min

7.1.6 Preparatory Thin Layer Chromatography

The pre-coated preparative TLC plate SIL G-200 UV$_{254}$ was purchased from MACHEREY-NAGEL GmbH (layer: 2.0mm silica gel with fluorescent indicator UV$_{254}$).

7.1.7 Preparative HPLC

The compounds were dissolved in 40% buffer B, and the purification was carried out with an injection loop volume of 2 mL.

Preparative HPLC:	Beckman System Gold Programmable Solvent Module 126 NMP
	Beckman Programmable Detector Module 166
Column:	Phenomenex Jupiter 10µ Proteo 90 Å, 250 x 21.2 mm 10 micron
Wavelength:	224 nm

Mobile phase:

Solvent A:	95% H_2O
	5% MeOH
	0.1% TFA

Solvent B:	95% MeOH
	5% H_2O
	0.1% TFA
Flow rate:	25ml/min

7.1.8 Chiral HPLC

Pump:	Waters 515 HPLC Pump
Detector:	LDC Analytical Spectromonitor 5000 Photodiode Array Detector
Column:	DAICEL Chemical Industries LTD. Chiralcel OD-H

Solvent A:	Hexane
Solvent B:	i-propanol
wavelength:	220nm
Standard Gradient:	1:1 60 min, 0.5 ml/min

7.1.9 Chemicals

Chemical names follow IUPAC nomenclature. Starting materials were purchased from Aldrich, Lancaster, Fluka, Merck, Roth and were used without purification.

Substance name	CAS-Number	Company
(z)-1-Ethoxy-2-(tributylstannyl)ethene	e2342g1	Activate scientific GmbH
1-Hydroxybenzotriazol	123333-53-9	Aldrich
6-Bromopicolinic acid	21190-87-4	Activate scientific GmbH
anhydrous Acetonitril	75-05-8	Roth
Benzyl chloroformate	501-53-1	Aldrich
Di-tert-butyl-dicarbonat, 98%	24424-99-5	Fluka
EDC-HCl	25952-53-8	Aldrich
Ethyl-6-bromo-2-Pyridinecarboxylate	21190-88-5	Chempur
Hydrogen chloride	7647-01-0	Roth
30% Hydrogen peroxide	7722-84-1	Roth
Lithium chloride	7447-41-8	Merck
Magnesium sulfate	7487-88-9	Roth
N,N'-Diisopropylethylamine	7087-68-5	Aldrich
N-Bromosuccinimid, 99%	128-08-5	Aldrich
n-BuLi (2M in Cyclohexane)	109-72-8	Aldrich
Palladium on carbon	7440-05-3	Aldrich
Platinum dioxide	1314-15-4	Merck
Potassium carbonate	584-08-7	Roth
Pyridine	110-86-1	Roth
Raney nickel catalyst	7440-02-0	Merck
Sodium azide	26628-22-8	Merck
Sodium bicarbonate	144-55-8	Merck
Sodium chloride	7647-14-5	Merck

Sodium hydride 60 % dispersion in mineral oil	7646-69-7	Aldrich
Sodium hydroxide	1310-73-2	Merck
Sulfuric acid	7664-93-9	Roth
Thionyl chloride	7719-09-7	Merck
Triethylamine	121-44-8	Merck
Trifluoroacetic acid	76-05-1	Fluka
(Trimethylsilyl)diazomethane 2.0M in Et_2O	18107-18-1	Aldrich
9-BBN 0.5M in THF	280-64-8	Aldrich
1,2-Dibromoethane	106-93-4	Fluka
1,4-Dioxane	123-91-1	Roth
3,4-Dimethoxyphenol	2033-89-8	Fluka
Chloroform	67-66-3	Roth
Dichloromethane	75-09-2	Roth
Dichloromethane dry	75-09-2	Roth
Tetrahydrofuran	109-99-9	Roth
Acetone	67-64-1	Roth
Methanol	67-56-1	Roth
Methanol HPLC	67-56-1	Roth
Acetonitrile HPLC	75-05-8	Roth
Toluene	108-88-3	Roth
Diethylether	60-29-7	Roth
DMF	68-12-2	Roth
TFA	76-05-1	Roth
Formic acid	64-18-6	Roth
DIPEA	7087-68-5	Fluka
Triethylamine	121-44-8	Merck
$MgSO_4$	7487-88-9	Roth
$KMnO_4$	7722-64-7	Merck
NaCl	7647-14-5	VWR
LiOH	1310-65-2	Sigma
n-BuLi 2M in cyclohexane	109-72-8	Aldrich
NaN_3	26628-22-8	Aldrich

KOH	1310-58-3	Roth
K_2CO_3	584-08-7	Roth
DMAP	1122-58-3	Fluka
NaHMDS 1M in THF	1070-89-9	Aldrich
$NaHCO_3$	144-55-8	Roth
NH4Cl	12125-02-9	Merck
HATU	148893-10-1	Nova Biochem
$CDCl_3$	865-49-6	Roth

7.1.10 Solvents

Solvents were purchased from commercial suppliers Roth and Aldrich with ROTISOLV®, ROTIPURAN®, ROTIDRY® and HPLC grade and were used without purification.

Solvent	Quality	Company
Acetic acid	ROTISOLV ≥99,9%	Roth
Acetone	ROTISOLV ≥99,8%	Roth
Acetonitril	ROTISOLV ≥99,9%	Roth
Anhydrous Methanol	ROTISOLV ≥99,9%	Roth
Chloroform	99 % for Synthesis	Roth
Cyclohexane	ROTIPURAN ≥99,5%	Roth
Dichloromethane	ROTIDRY ≥99,8%	Roth
Diethyl ether	ROTISOLV ≥99,8%	Roth
Dimethylformamide	ROTISOLV ≥99,9%	Roth
Ethyl acetate	ROTISOLV ≥99%	Roth
Methanol	ROTISOLV ≥99,9%	Roth
n-Hexane	ROTISOLV ≥99%	Roth
Pentane	ROTIPURAN ≥99%	Roth
Tetrahydrofuran	anhydrous, ≥99.9%	Aldrich

7.2 Chemical Synthesis

7.2.1 Synthesis of 6-(cyanomethyl)picolinic acid 22

To 100 ml anhydrous THF under argon at -78°C was added butyl lithium (6.02 g, 94mmol) followed by addition of acetonitrile (4.06g, 99mmol) and stirring for 30min. Then 6-bromopicolinic acid 21 (2.5g, 12.38mmol) in 100 ml anhydrous THF cooled on ice was added dropwise. After 2 h at -78°C and 30 min at room temperature, the reaction mixture was concentrated *in vacuo*, dissolved in DCM (100 ml) and extracted with saturated $NaHCO_3$ solution (3 x 100 ml). The aqueous layers were acidified with 10% HCl, and extracted with DCM (6 x 100 ml). The collected organic layers were dried over $MgSO_4$ and concentrated *in vacuo*. This crude product was used for next reaction without further purification.

TLC [20% MeOH, 0.2% TFA in $CHCl_3$]: R_f = 0.04

Yield: 1.76g, 10.9mmol (87.7%)

^{1}HNMR (300 MHz, $CDCl_3$): δ= 8.1(d, 1H, J=7.75 Hz), 8.05(t, 1H, J=7.77, 7.77Hz), 7.75(d, 1H, J=7.8 Hz), 4.08(s, 2H)

^{13}C NMR (75 MHz, $CDCl_3$): δ= 163.69, 150.06, 146.67, 140.26, 126.86, 123.68, 116.05, 26.47

HRMS :163.0504[M + H] [+], 185.0321[M + Na] [+], calculated 163.0508 [M + H] [+]

7.2.2 Synthesis of methyl 6-(cyanomethyl) picolinate 20

13.35 ml 2M $TMSCHN_2$ in Et_2O (3.05g, 26.7mmol) was added dropwise to crude 6-(cyanomethyl) picolinic acid 22 (1.31g, 8.1mmol) in 27 ml anhydrous MeOH at 0°C. After stirring at room temperature for 5h, the reaction was quenched with saturated $NaHCO_3$ solution (100 ml) and extracted with DCM (6 x 100 ml). The organic layers were dried over $MgSO_4$ and concentrated *in vacuo*. The pure product was obtained by flash chromatography with hexane: EtOAc 1:1.

TLC [Hexane: EtOAc 1:1]: R_f = 0.54

Yield: 750mg, 4.3mmol (52.7%)

^{1}HNMR (300 MHz, CDCl$_3$): δ= 8.01-8.06 (m, 1H), 7.87(t, 1H, J=7.79,7.79 Hz), 7.64(d, 1H), 4.02(s, 2H), 3.94(s, 3H)

^{13}C NMR (300 MHz, CDCl$_3$): δ= 164.95, 151.05, 148.11, 138.61, 125.49, 124.41, 116.60, 53.04, 26.59

HRMS: 177.0649 [M + H] [+], 199.0472 [M + Na] [+], calculated 177.0664[M + H] [+]

7.2.3 Synthesis of ethyl 6-cyanopicolinate 11

CuCN (31,1g, 348mmol) was added to a solution of ethyl 6-bromopicolinate **12** (16g, 69.5mmol) in 608 ml pyridine. The mixture was heated under reflux for 16 h, filtered through celite and concentrated *in vacuo*. Saturated NaHCO$_3$ solution (100 ml) was added and extracted with DCM (6 x 100 ml). The organic layers were dried over MgSO$_4$ and concentrated *in vacuo*. The mixture was purified by flash chromatography with hexane: EtOAc 1:1.

TLC [Hexane: EtOAc 1:1]: R$_f$ = 0.65

Yield: 7.3g, 41.4mmol (60%)

^{1}HNMR (600 MHz, CDCl$_3$): δ= 8.32(dd, 1H, J=1.15, 7.97Hz), 8.04(t, 1H, J=7.86, 7.86Hz), 7.88 (dd, 1H, J=1.13, 7.76Hz), 4.52(q, 2H, J=7.13, 7.13, 7.12Hz), 1.40(t, 3H, J=7.13, 7.13Hz)

^{13}C NMR (300 MHz, CDCl$_3$): δ= 163.76, 150.06, 138.70, 134,23, 131.40, 128.12, 116.62, 62.89, 14.44

HRMS: 177.0669[M + H], calculated 177.0664[M + H] [+]

7.2.4 Synthesis of ethyl 6-((tert-butoxycarbonylamino)methyl)picolinate 13

To a solution of ethyl 6-cyanopicolinate **11** (7.87g, 44.7mmol) in 350 ml MeOH was added Boc$_2$O (19.5g, 89mmol) and catalytic amounts of Raney nickel. The reaction mixture was degased with argon and stirred under 1 atm H$_2$ at room temperature for 24 h, filtered through celite and concentrated *in vacuo*. The mixture was purified by flash chromatography with EtOAc: DCM 1:5.

TLC [EtOAc: DCM 1:5]: R$_f$ = 0.34

Yield: 8.74g, 31.2mmol (68%)

^{1}HNMR (300 MHz, CDCl$_3$): δ= 7.98(d, 1H, J=7.73Hz), 7.79(t, 1H, J=7.76, 7.76Hz), 7.48 (d, 1H, J=7.78Hz), 5.51(s, 1H), 4.48-4.58(m,2H), 4.40-4.48(m,2H), 1.44(s, 9H), 1.34-1.42(m,3H)

^{13}C NMR (75 MHz, CDCl$_3$): δ= 165.01, 158.55, 155.95, 147.68, 137.62, 125.05, 123.65, 79.65, 61.88, 45.85, 28.35, 14.26

HRMS: 281.1505[M + H][+], calculated 281.1501[M + H][+]

7.2.5 Synthesis of methyl 6-(2-(tert-butoxycarbonylamino) ethyl) picolinate 23

To a solution of methyl 6-(cyanomethyl) picolinate **20** (0.75g, 4.3mmol) in 54 ml MeOH was added Boc$_2$O (1.858g, 8.5mmol) and catalytic amounts of Raney nickel. The reaction mixture was degased with argon and stirred under 1 atm H$_2$ at room temperature for 24 h, filtered through celite and concentrated *in vacuo*. The mixture was purified by flash chromatography with EtOAc: DCM 1:2.

TLC [EtOAc: DCM 1:2]: R$_f$ = 0.54

Yield: 860mg, 3.1mmol (76%)

^{1}HNMR (300 MHz, CDCl$_3$) δ= 7.90(dd, 1H, J=1.01,7.75Hz), 7.69(t, 1H, J=7.75, 7.75Hz), 7.31(d, 1H, J=7.73Hz), 3.92 (s, 3H), 3.48 (d, 2H, J=5.89Hz), 3.01(t, 2H, J=6.64, 6.64Hz), 1.34(s, 9H)

^{13}C NMR (300 MHz, CDCl$_3$) δ= 165.71, 159.92, 155.87, 147.51, 137.29, 126.70, 122.92, 78.97, 52.71, 39.90, 37.79, 28.31

HRMS : m/z: found 281.1457[M + H][+], 303.1287 [M + Na][+], calculated 281.1501[M + H][+]

7.2.6 Synthesis of ethyl 6-((tert-butoxycarbonylamino) methyl)piperidine-2-carboxylate 14

To a solution of ethyl 6-((tert-butoxycarbonylamino)methyl)picolinate **13** (8.74g, 31.2mmol) in 150 ml AcOH was added catalytic amounts of PtO$_2$ and degassed with argon in a hydrogenation reactor (Roth). The reaction was stirred at room

temperature under H_2 (40bar) for 3 days. **13** was not fully converted. The reaction mixture was filtered through celite, concentrated *in vacuo* and purified by flash chromatography with EtOAc. The retrieval of **13** was used with the same procedure until 100% converted.

TLC [EtOAc]: R_f = 0.38

Yield: 4.35g, 15.2mmol (49%)

^{1}HNMR (600 MHz, CDCl$_3$) δ= 5.07(s, 1H), 4.14-4.2(m, 2H),3.33(dd, 1H, J=2.83, 11.52 Hz), 3.23-3.35(m, 1H), 2.90-3.05(m, 1H), 2.66-2.70(m, 1H), 1.97-2.05(m, 3H), 1.86-1.92(m, 1H), 1.59-1.65(m, 1H), 1.4-1.48(m, 10H), 1.32-1.4(m, 1H), 1.03-1.12(m, 1H).

^{13}C NMR (300 MHz, CDCl$_3$) δ= 175.00, 156.25, 79.3, (60.92, 60.97), (58.7, 58.75), 55.68, 46, (29.06,29.1), (28.96,29.01), (28.37,28.41), 23.92, (14.13,14.17)

MS (ESI) m/z: found 287.2 [M + H] $^+$, calculated 287.20[M + H] $^+$

7.2.7 Synthesis of methyl 6-(2-(tert-butoxycarbonylamino) ethyl) piperidine-2-carboxylate 24 diastereomeric mixture

To a solution of methyl 6-(2-(tert-butoxycarbonylamino) ethyl) picolinate **23** (644mg, 2.3mmol) in 33 ml AcOH was added catalytic amounts of PtO$_2$ and degassed with argon in a hydrogenation reactor (Roth). The reaction was stirred at room temperature under H_2 (50bar) for 2 days, filtered through celite, concentrated *in vacuo* and purified by flash chromatography with EtOAc.

TLC [EtOAc]: R_f = 0.31

Yield: 646mg, 2.3mmol (98 %)

^{1}HNMR (300 MHz, CDCl$_3$) δ= 4.81-4.95 (m, 1H), 3.66 (s, 3H), 3.25-3.42(m, 1H),3.05-3.25 (m, 2H), 2.85-3.00 (m, 1H), 2.48-2.60 (m, 1H), 1.95-2.05(m, 1H), 1.85-1.95(m, 1H), 1.45-1.65(m, 3H), 1.38 (s, 9H),1.15-1.38(m, 2H),0.95-1.1(m, 1H)

^{13}C NMR (300 MHz, CDCl$_3$) δ= 173.46, 156.03, 78.98, 59.08, 54.12, 51.86, 37.48, 37.01, 31.73, 29.15, 28.34, 24.28

HRMS : m/z: found 287.1876 [M + H] $^+$, calculated 287.1971[M + H] $^+$

7.2.8 Synthesis of 1-benzyl 2-ethyl 6-((tert-butoxycarbonylamino) methyl) piperidine-1,2-dicarboxylate 15

To a solution of ethyl 6-((tert-butoxycarbonylamino)methyl)piperidine-2-carboxylate **14** (4.35g, 15.2mmol) in 50 ml DCM at 0°C was added dropwisely benzyl chloroformate (3.89g, 22.8mmol) followed by addition of N,N-diisopropylethylamine (7.85g, 60.8mmol). Atfer stirring at room temperature for 5 h, a saturated NH$_4$Cl solution (20 ml) was added. The mixture was extracted with DCM (4 x 20 ml). The organic layers were dried over MgSO$_4$, concentrated *in vacuo* and purified by flash chromatography with hexane: EtOAc 3:1

TLC [Hexane :EtOAc 3:1]: R$_f$ = 0.26

Yield: 6.14g, 14.6mmol (96%)

^{1}HNMR (300 MHz, CDCl$_3$) δ= 7.25-7.4(m, 5H), 5.2-5.4(m, 1H), 5.0-5.1(m, 1H), 4.7-5-0(m, 1H), 4.36-4.52(m, 1H), 4.06-4.3(m, 1H), 3.3-3.5(m, 1H), 2.9-3.14(m, 1H), 2.18-2.35(m, 1H), 1.5-1.8(m, 6H), 1.3-1.5(m, 10H), 1.1-1.3(m, 3H)

^{13}C NMR (300 MHz, CDCl$_3$) δ=173.4, 157.1, 156.4, 136.79, 128.68, 128.17, 127.96, 79.14, 67.8, 61.80, 53.4, 50.54, 42.58, 28.69, 26.26, 16.53, 14.33

MS (ESI) m/z: found 421.22[M + H] $^+$, calculated 421.23[M + H] $^+$

HRMS : m/z: found 421.2333 [M + H] $^+$, calculated 421.2339 [M + H] $^+$

7.2.9 Synthesis of 1-benzyl 2-methyl 6-(2-(tert-butoxycarbonylamino) ethyl) piperidine-1, 2-dicarboxylate 25

To a solution of methyl 6-(2-(tert-butoxycarbonylamino)ethyl)piperidine-2-carboxylate **24** (646mg, 2.3mmol) in 7 ml DCM at 0°C was added dropwisely benzyl chloroformate (578mg, 3.4mmol) followed by addition of N,N-diisopropylethylamine (1167mg, 9mmol). After stirring at room temperature for 6 h, a saturated NH$_4$Cl solution (20 ml) was added and extracted with DCM (4 x 20 ml). The organic layers were dried over MgSO$_4$, concentrated *in vacuo* and purified by flash chromatography with hexane: EtOAc 2:1

TLC [Hexane :EtOAc 2:1]: R$_f$ = 0.46

Yield: 812mg,1.9mmol (86%)

^{1}HNMR (300 MHz, CDCl$_3$) δ= 7.28-7.42(m, 5H), 5.02-5.26(m, 2H), 4.78-5.01(m,0.5H), 4.66-4.70(m,0.5H), 4.20-4.44(m,1H), 3.55-3.73(m,3H), 2.85-3.45(m,2H), 2.19-2.34(m,1H), 1.45-1.75(m,7H), 1.42(s,9H)

^{13}C NMR (75 MHz, CDCl$_3$) δ=172.89, 156.45, 156.05, 136.40, 128.50, 128.45, 128.10, 127.51, 126.92, 78.85, 67.55, 52.45, 52.08, 48.40, 37.50, 33.27, 28.70, 28.44, 25.84, 15.88

HRMS : m/z: found 421.2437 [M + H] $^+$, calculated 421.2339 [M + H] $^+$

7.2.10 Synthesis of benzyl 2-oxo-3,9-diazabicyclo[3.3.1]nonane-9-carboxylate 17

Step 1: 1-Benzyl 2-ethyl 6-((tert-butoxycarbonylamino)methyl)piperidine-1,2-dicarboxylate **15** (6.11g, 15mmol) in 50% TFA in DCM was stirred at room temperature for 1 h and then concentrated *in vacuo*. DCM was added and evaporated for 3 times to remove the TFA. The produced **16** was used for the next step without further purification.

Step 2: The crude product from step 1 in 300 ml pyridine was heated under reflux for 2 h. The mixture was concentrated *in vacuo* and purified by flash chromatography with EtOAc.

TLC [EtOAc]: R$_f$ = 0.23

Yield: 3.14g, 11.4mmol (76%)

^{1}HNMR (600 MHz, CDCl$_3$) δ= 7.28-7.42(m, 5H), 5.05-5.2(m, 2H), 4.63-4.77(m, 1H), 4.43-4.57(m, 1H), 3.63-3.77(m, 1H), 3.15-3.24(m, 1H), 1.89-1.99(m, 1H), 1.66-1.89(m, 5H)

^{13}C NMR (150 MHz, CDCl$_3$) δ=171.41, 154.19, 136.31, 128.77, 128.42, 128.15, 67.79, (54.18, 53.47), (45.94, 45.59), (44.98, 44.13), (30.59, 30.20), (27.84, 27.43), 18.12

HRMS : m/z: found 275.1390 [M + H] $^+$, calculated 275.1396 [M + H] $^+$

7.2.11 Synthesis of benzyl 2-oxo-3, 10-diazabicyclo [4.3.1] decane-10-carboxylate 27

Step 1: 1-Benzyl 2-methyl 6-(2-(tert-butoxycarbonylamino)ethyl)piperidine-1,2-dicarboxylate **25** (3.6g, 8.6mmol) in 360 ml 50% TFA in DCM was stirring at room temperature for 1 hour and then concentrated *in vacuo*. DCM was added and evaporated for three times to remove the TFA. The produced **26** was used for the next step without further purification.

TLC [10 %MeOH in CHCl$_3$]: R$_f$ = 0.31

Step 2: The crude product from step 1 was dissolved in 150 ml pyridine and heated under reflux for overnight. The reaction mixture was concentrated *in vacuo* followed by purification by flash chromatography with EtOAc.

TLC [EtOAc]: R$_f$ = 0.26

Yield: 840mg, 2.9mmol (33 %)

^{1}H-NMR (300 MHz, CDCl$_3$): δ= = 7.28-7.38(m, 5H), 6.52-6.74 (m, 1H), 5.12-5.24(m, 2H), 4.96-5.18 (m, 1H), 4.6-4.74(m, 1H), 3.14-3.22(m,1H), 2.88-2.96(m, 1H), 2.24-2.36 (m, 1H), 2.12-2.24(m, 1H), 1.88-1.96(m, 1H), 1.56-1.76(m, 4H), 1.48-1.56(m, 1H).

^{13}C-NMR (150 MHz, CDCl$_3$): δ= = 175.24, (156.0, 155.92), (136.37, 136.30), (128.58, 128.52), 128.23, 128.12, 127.00, 127.80, 67.63, (55.51, 55.28), (46.89, 46.44), (39.28, 39.26), (33.02, 32.88), (29.24, 28.91), (28.10, 27.92), (15.32, 15.26)

MS (ESI) m/z: found 289.15 [M + H] $^+$, calculated 289.12

HRMS : m/z: found 289.1546 [M + H] $^+$, calculated 289.1552 [M + H] $^+$

7.2.12 Synthesis of 4-(2-bromoethoxy)-1, 2-dimethoxybenzene 28a

28a was prepared as described. [196]

7.2.13 Synthesis of benzyl 3-(2-(3,4-dimethoxyphenoxy)ethyl)-2-oxo-3,9-diazabicyclo[3.3.1]nonane-9-carboxylate 29a

To a solution of benzyl 2-oxo-3,9-diazabicyclo[3.3.1]nonane-9-carboxylate **17** (100mg, 0.4mmol) in 2 ml dry THF under argon at 0°C was added NaH (26mg, 0.9mmol). After stirring for 15 min, **28a** (238mg, 0.9mmol) was added and stirred at

room temperature for 5 days. The reaction mixture was concentrated *in vacuo*, acidified with 10% HCl solution (5 ml) and extracted with DCM (4 x 10 ml). The organic phases were dried over $MgSO_4$, concentrated *in vacuo* and purified by flash chromatography with hexane :EtOAc 2:1

TLC [Hexane :EtOAc 1:2]: R_f = 0.31

Yield: 104mg, 0.2mmol (63%)

^{1}HNMR (300 MHz, $CDCl_3$) δ= 7.3-7.42(m, 5H), 6.74-6.8(m, 1H), 4.45-4.50(m, 1H), 4.34-4.42(m, 1H), 5.07-5.2(m, 2H), 4.42-4.82(m, 2H), 4.05-4.25(m, 2H), 3.9-4.05(m, 1H), 3.77-3.9(m, 7H), 3.38-3.62(m, 2H), 1.92-2.04 (m, 1H), 1.78-1.92 (m, 1H), 1.6-1.78 (m, 4H)

^{13}C NMR (75 MHz, $CDCl_3$) δ=168.6, 154.2, 153.21, 150.14, 144.01, 136.3, 128.77, 128.41, 128.18, 112.21, 104.20, 100.73, 67.71, 66.95, 56.68, 56.11, 54.5, 53.10, 46.79, 45.4, 30.4, 28.2, 18.50

HRMS : m/z: found 455.2176[M + H] $^+$,calculated 455.2182 [M + H] $^+$

7.2.14 Synthesis of benzyl 3-ethyl-2-oxo-3,9-diazabicyclo [3.3.1]nonane-9-carboxylate 29b

To a solution of benzyl 2-oxo-3,9-diazabicyclo[3.3.1]nonane-9-carboxylate **17** (500mg, 1.8mmol) in 15 ml dry THF under argon at 0°C was added NaH (109mg, 2.7mmol). After stirring for 15 min, ethyl iodide (421mg, 2.7mmol) was added and stirred at room temperature. The reaction was checked by TLC until **17** was fully converted. The mixture was purified by flash chromatography with 4% MeOH in $CHCl_3$

TLC [5% MeOH in $CHCl_3$]: R_f = 0.56

Yield: 538mg, 1.8mmol (95%)

^{1}HNMR (300 MHz, $CDCl_3$) δ= 7.25-7.45(m, 5H), 5.03-5.23(m, 2H), 4.65-4.77(m, 1H), 4.45-4.65(m, 1H), 3.55-3.78(m, 2H), 3.05-3.33(m, 2H),1.95-2.07(m, 1H), 1.55-1.90(m, 5H), 1.13-1.23(t, 3H,J=7.18, 7.18Hz)

HRMS : m/z: found 303.1703[M + H] $^+$,calculated 303.1709 [M + H] $^+$

7.2.15 Synthesis of 3-ethyl-3,9-diazabicyclo[3.3.1]nonan-2-one __31b__

To a solution of benzyl 3-ethyl-2-oxo-3,9-diazabicyclo[3.3.1]nonane-9-carboxylate __29b__ (100mg, 0.3mmol) in 1 ml anhydrous MeOH was added catalytic amounts of Palladium on carbon followed by degassing with H_2. After stirring under 1 atm H_2 at room temperature for 2 h, the reaction mixture was filtered through celite and concentrated *in vacuo*. A 20% HCl solution (5 ml) was added and extracted with DCM (4 x 10 ml). The aqueous layer was basified with saturated $NaHCO_3$ solution and extracted with DCM (4 x 10 ml). The organic layer was concentrated and used for the next step without further purification.

TLC [5% MeOH in $CHCl_3$]: R_f = 0.37

Yield: 45mg, 0.3mmol (81%)

^{1}HNMR (300 MHz, $CDCl_3$) δ= 3.6-3.73 (m, 2H), 3.53-3.57 (m, 1H), 3.35-3.43 (m, 1H), 3.22-3.35 (m, 1H), 3.13-3.21 (m, 1H), 1.55-2.03 (m, 6H), 1.15-1.23 (t, 3H, J=7.19, 7.19Hz)

^{13}C NMR (75 MHz, $CDCl_3$) δ=170.96, 54.63, 51.52, 46.06, 41.34, 32.17, 29.27, 18.51, 12.28

HRMS : m/z: found 169.1333[M + H]$^+$, calculated 169.1314 [M + H]$^+$

7.2.16 Synthesis of 1-(3-ethyl-2-oxo-3,9-diazabicyclo[3.3.1]nonan-9-yl)-2-(3,4,5-trimethoxyphenyl)ethane-1,2-dione __4c__

2-Oxo-2-(3, 4, 5-trimethoxyphenyl) acetic acid __33a__ (42mg, 0.2mmol) in 1 ml DMF was treated with oxalyl chloride (47mg, 0.5mmol) and stirred at 0°C for 3 h. The reaction mixture was first concentrated *in vacuo* and then dissolved in 1 ml DCM followed by addition of 3-ethyl-3,9-diazabicyclo[3.3.1]nonan-2-one __31b__ (30mg, 0.2mmol), DIPEA (28mg, 0.2mmol) and stirred at room temperature for 1 h. The reaction was quenched with saturated NH_4Cl solution (5 ml) and extracted with DCM (4 x 10 ml). The organic layers were dried over $MgSO_4$ and concentrated *in vacuo*. The mixture was purified by flash chromatography with hexane: EtOAc 2:1.

TLC [Hexane: EtOAc]: R_f = 0.09

HPLC [0-100% Solvent B, 30 min]: R_t = 18.5 min, purity (280 nm) = 99%

Yield: 20mg, 0.05mmol (28%)

^{1}HNMR (300 MHz, CDCl$_3$) δ= 7.23(s, 1H), 7.19(s, 1H), 5.17-5.22(m, 0.5H), 5.05-5.12(m, 0.5H), 4.13-4.18(m, 0.5H), 3.98-4.06(m, 0.5H), 3.94-3.97(m, 3H), 3.88-3.93(m, 6H), 3.62-3.89(m, 1.5H), 3.21-3.42 (m, 2H), 3.13-3.17(m, 0.5H), 2.15-2.25 (m, 1H), 1.72-2.05(m, 5H), 1.16-1.24(m, 3H)

^{13}C NMR (75 MHz, CDCl$_3$) δ= (189.91, 189.62), (166.69, 166.19), (164.21, 163.62), (153.70, 153.65), (144.78, 144.72), (128.17, 128.05), (107.40, 107.29), (61.31, 61.28), 56.65, 56.60, 56.31, (51.35, 50.55), (49.75, 48.35), (41.57, 41.47), (31.60, 30.68), (29.09, 28.45), (18.31, 18.21), 12.19

HRMS : m/z: found 391.1863[M + H] $^+$,calculated 391.1869 [M + H] $^+$

7.2.17 Synthesis of benzyl 3-(2-(3, 4-dimethoxyphenoxy) ethyl)-2-oxo-3, 10-diazabicyclo [4.3.1] decane-10-carboxylate <u>30a</u>

To a solution of benzyl 2-oxo-3, 10-diazabicyclo [4.3.1] decane-10-carboxylate <u>27</u> (70mg, 0.2mmol) in 2 ml dry THF under argon at 0℃ was added NaH (9mg, 0.4mmol) and stirred for 15 min followed by addition of 4-(2-bromoethoxy)-1,2-dimethoxybenzene <u>28a</u> (158mg, 0.6mmol). The reaction was stirred at room temperature for 3 days and concentrated *in vacuo*. A 10% HCl solution (5 ml) was added and extracted with DCM (4 x 10 ml). The organic phases were dried over MgSO$_4$, concentrated *in vacuo* and purified by flash chromatography with hexane: EtOAc 1:3.

TLC [Hexane: EtOAc 1:3]: R$_f$ = 0.49

Yield: 73mg, 0.2mmol (64%)

^{1}H-NMR (600 MHz, CDCl$_3$): δ= 7.24-7.36 (m, 5H), 6.56 (t, 1H), 6.49 (m, 1H), 6.46-6.48 (m, 1H), 5.12-5.2(m, 1H), 5.0-5.1 (m, 2H), 4.55-4.65(m, 1H), 4.0-4.15(m, 2H), 3.85-3.95 (m,1H), 3.81-3.84 (m, 6H), 3.55.3.65(m, 1H), 3.49-3.54 (m, 1H), 3.21-3.27(m, 1H), 2.3-2.4 (m, 1H), 2.15.2.25(m, 1H), 1.94-2.01 (m, 1H), 1.4-1.7(m, 5H)

^{13}C-NMR (150 MHz, CDCl$_3$): δ= = 172.23, 155.96, 153.14, 149.87, 143.63, 136.32, 128.55, 128.47, 128.06, 127.90, 127.76, 111.88, 103.79, 100.38, 67.54, 67.22, 56.41, 56.17, 55.85, 51.22, 47.79, 45.85, 32.24, 28.81, 28.79, 15.29

HRMS(EI) : m/z: found 468.2261 [M] $^+$, calculated 468.2260 [M] $^+$

7.2.18 Synthesis of benzyl 3-(3,4-dimethoxyphenethyl)-2-oxo- 3,10-diazabicyclo [4.3.1]decane-10-carboxylate __30b__

To a solution of benzyl 2-oxo-3, 10-diazabicyclo [4.3.1] decane-10-carboxylate __27__ (100mg, 0.3mmol) in 2 ml dry THF under argon at 0°C was added NaH (25mg, 0.9mmol) and stirred for 15 min followed by addition of commercially available 3,4-dimethoxyphenethyl bromide __28b__ (213mg, 0.9mmol). The mixture was stirred at room temperature for 2 days and concentrated *in vacuo*. A 10% HCl solution (5 ml) was added and extracted with DCM (4 x 10 ml). The organic phases were dried over MgSO$_4$, concentrated *in vacuo* and purified by flash chromatography with hexane: EtOAc 1:2.

TLC [Hexane: EtOAc 1:2]: R$_f$ = 0.44

Yield: 39mg, 0.1mmol (25%)

^{1}H-NMR (600 MHz, CDCl$_3$): δ =7.27-7.39 (m, 5H), 6.72-6.78 (m, 3H), 5.13-5.17 (m, 2H), 5.09-5.13 (m, 0.5H), 4.99-5.05(m, 0.5H), 4.45-4.65(m, 1H), 3.8-3.9(m, 6H), 3.45-3.77(m, 4H), 3.27-3.37(m, 1H), 2.85-2.95(m, 1H), 2.70-2.85 (m,2H), 2.30-2.45 (m, 1H),2.00-2.20(m, 1H), 1.50-1.80(m, 3H), 0.86-0.94(m, 1H)

^{13}C-NMR (150 MHz, CDCl$_3$): δ= (171.81, 171.85), (155.71, 155.90), 148.90, (147.58, 147.52), 136.40, (131.58, 131.23), (128.55, 128.52), (128.17, 128.10), (127.95, 127.80), (120.74, 120.68), (112.05, 111.93), (111.19, 111.14), (67.52, 67.45), 56.17, (55.88, 55.85), 53.65, 53.20, (46.55, 46.27), (46.20, 45.73), (33.79, 33.72), (33.25, 31.90), (28.76, 28.65), (15.33, 15.24)

HRMS : m/z: found 468.2484 [M] $^+$, calculated 453.2389 [M] $^+$

7.2.19 Synthesis of 3- (2- (3, 4- dimethoxyphenoxy) ethyl) -3, 9-diazabicyclo [3.3.1]nonan-2-one __31a__

To a solution of benzyl 3-(3,4-dimethoxyphenethyl)-2-oxo-3,9-diazabicyclo[3.3.1]nonane-9-carboxylate __30a__ (104mg, 0.2mmol) in 1 ml anhydrous MeOH, catalytic amounts of palladium on carbon was added. The reaction mixture was degassed with H$_2$ and stirred at room temperature under 1 atm H$_2$ for 2 h, filterted through celite, concentrated *in vacuo* and used for the next step without further purification.

TLC [MeOH: CHCl$_3$ 1:9]: R$_f$ = 0.4

Yield: 73mg, 0.2mmol (100%)

^{1}HNMR (600 MHz, CDCl$_3$) δ= 6.80(d, 1H, J=8.75 Hz), 6.51(s, 1H), 6.39-6.44(m, 1H), 4.15-4.25(m, 2H), 3.9-4(m, 1H), 3.8-3.89(m, 7H), 3.54-3.64(m, 2H), 3.45-3.51(m, 1H), 3.35-3.43(m, 1H), 2.39(s, 1H), 1.55-2(m, 6H)

^{13}C NMR (300 MHz, CDCl$_3$) δ= 171.35, 153.08, 149.89, 143.71, 111.95, 104.02, 100.53, 66.81, 56.45, 55.9, 54.4, 54.3, 46.6, 45.9, 31.8, 28.9, 18.22

HRMS : m/z: found 321.1808[M + H] $^+$, calculated 321.1814[M + H] $^+$

7.2.20 Synthesis of 3-(2-(3, 4-dimethoxyphenoxy) ethyl)-3, 10-diazabicyclo [4.3.1] decan-2-one 32a

To a solution of benzyl 3-(2-(3, 4-dimethoxyphenoxy) ethyl)-2-oxo-3, 10-diazabicyclo [4.3.1] decane-10-carboxylate **30a** (60mg, 0.1mmol) in 1 ml anhydrous MeOH, catalytic amounts of palladium on carbon was added. The reaction mixture was degassed with H$_2$ and stirred under 1 atm H$_2$ at room temperature for 1 h, filtered through celite, concentrated *in vacuo* and used for the next step without further purification.

TLC [10% MeOH in CHCl$_3$]: R$_f$ = 0.17

Yield: 41mg, 0.1mmol (97%)

^{1}H-NMR (600 MHz, CDCl$_3$): δ= 6.76 (d, 1H), 6.50 (d, 1H), 6.40 (m, 1H), 4.08-4.15 (m, 3H), 3.85(s, 3H), 3.83 (s, 3H), 3.75-3.82(m, 3H), 3.33-3.35 (m, 1H), 3.2-3.26 (m, 1H), 2.23-2.24 (m, 1H), 1.98-2.12(m, 2H), 1.5-1.75 (m, 6H)

^{13}C-NMR (150 MHz, CDCl$_3$): δ= 172.23, 153.27, 149.85, 143.56, 111.90, 103.89, 100.48, 67.32, 57.97, 56.43, 55.86, 51.05, 47.99, 45.91, 33.79, 30.28, 29.68, 29.85.

MS (ESI) m/z: found 335.13 [M + H] $^+$, calculated 335.19[M + H] $^+$

7.2.21 Synthesis of 3-(3,4-dimethoxyphenethyl)-3,10-diazabicyclo[4.3.1]decan-2-one 32b

To a solution of benzyl 3-(3,4-dimethoxyphenethyl)-2-oxo-3,10-diazabicyclo[4.3.1]decane-10-carboxylate **30b** (10mg, 0.02mmol) in 1 ml anhydrous

MeOH, catalytic amounts of palladium on carbon was added. The reaction mixture was degassed with H_2 and stirred under 1 atm H_2 at room temperature for 1 h, filtered through celite, concentrated *in vacuo* and used for the next step without further purification.

TLC [10% MeOH in $CHCl_3$]: R_f = 0.51

Yield: 5mg, 0.02mmol (71%)

MS (ESI) m/z: found 319.42 [M + H][+], calculated 319.20[M + H][+]

7.2.22 Synthesis of 2-oxo-2-(3, 4, 5-trimethoxyphenyl) acetic acid <u>33a</u>

1-(3,4,5-Trimethoxyphenyl)ethanone (2.93g, 13.9mmol) and selenium dioxide (2.32g, 20.9mmol) in 60 ml pyridine were heated to 100°C for 14 h. The mixture was filterted through celite, concentrated *in vacuo* and purified by flash chromatography with hexane: EtOAc: AcOH 1:15:1.

TLC [Hexane: EtOAc: AcOH 1:15:1]: R_f = 0.14

Yield: 2.19g, 9.1mmol (65%)

^{1}HNMR (600 MHz, $CDCl_3$) δ= 3.91(s, 6H), 3.95(s, 3H),7.50 (s, 2H)

^{13}C NMR (150 MHz, $CDCl_3$) δ= 56.31, 61.03, 108.04, 127.55, 144.19, 153.06, 165.74, 186.94

HRMS(EI): m/z: found 240.0624[M][+], calculated 240.0634[M][+]

7.2.23 Synthesis of 3,3-dimethyl-2-oxopentanoic acid   <u>33b</u>

To a solution of NaOH (175mg, 4.4mmol) and $KMnO_4$ (543mg, 3.4mmol) in 5 ml water at 0°C was added 3,3-dimethyl-2-pentanone (200mg, 1.8mmol). After stirring for 1 h at 0°C and 3 days at room temperature, the reaction was acidified with concentrated HCl and extracted with DCM (4 x 10 ml). The organic phases were dried over $MgSO_4$, concentrated *in vacuo* and purified by flash chromatography with hexane: EtOAc 5:1.

TLC [Hexane: EtOAc 5:1]: R_f = 0.45

Yield: 97mg, 0.7mmol (39%)

^{1}HNMR (300 MHz, CDCl$_3$) δ=1.61(q, 2H,J=7.49,7.49,7.51Hz), 1.21(s, 6H), 0.91(t,3H, J=7.49,7.49Hz),

^{13}C NMR (150 MHz, CDCl$_3$) δ= 9.18, 24.38, 33.13, 42.49, 185.25

7.2.24 Synthesis of 1-(3-(2-(3,4-dimethoxyphenoxy)eth.yl)-2-oxo-3,9-diazabicyclo [3.3.1]nonan-9-yl)-2-(3,4,5-trimethoxyphenyl)ethane-1,2-dione 4a

3-(2-(3,4-Dimethoxyphenoxy)ethyl)-3,9-diazabicyclo[3.3.1]nonan-2-one **31a** (35mg, 0.1mmol) in 6 ml DCM was treated sequentially with 2-oxo-2-(3, 4, 5-trimethoxyphenyl) acetic acid **33a** (29mg, 0.1mmol), EDC-HCl (20mg, 0.1mmol), HOBt (18mg, 0.1mmol), TEA (13mg, 0.1mmol) at room temperature and stirred overnight. The reaction was quenched with saturated NH$_4$Cl solution (5 ml) and extracted with DCM (4 x 10 ml). The organic layers were dried over MgSO$_4$ and concentrated *in vacuo*. The mixture was purified by flash chromatography with EtOAc.

TLC [EtOAc]: R$_f$ = 0.54

HPLC [0-100% Solvent B, 30 min]: R$_t$ = 21.5 min, purity (280 nm) = 99%

Yield: 14mg, 0.03mmol (24%)

^{1}HNMR (600 MHz, CDCl$_3$) δ= 7.19(d, 2H, J=22.63), 6.72-6.8(m, 1H), 6.42-6.48(m, 1H), 6.34-6.39(m, 1H), 5.22(s, 0.5H), 5.07(s, 0.5H), 4.17-4.27(m, 1.5H), 4.08-4.16(m, 1.5H), 4.04-4.07(m, 0.5H), 3.97-4.04(m, 1.5H), 3.94(d, 3H, J=7.39), 3.79-3.92(m, 12H), 3.62-3.65(m, 0.5H), 3.47-3.56(m, 1.5H), 2.13-2.18(m, 0.5H), 1.93-2.02(m, 1.5H), 1.79-1.9(m, 2H), 1.7-1.78(m, 2H)

^{13}C NMR (300 MHz, CDCl$_3$) δ= (189.57, 189.30), (167.24, 166.73), (163.90, 163.38), 153.43, 153.39, (152.77, 152.76), (149.92, 149.90), (144.48, 144.46), (143.88, 143.85), (127.86, 127.74), (111.87, 111.85), (107.09, 107.00), (103.94, 103.85), (100.36, 100.35), (66.81, 66.80), (61.07, 61.04), 60.38, (56.39, 56.36), (56.29,56.14), (55.89, 55.86), (53.39, 52.68), 51.17, 49.36, (46.71, 46.55), 42.84, (31.35, 30.49), (28.95, 28.30), (18.03, 17.92)

HRMS(EI) : m/z: found 542.2264 [M] [+], calculated 542.2264 [M] [+]

7.2.25 Synthesis of 1-(3-(2-(3,4-dimethoxyphenoxy)ethyl)-2-oxo-3,9-diazabicyclo[3.3.1]nonan-9-yl)-3,3-dimethylpentane-1,2-dione __4b__

3-(2-(3,4-Dimethoxyphenoxy)ethyl)-3,9-diazabicyclo[3.3.1]nonan-2-one __31a__ (20mg, 0.06mmol) in 3 ml DCM was treated sequentially with 3,3-dimethyl-2-oxopentanoic acid __33b__ (18mg, 0.13mmol), EDC-HCl (23mg, 0.13mmol), HOBt (17mg, 0.13mmol), TEA (8mg, 0.08mmol) at room temperature and stirred overnight. The reaction was quenched with saturated NH_4Cl solution (5 ml) and extracted with DCM (4 x 10 ml). The organic layers were dried over $MgSO_4$ and concentrated *in vacuo*. The mixture was purified by flash chromatography with EtOAc.

TLC [EtOAc]: R_f = 0.6

HPLC [0-100% Solvent B, 16 min]: R_t = 14.9 min, purity (280 nm) = 98%

Yield: 21mg, 0.05mmol (76%)

^{1}HNMR (600 MHz, CDCl$_3$) δ= 6.74 (d, 1H, J=8.76 Hz), 6.44(t, 1H, J=2.86, 2.86 Hz), 6.35(dt, 1H, J=2.95, 2.95, 8.74Hz), 5.04 (s, 0.5H), 4.89(s, 0.5H), 4.16(ddd, 2H, J=6.88, 11.94, 14.20Hz), 3.85-4.03(m, 2.5H), 3.83(d, 3H, J=2.67Hz), 3.80(s, 3H), 3.69-3.75(m, 1H), 3.56-3.63(m, 0.5H), 3.46-3.54(m, 1H),1.95-2.1(m, 1H), 1.75-1.9(m, 3H), 1.65-1.57(m, 4H), 1.16-1.26(m, 3H), 1.11(d, 3H, J=5.56 Hz), 0.78-0.88(m, 3H)

^{13}C NMR (300 MHz, CDCl$_3$) δ= (207.03, 206.85), (167.30, 166.9), (164.44, 163.63), (152.85, 152.84), 149.88, 143.81, (111.92, 111.87), (103.99, 103.83), (100.43, 100.42), (67.92, 25.57), (66.82, 66.59), (56.39, 56.09), (55.86, 55.83), (53.36, 52.50), (50.76, 42.32), (48.16, 46.47), (46.71, 46.64), (32.40, 32.32), (31.26, 27.96), (30.19, 28.51), (23.63, 23.37), (23.33, 22.84), (18.00, 17.94), (8.84, 8.71)

HRMS : m/z: found 446.2413[M + H], calculated 446.2417[M + H] $^+$

7.2.26 Synthesis of 1-(3-(2-(3,4-dimethoxyphenoxy)ethyl)-2-oxo-3,10-diazabicyclo [4.3.1]decan-10-yl)-3,3-dimethylpentane-1,2-dione __5b__

To a solution of 3-(2-(3, 4-dimethoxyphenoxy) ethyl)-3, 10-diazabicyclo [4.3.1] decan-2-one __32a__ (22mg, 0.06mmol) in 3 ml DCM was added sequentially 3,3-dimethyl-2-oxopentanoic acid __33b__ (19mg, 0.1mmol), EDC-HCl (25mg, 0.1mmol), HOBt (17mg, 0.1mmol), TEA (8mg, 0.08mmol) at room temperature and stirred overnight. The reaction was quenched with saturated NH_4Cl solution (5 ml), extracted with DCM (4 x

10 ml). The organic layers were dried over $MgSO_4$ and concentrated *in vacuo*. The reaction mixture was purified by flash chromatography with EtOAc.

TLC [EtOAc]: R_f = 0.69

HPLC [0-100% Solvent B, 16 min]: R_t = 10.2 min, purity (280 nm) = 98%

Yield: 18mg, 0.04mmol (60%)

^{1}H-NMR (600 MHz, $CDCl_3$): δ= 6.77(d, J=8.75) 1H, 6.47-6.5(m,1H), 6.37-6.4(m, 1H), 5.36-5.38 (m, 0.5H), 4.88-4.94 (m, 0.5H), 4.14-4.17(m, 1H), 4.09-4.14(m, 1H), 4.01-4.07(m, 1.5H), 3.96-4.01 (m, 0.5H), 3.92-3.955 (m, 0.5H), 3.85-3.88 (m, 0.3H), 3.85(s, 3H), 3.832-3.84(m, 0.2H), 3.83(d, J=1.69, 3H), 3.77-3.81(m, 0.5H), 3.66-3.77(m, 1.5H), 3.56-3.62(m, 0.5H), 3.28-3.35(m, 1H), 2.44-2.50(m, 1H), 2.36-2.42(m, 1H), 2.27-2.34(m, 1H), 2.16-2.23(m, 1H), 1.99-2.08(m, 1H), 1.78-1.86(m, 1H), 1.52-1.74(m, 6H), 1.24(s, 1.5H), 1.12-1.19(m, 4.5H), 0.82-0.91(m, 3H)

^{13}C-NMR (150 MHz, $CDCl_3$): δ= (208.39, 207.54), (170.67, 170.39), (167.50, 166.19), (153.11, 153.06), 149.85, (143.68, 143.65), (111.92, 111.85), (103.95, 103.90), (100.53, 100.47), (67.20, 67.17), (58.59, 49.40) (56.41, 56.40), 55.85, (52.74, 43.06), (51.32, 51.13), (47.73, 47.39), (46.71, 46.52), (32.57, 31.90), (32.54, 32.53), (30.02, 28.72), (29.25, 29.11), (24.11, 23.39), (23.05, 22.7), (15.81, 15.67), (8.74,8.73)

HRMS(EI) : m/z: found 460.2571 [M] $^+$, calculated 460.2573 [M] $^+$

7.2.27 Synthesis of 1-(3-(3,4-dimethoxyphenethyl)-2-oxo-3,10-diazabicyclo [4.3.1]decan-10-yl)-2-(3,4,5-trimethoxyphenyl)ethane-1,2-dione **5d**

To a solution of 3-(3,4-dimethoxyphenethyl)-3,10-diazabicyclo[4.3.1]decan-2-one **32b** (27mg, 0.09mmol) in 3 ml DCM were added sequentially 2-oxo-2-(3, 4, 5-trimethoxyphenyl) acetic acid **33a** (23mg, 0.1mmol), EDC-HCl (20mg, 0.1mmol), HOBt (14mg, 0.1mmol) and TEA (10mg, 0.1mmol) at room temperature followed by stirring overnight. The reaction was quenched with saturated NH_4Cl solution (5 ml) and extracted with DCM (4 x 10 ml). The organic layers were dried over $MgSO_4$ and concentrated *in vacuo*. The reaction mixture was purified by flash chromatography with EtOAc.

TLC [EtOAc]: R_f = 0.42

HPLC [0-100% Solvent B, 16 min]: R_t = 14.4 min, purity (280 nm) = 99%

Yield: 35mg, 0.07mmol (75%)

^{1}H-NMR (600 MHz, CDCl$_3$): δ= 7.17(d, 2H ,J=2.09), 6.74-6.82 (m, 5H), 4.27-4.30(m, 1H), 3.94(d, 3H, J=4.9), 3.90(d, 6H, J=3.27), 3.87(d, 3H, J=2.64), 3.85(d, 3H, J=2.45), 3.80-3.84(m, 1H), 3.66-3.78 (m, 2H), 3.54-3.66 (m, 1H), 2.96-3.03 (m, 1H), 2.78-2.87 (m, 2H), 2.50-2.58 (m, 1H), 2.32-2.38 (m, 1H), 2.23-2.31 (m, 1H), 2.05-2.12 (m, 1H), 1.77-1.91 (m, 2H), 1.69-1.76 (m, 1H), 1.51-1.59 (m, 1H)

^{13}C NMR (150 MHz, CDCl$_3$):δ= (190.59, 190.23), 171.11, (170.02, 169.72), (166.95, 165.85), (155.48, 153.44), (148.95, 148.91), (147.63, 147.61), (144.44, 144.38), (131.40, 131.30), (127.99, 127.81), (120.78, 120.77), (112.05, 111.97), (111.33, 111.28), (106.94, 106.78), (61.06, 61.05), 58.71, (56.38, 56.35), (55.92, 55.89), (55.86, 55.85), (53.63, 53.35), 53.05, 49.61, (46.38, 46.26), 43.15, (33.89, 33.75), (33.25, 32.06), 30.15, (29.65, 29.45), (29.2, 28.95), 21.03, (15.78, 15.58), 14.18

MS (ESI) m/z: found 541.27 [M + H] $^{+}$, calculated 541,25

HRMS(EI) : m/z: found 540.2479 [M] $^{+}$, calculated 540.2472 [M] $^{+}$

7.2.28 Synthesis of 1-(3-(2-(3,4-dimethoxyphenoxy)ethyl)-2-oxo-3,10-diazabicyclo [4.3.1]decan-10-yl)-2-(3,4,5-trimethoxyphenyl)ethane-1,2-dione **5a**

3-(2-(3,4-Dimethoxyphenoxy) ethyl)-3,10-diazabicyclo [4.3.1] decan-2-one **32a** (20mg, 0.06mmol) in 3 ml DCM were treated sequentially with 2-oxo-2-(3, 4, 5-trimethoxyphenyl) acetic acid **33a** (16mg, 0.07mmol), EDC-HCl (14mg, 0.07mmol), HOBt (10mg, 0.07mmol) and TEA (7mg, 0.07mmol) at room temperature followed by stirring for 6 h. The reaction was quenched with saturated NH$_4$Cl solution (5 ml) and extracted with DCM (4 x 10 ml). The organic layers were dried over MgSO$_4$ and concentrated *in vacuo*. The reaction mixture was purification by flash chromatography with EtOAc.

TLC [EtOAc]: R$_f$ = 0.23

HPLC [0-100% Solvent B, 30 min]: R$_t$ = 23.2 min, purity (280 nm) = 98%

Yield: 22mg, 0.04mmol (67%)

^{1}H-NMR (600 MHz, CDCl$_3$): δ= 7.2(d, 2H, J=3.95), 6.78-6.82 (m, 1H), 6.51-6.55 (m, 1H), 6.4-6.46 (m, 1H), 5.59(s, 0.5H), 5.12(s, 0.5H), 4.0-4.36 (m, 5H), 3.97 (d, 3H,

J=2.62), 3.92 (d, 6H, J=2.23), 3.88(d, 3H, J=2.67), 3.86(d, 3H, J=2.02), 3.6-3.7(m, 1H), 3.36-3.46 (m, 1H), 2.4-2.6 (m, 2H), 1.5-1.8 (m, 6H)

^{13}C-NMR (150 MHz, CDCl$_3$): δ=(190.62, 190.22), (170.56, 170.30), 167.04, 165.98, (153.54, 153.49), (153.14, 153.13), 149.95, (144.51, 144.48), (143.80, 143.77), (128.04, 127.86), (112.02, 111.99), 107.01, 106.88, (104.15, 104.09), (100.65, 100.55), (67.33, 67.29), (61.09, 61.07), 58.68, 56.46, 56.45, 56.39, 55.91, 53.09, (51.27, 51.23), 49.81, (47.58, 43.38), (29.7, 29.66), 29.47, 29.03

HRMS(EI) : m/z: found 556.2417 [M] $^+$, calculated 556.2421 [M] $^+$

7.2.29 Synthesis of 1-(3-(2-(3,4-dimethoxyphenoxy)ethyl)-2-oxo-3,10-diazabicyclo [4.3.1]decan-10-yl)-2-((1S)-2-ethyl-1-hydroxycyclohexyl)ethane-1,2-dione 5c

2-((1S,2R)-2-Ethyl-1-hydroxycyclohexyl)-2-oxoacetic acid (25mg, 0.1mmol)[196] in 3 ml DCM was treated sequentially with HATU (55mg, 0.1mmol), TEA (15mg, 0.1mmol), and 3-(2-(3,4-dimethoxyphenoxy)ethyl)-3,10-diazabicyclo[4.3.1]decan-2-one **32a** (40mg, 0.1mmol) at room temperature followed by stirring overnight. The reaction was quenched with saturated NH$_4$Cl solution (5 ml) and extracted with DCM (4 x 10 ml). The organic layers were dried over MgSO$_4$ and concentrated *in vacuo*. The mixture was purified by preparative TLC in EtOAc.

TLC [EtOAc]: R$_f$ = 0.63

HPLC [0-100% Solvent B, 30 min]: R$_t$ = 23.2 min, purity (280 nm) = 98%

Yield: 14mg, 0.03mmol (23%)

^{1}HNMR (600 MHz, CDCl$_3$) δ= 6.78-6.84(m, 1H), 6.52-6.56(m, 1H), 6.38-6.44(m, 1H), 5-5.06(m, 1H), 4.68-6.76(m, 0.5H), 4.05-4.13(m, 0.5H), 3.93-4.03(m, 2H), 3.74-3.84(m, 2H), 3.64-3.74(m, 6H), 3.46-3.64(m, 2H), 3.2-3.3(m, 2H), 2.05-2.3(m, 2H), 1.75-1.95(m, 1H), 1.35-1.7(m, 9H), 1.05-1.3(m, 4H), 0.78-0.86(m, 1H), 0.65-0.85(m, 3H)

^{13}C NMR (100 MHz, CDCl$_3$) δ= (209.75, 209.20, 208.90, 208.75), (170.27, 170.25, 169.95, 169.75), (168.00, 167.95, 167.70, 167.30), (153.30, 153.27, 153.25), (150.15, 150.13), (143.71,143.67), (113.33, 113.27), (104.80, 104.77, 104.65), (101.28, 101.26, 101.24, 101.16), (81.66, 81.26, 81.19, 81.17), (66.37, 66.30, 66.26, 66.18), 58.13, 56.54, 55.90, (52.80, 52.66), (50.18, 50.12, 50.08, 50.02), (49.15,

49.25), (46.82, 46.65, 46.48, 46.35), (43.90, 43.50, 43.46, 43.37), (32.20, 32.05, 31.95, 31.80), (29.45, 29.40, 29.30, 29.25), (29.23, 29.17, 29.15, 29.13), (28.85, 28.83, 28.73, 28.67), (25.23, 25.15, 25.07, 25.03), (23.23, 23.07, 23.03, 22.52), (20.67, 20.57, 20.50, 20.47), (15.85, 15.75, 15.65), (12.37, 12.27, 12.25, 12.23)

HRMS : m/z: found 517.3024 [M] $^+$, calculated 517.2914[M + H] $^+$

7.2.30 Synthesis of 1-tert-butyl 2-(2-(3,4-dimethoxyphenoxy)ethyl) piperidine-1,2-dicarboxylate <u>38</u>

<u>38</u> was prepared as described. [196]

7.2.31 Synthesis of 2-(3,4-dimethoxyphenoxy)ethyl piperidine-2-carboxylate <u>39</u>

1-tert-Butyl 2-(2-(3,4-dimethoxyphenoxy)ethyl) piperidine-1,2-dicarboxylate <u>38</u> (456mg, 1.1mmol) in 10 ml 20% TFA in DCM was stirred at room temperature for 2 h. The reaction mixture was concentrated *in vacuo* and used for next step without further purification .

TLC [Hexane: EtOAc: TEA 7.5:2.3:0.4]: R_f = 0.19

Yield: 344mg, 1.1mmol (100%)

^{1}H NMR (600 MHz, CDCl$_3$) δ= 6.76 (d, 1H, J= 9 Hz), 6.50 (d, 1H, J= 3 Hz), 6.35 (dd, 1H, J= 3, 9 Hz), 4.45-4.54(m, 2H), 4.11 (t, 2H, J= 4.2 Hz), 3.92 (dd, 1H, J= 3.6, 11.4 Hz), 3.83 (s, 3H), 3.82 (s, 3H), 3.55 (d, 1H, J= 12.6 Hz), 2.99-3.04 (m, 1H), 2.24-2.28 (m, 1H), 1.82-1.97 (m, 4H), 1.54-1.61 (m, 1H),

^{13}C NMR (150 MHz, CDCl$_3$) δ= 168.48, 152.71, 149.91, 143.98, 111.74, 103.94, 100.97, 65.85, 64.71, 56.83, 56.39, 55.81, 44.14, 25.60, 21.74, 21.50,

HRMS(EI): m/z: found 309.1580 [M] $^+$, calculated 309.1576 [M] $^+$

7.2.32 Synthesis of 2-(3,4-dimethoxyphenoxy)ethyl 1-(2-oxo-2-(3,4,5-trimethoxyphenyl)acetyl)piperidine-2-carboxylate <u>6a</u>

2-(3,4-Dimethoxyphenoxy)ethyl piperidine-2-carboxylate **39** (50mg, 0.2mmol) in 10 ml acetonitrile under argon was treated sequentially with DIPEA (63mg, 0.5mmol), 2-oxo-2-(3, 4, 5-trimethoxyphenyl) acetic acid **33a** (44mg, 0.2mmol) and HATU (58mg, 0.2mmol). After stirring at room temperature for 3 days, it was concentrated *in vacuo* followed by addition of 5 ml H_2O and extraction with DCM (3 x 10 ml). The organic phases were dried over $MgSO_4$, concentrated *in vacuo* and purified by flash chromatography with hexane: EtOAc 3:1

TLC [Hexane: EtOAc 1:1]: R_f = 0.32

HPLC [0-100% Solvent B, 16 min]: R_t = 15.5 min, purity (280 nm) = 99%

Yield: 36mg, 0.07mmol (42%)

^{1}HNMR (300 MHz, $CDCl_3$) δ= 7.33-7.39(m,1.5H), 7.21-7.23(m, 0.5H), 6.73-6.8(m, 1H), 6.46-6.54(m, 1H), 6.3-6.43(m, 1H), 5.41-5.46(m, 1H), 4.5-4.65(m, 2H), 4.1-4.2(m, 2H), 3.94(d, 9H, J=1.96Hz), 3.84(d, 6H, J=2.16 Hz),3.22-3.54(m, 2H),2.2-2.44(m, 2H), 1.73-1.88(m, 2H), 1.51-1.69(m, 2H)

^{13}C NMR (300 MHz, $CDCl_3$) δ= (190.83, 190.34), (170.44, 170.19), (167.89, 166.87), (153.54, 153.27), (152.92, 152.78), (149.96, 149.92), (144.01, 143.99), (128.11, 128.01), (111.78, 111.76), 107.25, 107.00, (104.05, 104.0), (101.16, 101.08), (66.34, 66.27), (63.80, 63.78), (60.98, 60.35), 56.43, 56.41, 56.31, 55.87, 51.75, 44.26, 26.31, 24.75, (21.16, 21.02)

HRMS(EI) : m/z: found 531.2105 [M] $^+$, calculated 531.2104 [M] $^+$

7.2.33 Synthesis of 2-(3,4-dimethoxyphenoxy)ethyl 1-(3,5-dichlorophenylsulfonyl)piperidine-2-carboxylate 6e

2-(3,4-Dimethoxyphenoxy)ethyl piperidine-2-carboxylate **39** (50mg, 0.16mmol) in 1 ml DCM was treated with DIPEA (63mg, 0.49mmol) and stirred for 30min at room temperature followed by addition of 3,5-dichlorobenzene sulfony chloride **34a** (40mg, 0.16mmol). After stirring overnight at room temperature, the reaction was quenched with saturated NH_4Cl solution (5 ml), extracted with DCM (4 x 10 ml). The organic layers were dried over $MgSO_4$ and concentrated *in vacuo*. The mixture was purified with preparative TLC in cyclohexane:EtOAc 3:1.

TLC [Cyclohexane: EtOAc 3:1]: R_f = 0.57

HPLC [0-100% Solvent B, 30 min]: R_t = 27.2 min, purity (280 nm) = 99%

Yield: 17mg, 0.03mmol (20%)

^{1}HNMR (600 MHz, CDCl$_3$) δ= 7.64(d, 2H, J=1.85Hz), 7.49 (t, 1H, J=1.86, 1.86Hz), 6.76(d, 1H, J=8.76Hz), 6.48(d, 1H, J=2.8Hz), 6.34(dd, 1H, J=2.83, 8.73Hz), 4.75-4.8(m, 1H), 4.35-4.4(m, 1H), 4.25-4.3(m, 1H), 4.03-4.08(m, 1H), 3.97-4.03(m, 1H), 3.83(d, 6H, J=7.88Hz), 3.72-3.77(m, 1H), 3.16-3.24(m, 1H), 2.16-2.21(m, 1H), 1.73-1.85(m, 1H), 1.65-1.71(m, 1.8H), 1.47-1.63(m, 2H), 1.33-1.36(m, 0.5H)

^{13}C NMR (300 MHz, CDCl$_3$) δ= 170.23, 152.82, 149.92, 143.99, 142.67, 135.64, 132.29, 125.55, 111.76, 103.99, 101.06, 66.13, 63.48, 56.41, 55.85, 55.31, 42.88, 27.92, 24.73, 19.88

HRMS : m/z: found 518.1343 [M + H] $^+$, calculated 518.0807 [M + H] $^+$

7.2.34 Synthesis of 2-(3,4-dimethoxyphenoxy)ethyl 1-(benzo[d]thiazol-6-ylsulfonyl)piperidine-2-carboxylate 6f

2-(3,4-Dimethoxyphenoxy)ethyl piperidine-2-carboxylate **39** (50mg, 0.16mmol) in 1 ml DCM under argon was treated sequentially with DIPEA (42mg, 0.32mmol) and 1,3-benzothiazole-6-sulfonyl chloride **34b** (76mg, 0.32mmol). After stirring at room temperature overnight, the reaction was quenched with saturated NH$_4$Cl solution (5 ml) and extracted with DCM (4 x 10 ml). The organic layers were dried over MgSO$_4$ and concentrated *in vacuo*. The mixture was purified by flash chromatography with cyclohexane: EtOAc 1:1.

TLC [Cyclohexane: EtOAc 1:1]: R$_f$ = 0.3

HPLC [0-100% Solvent B, 30min]: R$_t$ = 23.7 min, purity (280 nm) = 98%

Yield: 39mg, 0.077mmol (48%)

^{1}HNMR (300 MHz, CDCl$_3$) δ= 9.18-9.22(m, 1H), 8.47-8.51(m, 1H), 8.19-8.24(m, 1H),7.90-7.96 (m, 1H), 6.75-6.81(m, 1H), 6.47-6.51(m, 1H), 6.31-6.37(m, 1H), 4.85-4.91 (m, 1H), 4.09-4.38 (m, 2H), 3.89-4.05(m, 2H), 3.83-3.89 (d, 6H, J=2.01Hz), 3.74-3.83(m, 1H),3.21-3.34(m, 1H),2.15-2.25(m, 1H), 1.74-1.88(m, 1H), 1.62-1.74(m, 2H), 1.3-1.62(m, 2H)

^{13}C NMR (75 MHz, CDCl$_3$) δ= 170.56, 157.63, 155.2, 152.84, 149.94, 144.01, 137.34, 133.95, 124.98, 123.98, 122.00, 111.80, 104.07, 101.09, 66.16, 63.37, 56.44, 55.89, 55.21, 42.80, 27.94, 24.75, 19.98

HRMS : m/z: found 507.1779 [M + H] $^+$, calculated 507.1260 [M + H] $^+$

7.2.35 Synthesis of 2-(3,4-dimethoxyphenoxy)ethyl 1-(2-oxo-2,3-dihydrobenzo[d]thiazol-6-ylsulfonyl)piperidine-2-carboxylate 6g

2-(3,4-Dimethoxyphenoxy)ethyl piperidine-2-carboxylate **39** (50mg, 0.16mmol) in 1 ml DCM under argon was treated sequentially with DIPEA (42mg, 0.32mmol) and 2-oxo-2,3-dihydrobenzo[d]thiazole-6-sulfonyl chloride **34c** (81mg, 0.32mmol). After strring at room temperature overnight, the reaction was quenched with saturated NH$_4$Cl solution (5 ml) and extracted with DCM (4 x 10 ml). The organic layers were dried over MgSO$_4$ and concentrated *in vacuo*. The mixture was purified with preparative HPLC using a gradient of 40-50% buffer B in 16 minutes.

TLC [Cyclohexane: EtOAc 1:1]: R$_f$ = 0.74

HPLC [0-100% Solvent B, 30 min]: R$_t$ = 22.0 min, purity (280 nm) = 99%

Yield: 28mg, 0.05mmol (33%)

^{1}HNMR (400 MHz, DMSO-D$_6$) δ= 12.30(s, 1H), 8.05(d, 1H, J=1.86Hz), 7.62(dd,1H, J=1.96, 8.44Hz), 7.19(d, 1H, J=8.45Hz), 6.79(d, 1H, J=8.81Hz), 6.49(d, 1H, J=2.83Hz), 6.35(dd, 1H, J=2.85, 8.75Hz), 4.57-4.68(m,1H), 4.10-4.28(m, 2H), 3.91-4.07(m,2H), 3.68(s, 3H), 3.64(s, 3H), 3.54-3.62(m,1H), 3.01-3.14(m, 1H), 1.87-1.98(m,1H), 1.44-1.62(m, 3H), 1.04-1.29(m, 2H)

^{13}C NMR (100 MHz, DMSO-D6) δ= 170.75, 170.61, 152.97, 150.09, 143.80, 140.23, 133.95, 126.03, 124.64, 122.46, 113.10, 111.91, 104.79, 101.36, 66.31, 63.65, 56.48, 55.89, 55.13, 42.72, 27.64, 24.39, 19.82

HRMS : m/z: found 523.1185 [M + H] $^+$, calculated 523.1209 [M + H] $^+$

7.2.36 Synthesis of 9-(3,5-dichlorophenylsulfonyl)-3-(2-(3,4-dimethoxyphenoxy)ethyl)-3,9-diazabicyclo [3.3.1]nonan-2-one 4e

3-(2-(3,4-Dimethoxyphenoxy)ethyl)-3,9-diazabicyclo[3.3.1]nonan-2-one **31a** (24mg, 0.08mmol) in 3 ml DCM was treated with DIPEA (12mg, 0.09mmol) and stirred for 30min at room temperature followed by addition of 3,5-dichlorobenzene sulfonyl chloride **34a** (22mg, 0.09mmol). After stirring for 6 h at room temperature, the reaction was quenched with saturated NH$_4$Cl solution (5 ml) and extracted with DCM (4 x 10 ml). The organic layers were dried over MgSO$_4$ and concentrated *in vacuo*. The mixture was purified by flash chromatography with hexane: EtOAc 1:1.

TLC [EtOAc]: R_f = 0.48

HPLC [0-100% Solvent B, 30 min]: R_t = 23.8 min, purity (280 nm) = 99%

Yield: 21mg, 0.04mmol (53%)

^{1}HNMR (600 MHz, CDCl$_3$) δ= 7.66-7.73(m, 2H), 7.33-7.39(m, 1H), 6.74-6.79(m, 1H), 6.36-6.41(m, 1H), 6.28-6.33(m, 1H), 4.43(s, 1H), 4.28-4.33(m, 1H), 4.04-4.10(m, 1H), 3.88-3.94(m, 1H), 3.73(d, 6H, J= 6.56 Hz), 3.65-3.72(m, 1.5H), 3.55-3.62(m, 1H), 3.3-3.37(m, 1.5H), 1.88-2.02(m, 2H), 1.72-1.84(m, 2H), 1.54-1.72(m, 2H)

^{13}C NMR (300 MHz, CDCl$_3$) δ= 166.85, 152.74, 149.83, 143.85, 142.76, 136.14, 132.87, 125.29, 111.92, 103.94, 100.36, 66.89, 56.45, 55.85, 55.12, 52.12, 47.40, 46.57, 31.46, 28.13, 17.27

HRMS(EI) : m/z: found 528.0893 [M] $^+$, calculated 528.0889[M] $^+$

7.2.37 Synthesis of 9-(benzo[d]thiazol-6-ylsulfonyl)-3-(2-(3,4-dimethoxyphenoxy)ethyl)-3,9-diazabicyclo[3.3.1]nonan-2-one 4f

3-(2-(3,4-Dimethoxyphenoxy)ethyl)-3,9-diazabicyclo[3.3.1]nonan-2-one **31a** (32mg, 0.1mmol) in 3 ml DCM was treated with DIPEA (15mg, 0.12mmol) and stirred for 30min at room temperature followed by addition of 1,3-benzothiazole-6-sulfonyl chloride **34b** (28mg, 0.12mmol). The reaction was stirred overnight at room temperature. The reaction was quenched with saturated NH$_4$Cl solution (5 ml) and extracted with DCM (4 x 10 ml). The organic layers were dried over MgSO$_4$ and concentrated *in vacuo*. The mixture was purified with preparative TLC in 10% MeOH in CHCl$_3$.

TLC [EtOAc]: R_f = 0.47

HPLC [0-100% Solvent B, 16 min]: R_t = 19.5 min, purity (280 nm) = 99%

Yield: 8mg, 0.02mmol (15%)

^{1}HNMR (600 MHz, CDCl$_3$) δ= 9.13(s, 1H), 8.51(d, 1H, J= 1.33Hz), 8.18(d, 1H, J= 8.62Hz), 7.93 (dd, 1H, J= 1.87, 8.63Hz), 6.72(d, 1H, J=8.79Hz), 6.31(d, 1H, J= 2.82Hz), 6.18-6.23(m, 1H), 4.43-4.46(m, 1H),4.35-4.39(m, 1H), 3.92-3.98(m, 1H), 3.78-3.83(m, 6H), 3.7-3.74(m, 1H), 3.5-3.59(m, 2H), 3.29-3.33(m, 1H), 2.97-3.05(m, 1H), 1.96-2.01(m, 1H), 1.9-1.96(m, 1H), 1.76-1.84(m, 1H), 1.7-1.75(m, 1H), 1.6-1.68(m, 2H)

^{13}C NMR (300 MHz, CDCl$_3$) δ= 167.25, 158.13, 155.6, 152.66, 149.80, 143.76, 136.86, 134.3, 124.55, 124.38, 122.18, 111.83, 103.86, 100.29, 66.60, 56.39, 55.84, 55.03, 51.90, 47.21, 46.23, 31.53, 28.04, 17.30

HRMS(EI) : m/z: found 517.1340 [M] $^+$, calculated 517.1341 [M] $^+$

7.2.38 Synthesis of 10-(3,5-dichlorophenylsulfonyl)-3-(2-(3,4-dimethoxyphenoxy)ethyl)-3,10-diazabicyclo [4.3.1]decan-2-one 5e

3-(2-(3,4-Dimethoxyphenoxy) ethyl)-3,10-diazabicyclo [4.3.1] decan-2-one **32a** (22mg, 0.07mmol) in 3 ml DCM was treated with DIPEA (10mg, 0.08mmol) and stirred for 30min at room temperature followed by addition of 3,5-dichlorobenzen sulfony chloride **34a** (19mg, 0.08mmol). After stirring overnight at room temperature, the reaction was quenched with saturated NH$_4$Cl solution (5 ml) and extracted with DCM (4 x 10 ml). The organic layers were dried over MgSO$_4$ and concentrated *in vacuo*. The mixture was purified by flash chromatography with cyclohexane: EtOAc 2:1.

TLC [Cyclohexane/EtOAc 1:1]: R$_f$ = 0.40

HPLC [0-100% Solvent B, 30 min]: R$_t$ = 25.5 min, purity (280 nm) = 99%

Yield: 16mg, 0.03mmol (45%)

^{1}HNMR (600 MHz, CDCl$_3$) δ= 7.69(s, 1H), 7.68(s, 1H), 7.48-7.53(m, 1H), 6.74-6.8(m, 1H),6.47-6.5(m, 1H),6.36-6.41(m, 1H), 4.68-4.72(m, 1H), 4.34-4.42(m, 1H), 4.07-4.17(m, 2H), 3.98-4.07(m, 1H), 3.93-3.98(m, 1H), 3.86(s, 3H), 3.82(s, 3H), 3.64-3.68(m, 2H), 3.43-3.48(m, 0.5H), 3.31-3.4(m, 1.5H), 2.2-2.3(m, 2H), 1.95-2.05(m, 2H), 1.55-1.75(m, 2H)

^{13}C NMR (300 MHz, CDCl$_3$) δ= 170.50, 153.15, 149.9, 144.15, 143.75, 136.30, 132.63, 124.92, 111.98, 104.06, 100.56, 67.25, 57.05,56.45, 55.90, 51.42, 51.36, 49.1, 48.2, 32.7, (28.35,27.9), (14.8, 14.1)

HRMS(EI) : m/z: found 542.1045 [M] $^+$, calculated 542.1045 [M] $^+$

7.2.39 Synthesis of 10-(benzo[d]thiazol-6-ylsulfonyl)-3-(2-(3,4-dimethoxyphenoxy)ethyl)-3,10-diazabicyclo [4.3.1]decan-2-one 5f

3-(2-(3, 4-Dimethoxyphenoxy) ethyl)-3, 10-diazabicyclo [4.3.1] decan-2-one **32a** (24mg, 0.07mmol) in 3 ml DCM was treated with DIPEA (11mg, 0.09mmol) and stirred for 30min at room temperature followed by addition of 1,3-benzothiazole-6-sulfonyl chloride **34b** (20mg, 0.09mmol). After stirring overnight at room temperature, the reaction was quenched with saturated NH_4Cl solution (5 ml), extracted with DCM (4 x 10 ml). The organic layers were dried over $MgSO_4$ and concentrated *in vacuo*. The mixture was purified with preparative TLC in 10% MeOH in $CHCl_3$.

TLC [EtOAc]: R_f = 0.54

HPLC [0-100% Solvent B, 30 min]: R_t = 20.7 min, purity (280 nm) = 99%

Yield: 5mg, 0.01mmol (13%)

^{1}HNMR (600 MHz, $CDCl_3$) δ= 9.18(s, 1H), 8.48-8.52(m, 1H), 8.23 (d, 1H, J= 8.63Hz), 7.93(dd, 1H, J=1.86, 8.64Hz), 6.77(d, 1H, J= 8.78Hz), 6.47(d, 1H, J= 2.84Hz), 6.36-6.39(m, 1H), 4.74-4.78(m, 1H), 4.42-4.48(m, 1H), 4.09-4.15(m, 2H), 4.02-4.08(m, 1H), 3.95-3.99(m, 1H), 3.84(s, 3H), .815-3.825(m, 3H), 3.6-3.65(m, 2H), 3.3-3.35(m, 1H), 3.05-3.1(m, 1H), 2.25-2,33(m, 1H), 2.15-2.2(m, 1H), 1.97-2.03(m, 1H), 1.7-1.85(m, 1H),1.55-1.63(m, 1H), 1.1-1.2(m, 1H)

^{13}C NMR (300 MHz, $CDCl_3$) δ= 166.1, 153.15, 150.70, 148.4, 145.1, 138.93, 133.75, 129.62, 119.86, 119.35, 116.84, 107.10, 99.21, 95.75, 62.45, 52.15, 51.65, 51.12, 44.03, 43.52, 37.15, 24.93, 27.95, 23.02, 17.85

HRMS : m/z: found 532.1560 [M] $^+$, calculated 532.1576[M + H] $^+$,

7.2.40 Synthesis of 6-(3-(2-(3,4-dimethoxyphenoxy)ethyl)-2-oxo-3,9-diazabicyclo [3.3.1]nonan-9-ylsulfonyl)benzo[d]thiazol-2(3H)-one **4g**

3-(2-(3,4-Dimethoxyphenoxy)ethyl)-3,9-diazabicyclo[3.3.1]nonan-2-one **31a** (40mg, 0.13mmol) in 3 ml DCM was treated with DIPEA (32mg, 0.25mmol) and stirred for 30min at room temperature followed by addition of 2-oxo-2,3-dihydrobenzo[d]thiazole-6-sulfonyl chloride **34c** (62mg, 0.25mmol). After stirring overnight at room temperature, the reaction was quenched with saturated NH_4Cl solution (5 ml) and extracted with DCM (4 x 10 ml). The organic layers were dried over $MgSO_4$ and concentrated *in vacuo*. The mixture was purified by preparative HPLC using a gradient of 50-57% buffer B in 16 minutes.

TLC [EtOAc]: R_f = 0.38

HPLC [0-100% Solvent B, 16 min]: R_t = 13.0 min, purity (280 nm) = 99%

Yield: 35mg, 0.07mmol (53%)

^{1}HNMR (300 MHz, DMSO) δ= 12.33-12.40(m, 1H), 8.11-8.15(m, 1H), 7.64-7.71(m, 1H), 7.20-7.26(m, 1H), 6.75-6.85(m, 1H), 6.44-6.48(m, 1H), 6.23-6.32(m, 1H), 4.19-4.28(m, 1H), 4.12-4.18(m, 1H), 3.71-3.83(m, 2H), 3.69(s, 3H), 3.66(s, 3H), 3.36-3.50(m, 2H), 3.20-3.29(m, 1H), 2.97-3.10(m, 1H), 1.35-1.82(m, 6H)

^{13}C NMR (75 MHz, DMSO) δ= 170.69, 166.56, 152.95, 150.12, 143.74, 140.65, 133.40, 126.15, 124.90, 122.45, 113.20, 112.11, 104.48, 101.25, 65.55, 56.51, 55.92, 54.85, 50.70, 47.20, 45.41, 31.27, 28.09, 17.25

HRMS (EI) m/z: found 533.1299[M]$^+$, calculated 533.1290[M]$^+$

7.2.41 Synthesis of 6-(3-(2-(3,4-dimethoxyphenoxy)ethyl)-2-oxo-3,10-diazabicyclo [4.3.1]decan-10-ylsulfonyl)benzo[d]thiazol-2(3H)-one 5g

3-(2-(3,4-Dimethoxyphenoxy) ethyl)-3,10-diazabicyclo [4.3.1] decan-2-one **32a** (15mg, 0.05mmol) in 3 ml DCM was treated with DIPEA (12mg, 0.09mmol) and stirred for 30min at room temperature followed by addition of 2-oxo-2,3-dihydrobenzo[d]thiazole-6-sulfonyl chloride **34c** (22mg, 0.09mmol). After stirring overnight at room temperature, the reaction was quenched with saturated NH$_4$Cl solution (5 ml) and extracted with DCM (4 x 10 ml). The organic layers were dried over MgSO$_4$ and concentrated *in vacuo*. The mixture was purified by preparative HPLC using a gradient of 55-65% buffer B in 16mins.

TLC [EtOAc]: R_f = 0.54

HPLC [0-100% Solvent B, 16 min]: R_t = 13.6 min, purity (280 nm) = 99%

Yield: 5mg, 0.01mmol (20%)

^{1}HNMR (300 MHz, DMSO) δ= 12.07-12.13(s, 1H), 7.85-7.88(m, 1H), 7.56-7.61(m, 1H), 7.12-7.18(m, 1H), 6.68-6.73(m, 1H), 6.67-6.73(m, 1H), 6.41-6.46(m, 1H), 6.29-6.34(m, 1H),4.54-4.60(m, 1H), 4.20-4.29(m, 1H),3.93-4.02(m, 2H), 3.75-3.93(m, 2H), 3.65-3.75(m, 8H), 3.20-3.27(m, 1H),2.15-2.25(m, 1H),1.95-2.05(m, 1H),1.87-1.93(m, 1H),1.05-1.45(m, 3H)

^{13}C NMR (75 MHz, DMSO) δ= 175.49, 175.30, 157.94, 154.62, 148.30, 144.97, 139.84, 129.90, 126.01, 125.95, 117.40, 113.70, 109.12, 105.60, 71.41, 61.47, 61.20, 60.57, 55.53, 53.13, 52.60, 37.32, 32.66, 32.36, 19.54

HRMS (EI) m/z: found 547.1446[M] [+], calculated 547.1447[M] [+]

7.2.42 Synthesis of 3,9-diazabicyclo[3.3.1]nonan-2-one 35

To a solution of benzyl 2-oxo-3,9-diazabicyclo[3.3.1]nonane-9-carboxylate **17** (84mg, 0.3mmol) in 1 ml anhydrous MeOH were added catalytic amounts of palladium on carbon followed by degassing with H_2. After stirring under 1 atm H_2 at room temperature for 2 h, the reaction mixture was filtered through celite, concentrated *in vacuo* and used for the next step without further purification.

TLC [20% MeOH in CHCl$_3$]: R$_f$ = 0.17

Yield: 35mg, 0.25mmol (82%)

7.2.43 Synthesis of 3,10-diazabicyclo[4.3.1]decan-2-one 36

To a solution of benzyl 2-oxo-3, 10-diazabicyclo [4.3.1] decane-10-carboxylate **27** (33mg, 0.1mmol) in 1 ml anhydrous MeOH were added catalytic amounts of palladium on carbon followed by degassing with H_2. After stirring under 1 atm H_2 at room temperature for 3 h, the reaction mixture was filtered through celite, concentrated *in vacuo* and used for the next step without further purification.

TLC [20% MeOH in CHCl$_3$]: R$_f$ = 0.26

Yield: 17mg, 0.1mmol (100%)

7.2.44 Synthesis of 6-(2-oxo-3,9-diazabicyclo [3.3.1]nonan-9-ylsulfonyl)benzo[d]thiazol-2(3H)-one 4h

3,9-Diazabicyclo[3.3.1]nonan-2-one **35** (25mg, 0.2mmol) in 1 ml DCM under argon was treated with DIPEA (69mg, 0.5mmol) and stirred for 30min at room temperature followed by addition of 2-oxo-2,3-dihydrobenzo[d]thiazole-6-sulfonyl chloride **34c** (53mg, 0.2mmol). After stirring overnight at room temperature, the reaction was quenched with saturated NH$_4$Cl solution (5 ml) and extracted with DCM (4 x 10 ml). The organic layers were dried over MgSO$_4$ and concentrated *in vacuo*. The mixture was purified by preparative HPLC using a gradient of 45% buffer B in 16mins.

TLC [10% MeOH in DCM]: R_f = 0.71

HPLC [0-100% Solvent B, 16 min]: R_t = 10.2 min, purity (280 nm) = 99%

Yield: 27mg, 0.08mmol (43%)

^{1}HNMR (600 MHz, DMSO-D_6) δ= 8.13(d, 1H, J=1.88Hz), 7.68 (dd, 1H, J=1.98, 8.44Hz), 7.60(s, 1H), 7.21(d, 1H, J=8.39Hz), 4.12-4.15(m, 1H), 4.01-4.04(m, 1H), 3.17-3.25(m, 1H), 2.93-2.97(m, 1H), 1.57-1.73(m, 5H), 1.40-1.50(m, 1H)

^{13}C NMR (300 MHz, DMSO) δ= 170.80, 167.59, 140.59, 133.66, 126.07, 124.82, 122.52, 112.14, 54.62, 46.17, 44.07, 31.11, 27.63, 17.59

HRMS(EI+) : m/z: found 353.0458 [M] $^+$, calculated 353.0504 [M] $^+$

7.2.45 Synthesis of 6-(2-oxo-3,10-diazabicyclo[4.3.1]decan-10-ylsulfonyl)benzo[d]thiazol-2(3H)-one 5h

3,10-Diazabicyclo[4.3.1]decan-2-one **36** (17mg, 0.1mmol) in 1 ml DCM under argon was treated with DIPEA (43mg, 0.3mmol) and stirred for 30min at room temperature followed by addition of 2-oxo-2,3-dihydrobenzo[d]thiazole-6-sulfonyl chloride **34c** (33mg, 0.1mmol). After stirring overnight at room temperature, the reaction was quenched with saturated NH$_4$Cl solution (5 ml) and extracted with DCM (4 x 10 ml). The organic layers were dried over MgSO$_4$ and concentrated *in vacuo*. The mixture was purified by preparative HPLC using a gradient of 45% buffer B in 16mins.

TLC [10% MeOH in DCM]: R_f = 0.72

HPLC [0-100% Solvent B, 16 min]: R_t = 10.6 min, purity (280 nm) = 98%

Yield: 5mg, 0.01mmol (12%)

^{1}HNMR (600 MHz, DMSO) δ= 8.19(d, 1H, J=1.93Hz), 7.90-7.95 (m, 1H), 7.73(dd, 1H, J=1.98Hz, 8.43Hz), 7.25(d, 1H, J=8.44Hz), 4.39-4.43(m, 1H), 4.25-4.31(m, 1H), 3.25-3.30(m, 1H), 2.84-2.9(m, 1H), 2.03-2.17(m, 1H), 1.85-1.93(m, 1H), 1.67-1.77(m, 1H), 1.42-1.50(m, 1H), 1.17-1.33(m, 2H), 1.05-1.15(m, 2H)

^{13}C NMR (300 MHz, DMSO) δ= 172.4, 170.8, 140.4, 135.3, 125.5, 124.9, 122.1, 112.3, 56.3, 49.1, 38.9, 33.25, 28.0, 26.9, 14.8

HRMS : m/z: found 368.0736 [M + H] $^+$, calculated 368.0739 [M + H] $^+$

7.2.46 Synthesis of 10-(3,5-dichloro-4-hydroxyphenylsulfonyl)-3-(2-(3,4-dimethoxyphenoxy)ethyl)-3,10-diazabicyclo[4.3.1]decan-2-one 5i

3-(2-(3, 4-dimethoxyphenoxy) ethyl)-3, 10-diazabicyclo [4.3.1] decan-2-one **32a** (24mg, 0.07mmol) in 3 ml DCM was treated with DIPEA (23mg, 0.09mmol) and stirred for 30min at room temperature followed by addition of 3,5-dichloro-4-hydroxy benzenesulfonylchloride **34d** (23mg, 0.09mmol). After stirring overnight at room temperature, the reaction was quenched with saturated NH$_4$Cl solution (5 ml) and extracted with DCM (4 x 10 ml). The organic layers were dried over MgSO$_4$ and concentrated *in vacuo*. The mixture was purified by flash chromatography with EtOAc followed by 10% MeOH in CHCl$_3$.

TLC [EtOAc]: R$_f$ = 0.6

HPLC [0-100% Solvent B, 30 min]: R$_t$ = 21.5 min, purity (280 nm) = 98%

Yield: 10mg, 0.02mmol (25 %)

^{1}HNMR (300 MHz, CDCl$_3$) δ= 7.78(s, 2H), 6.76-6.82(m, 1H), 6.5-6.54(m, 1H), 6.38-6.44(m, 1H), 4.68-4.74(m, 1H), 4.3-4.45(m, 1H), 3.93-4.24(m, 3H), 3.85-3.9(m, 7H), 3.6-3.73(m, 3H), 3.3-3-45(m, 1H), 2.2-2.4(m, 2H), 1.95-2.1(m, 2H), 1.6-1.7(m, 1H), 1.35-1.45(m, 1H)

^{13}C NMR (75 MHz, CDCl$_3$) δ=170.4, 153.14, 151.5, 149.9, 143.7, 134.4, 126.83, 122.09, 111.99, 104.07, 100.59, 67.25, 56.93, 56.46, 55.91, 51.43, 51.35, 48.91, 48.27, 31.92, 22.69, 14.11

HRMS(EI) : m/z: found 558.0993 [M]$^+$, calculated 558.0994 [M]$^+$

7.2.47 Synthesis of tert-butyl allyl(2-(3,4-dimethoxyphenoxy)ethyl)carbamate 48

To a solution of tert-butyl N-allylcarbamate (144mg, 0.92mmol) in 1ml DMF was added NaH (22mg, 0.92mmol) under argon and the reaction mixture was stirred for 30min at 0°C followed by addition of 4-(2-bromoethoxy)-1,2-dimethoxybenzene **28a** (200mg, 0.77mmol) and stirring at 0°C for 2 h. To the mixture a saturated NH$_4$Cl solution (10ml) was added and extracted with DCM (5 x 10 ml). The organic layers were dried over MgSO$_4$, filtered and concentrated *in vacuo*. The pure product was obtained by flash chromatography with cyclohexane: EtOAc 5:1.

TLC [cyclohexane: EtOAc 5:1]: R_f = 0.26

Yield: 178mg, 0.53mmol (69%)

^{1}HNMR (400 MHz, CDCl$_3$) δ= 6.76(d,1H, J=8.75Hz), 6.49(s,1H), 6.31-6.43(m,1H), 5.70-5.90(m,1H), 5.02-5.23(m,2H), 3.98-4.08(m,2H), 3.88-3.98(m,2H), 3.84(s,3H), 3.81(s,3H), 3.55 (s,2H), 1.45(s,9H)

MS(ESI) : m/z: found 337.93 [M+Na][+], calculated 338.19 [M+H][+]

7.2.48 Synthesis of tert-butyl 2-(3,4-dimethoxyphenoxy)ethyl(4-(trimethylsilyl)but-2-enyl)carbamate 50

To a solution of tert-butyl allyl(2-(3,4-dimethoxyphenoxy)ethyl)carbamate **48** (100mg, 0.30mmol) and allyltrimethylsilane (135mg, 1.18mmol) in 3ml DCM was added Grubbs catalyst generation I (24mg, 0.03mmol, Sigma-Aldrich) and heated under reflux overnight. The mixture was filtered through celite and concentrated *in vacuo*. The pure product was obtained by flash chromatography with cyclohexane: EtOAc 6:1.

TLC [cyclohexane: EtOAc 6:1]: R_f = 0.38

Yield: 85mg, 0.20mmol (67%)

^{1}HNMR (400 MHz, CDCl$_3$) δ= 6.73-6.82(m,1H), 6.46-6.56(m,1H), 6.35-6.45(m,1H), 5.45-5.67(m,1H), 5.18-5.45(m,1H), 3.87-4.15(m,4H), 3.86(s,3H), 3.84(s,3H), 3.43-3.63(m,2H), 1.50-1.75(m,2H), 1.47(s,9H), -0.09-0.03(m,9H)

^{13}C NMR (100 MHz, CDCl$_3$) δ=155.50, 153.33, 149.89, 143.55, 129.55, 123.57, 111.91, 103.80, 100.82, 79.54, 67.02, 56.45, 55.82, 50.01, 45.50, 28.45, 22.69, -1.81

MS(ESI) : m/z: found 446.93 [M+Na][+], calculated 446.60 [M+Na][+]

7.2.49 Synthesis of N-(2-(3,4-dimethoxyphenoxy)ethyl)-4-(trimethylsilyl)but-2-en-1-amine 51

Excess amount of SiO$_2$ was added to tert-butyl 2-(3,4-dimethoxyphenoxy)ethyl(4-(trimethylsilyl)but-2-enyl)carbamate **50** (220mg, 0.52mmol) and stirred at 150°C *in vacuo* for 2 h. The SiO$_2$ was washed with EtOAc for 3 times and the organic layers were collected and concentrated *in vacuo.* The compound was used for the next step without further purification.

TLC [5% TEA in EtOAc]: R_f = 0.6

Yield: 143mg, 0.44mmol (85%)

MS(ESI): m/z: found 323.93 [M+H]$^+$, calculated 324.20 [M+H]$^+$

7.2.50 Synthesis of (S)-N-(2-(3,4-dimethoxyphenoxy)ethyl)-6-oxo-N-(4-(trimethylsilyl)but-2-enyl)piperidine-2-carboxamide 53

To a solution of (S)-6-oxo-2-piperidinecarboxylic acid **52** (109mg, 0.76mmol) in 5ml DCM was added sequentially DIPEA (205mg, 1.58mmol), HOAt(104mg, 0.76mmol) and EDC-HCl(118mg, 0.76mmol) followed by stirring for 30 min at room temperature and addition of N-(2-(3,4-dimethoxyphenoxy)ethyl)-4-(trimethylsilyl)but-2-en-1-amine **51** (205mg, 0.63mmol). After 24 h, brine (10ml) was added and extracted with DCM (5 x 10 ml). The organic layers were dried over MgSO$_4$, filtered and concentrated *in vacuo*. The pure product was obtained by flash chromatography with 5% TEA in EtOAc.

TLC [5% TEA in EtOAc]: R_f = 0.27

Yield: 260mg, 0.58mmol (90%)

MS(ESI) : m/z: found 449.57 [M+H]$^+$, calculated 449.24[M+H]$^+$

7.2.51 Synthesis of (S)-tert-butyl 2-((2-(3,4-dimethoxyphenoxy)ethyl)(4-(trimethylsilyl)but-2-enyl)carbamoyl)-6-oxopiperidine-1-carboxylate 54

To a solution of (S)-N-(2-(3,4-dimethoxyphenoxy)ethyl)-6-oxo-N-(4-(trimethylsilyl)but-2-enyl)piperidine-2-carboxamide **53** (1070mg, 2.39mmol) in 15ml THF was added 1M BuLi solution in hexanes (184mg, 2.87mmol) dropwise under argon at -78°C and stirred for 1 h followed by addition of di-tert-butyl dicarbonate (1040mg, 4.78mmol). After stirring at -78°C overnight, a saturated NH$_4$Cl solution (20ml) was added at room temperature and extracted with DCM (6 x 20ml). The organic layers were dried over MgSO$_4$, filtered and concentrated *in vacuo*. The pure product was obtained by flash chromatography with cyclohexane: EtOAc 1:1.

TLC [cyclohexane: EtOAc 1:1]: R_f = 0.4

Yield: 947mg, 1.73mmol (72%)

¹HNMR (400 MHz, CDCl₃) δ= 6.72-6.79(m,1H), 6.44-6.53(m,1H), 6.31-6.42(m,1H), 5.55-5.75(m,1H), 5.15-5.45(m,1H), 4.95-5.05(m,1H), 3.95-4.25(m,4H), 3.77-3.90(m,6H), 3.55-3.77(m,2H), 2.54-2.65(m,1H), 2.35-2.50(m,1H), 1.50-1.65(m,4H), 1.38-1.49(m,9H), 0(t,9H,J=12.30,12.30Hz)

¹³C NMR (100 MHz, CDCl₃) δ= 171.37, 171.13, 153.13, 153.09, 149.76, 143.51, 131.93, 122.53, 111.80, 103.95, 100.51, 83.04, 66.64, 55.82, 55.57, 51.36, 45.29, 34.40, 27.96, 25.84, 22.91,19.13, -1.92

MS(ESI) : m/z: found 571.34 [M+H] ⁺, calculated 571.28[M+H] ⁺

7.2.52 Synthesis of (1S,5S,6R)-3-(2-(3,4-dimethoxyphenoxy)ethyl)-5-vinyl-3,10-diazabicyclo[4.3.1]decan-2-one 57

To a solution of (S)-tert-butyl 2-((2-(3,4-dimethoxyphenoxy)ethyl)(4-(trimethylsilyl)but-2-enyl)carbamoyl)-6-oxopiperidine-1-carboxylate **54** (100mg, 0.18mmol) in 1ml THF under argon was added dropwise DIBAL-H (78mg, 0.55mmol) and stirred at -78°C for 1 h followed by removal of the solvent *in vacuo*. The oily residue in 1ml DCM was treated dropwise with 1ml 10% TFA in DCM at -78°C followed by stirring at 0°C for 2 h, addition of 1mL TFA and stirring for another 2 h. A saturated NaHCO₃ solution (10ml) was added and extracted with DCM (6 x 10ml). The organic layers were dried over MgSO₄, filtered and concentrated *in vacuo*. The pure product was obtained by preparative TLC with 5% MeOH and 5% TEA in EtOAc.

TLC [5% MeOH, 5% TEA in EtOAc]: R_f = 0.38

Yield: 50mg, 0.14mmol (76%)

¹HNMR (400 MHz, CDCl₃) δ= 6.77(d, 1H, J=8.76Hz), 6.49(d, 1H, J=2.81Hz), 6.38(dd, 1H, J=2.84,8.73Hz), 5.65-5.76(m, 1H), 5.07(s, 1H), 5.01-5.05(m, 1H), 4.22-4.30(m, 1H), 4.13-4.20(m,1H), 3.99-4.10(m,2H), 3.84-3.90(m,1H), 3.83(s,3H), 3.82(s,3H), 3.55-3.78(m,1H), 3.26-3.35(m,1H), 2.97-3.04(m,1H), 2.73-2.83(m,1H), 2.23-2.32(m,1H), 1.69-1.82(m,2H), 1.48-1.68(m,4H)

¹³C NMR (100 MHz, CDCl₃) δ= 172.90, 153.11, 149.81, 143.56, 138.58, 115.55, 111.77, 103.46, 100.48, 67.33, 57.00, 56.40, 55.79, 52.73, 52.51, 51.34, 48.88, 28.70, 27.28, 16.24

MS(ESI) : m/z: found 361.09 [M+H] ⁺, calculated 361.21[M+H] ⁺

7.2.53 Synthesis of (1S,5S,6R)-10-(3,5-dichlorophenylsulfonyl)-3-(2-(3,4-dimethoxyphenoxy)ethyl)-5-vinyl-3,10-diazabicyclo[4.3.1]decan-2-one 71

A solution (1S,5S,6R)-3-(2-(3,4-dimethoxyphenoxy)ethyl)-5-vinyl-3,10-diazabicyclo[4.3.1]decan-2-one **57** (80mg, 0.22mmol) in 1mL DCM under argon was treated with DIPEA (34.4mg, 0.266mmol) and stirred for 30 min at room temperature followed by addition of 3,5-dichlorobenzene sulfonyl chloride **34a** (65mg, 0.27mmol). After stirring overnight at room temperature, the pure product was obtained by preparative TLC with cyclohexane: EtOAc 1:1.

TLC [cyclohexane: EtOAc 1:1]: R_f = 0.68

Yield: 60mg, 0.11mmol (48%)

^{1}HNMR (600 MHz, CDCl$_3$) δ= 7.68(d, 2H, J=1.85Hz), 7.53(t, 1H, J=1.85, 1.85Hz), 6.76(d, 1H, J=8.77Hz), 6.46(d, 1H, J=2.79Hz), 6.36(dd, 1H, J=2.81, 8.75Hz), 5.77-5.86(m, 1H), 5.05-5.16(m, 2H), 4.65-4.71(m,1H), 4.07-4.21(m,3H), 3.99-4.05(m,1H), 3.94-3.98(m,1H), 3.83(s,3H), 3.82(s,3H), 3.45-3.53(m,1H), 3.22-3.3(m,1H), 2.67-2.76(m,1H), 2.24(d,1H, J=13.52Hz), 1.42-1.53(m,3H), 1.14-1.22(m,2H)

^{13}C NMR (150 MHz, CDCl$_3$) δ= 170.18, 153.04, 149.83, 144.05, 143.66, 137.52, 136.31, 132.67, 124.84, 116.54, 111.81, 103.52, 100.52, 67.29, 56.80, 56.40, 55.79, 54.92, 53.39, 51.60, 49.25, 27.60, 26.27, 15.41

MS(ESI) : m/z: found 570.62 [M+H] [+], calculated 570.51[M+H] [+]

7.2.54 Synthesis of (1S,5S,6R)-10-(3,5-dichlorophenylsulfonyl)-5-(1,2-dihydroxyethyl)-3-(2-(3,4-dimethoxyphenoxy)ethyl)-3,10-diazabicyclo [4.3.1] decan-2-one 72 diastereomeric mixture

To a solution of (1S,5S,6R)-10-(3,5-dichlorophenylsulfonyl)-3-(2-(3,4-dimethoxyphenoxy)ethyl)-5-vinyl-3,10-diazabicyclo[4.3.1]decan-2-one **71** (20mg, 0.04mmol) in 2ml t-BuOH and water (1:1) was added AD-mix-alpha (308 mg) at room temperature and stirred two days. The pure product was obtained by preparative TLC with 1% AcOH in cyclohexane: EtOAc 1:4.

TLC [1% AcOH in cyclohexane: EtOAc 1:4]: R_f = 0.35

HPLC [40-42% Solvent B, 30 min]: R_t = 17.5 min, purity (280 nm) = 99%

Yield: 12mg, 0.03mmol (57%)

^{1}HNMR (300 MHz, CDCl$_3$) δ= 7.68-7.72(m,2H), 7.52-7.56(m,1H), 6.74-6.81(m,1H), 6.54-6.58(m,1H), 6.38-6.44(m,1H), 4.67-4.74(m,1H), 3.90-4.35(m,6H), 3.85(s,3H), 3.82(s,3H), 3.30-3.80(m,6H), 2.08-2.30(m,3H), 1.35-1.55(m,3H), 0.82-0.85(m,1H)

^{13}C NMR (75 MHz, CDCl$_3$) δ=169.95, 153.09, 149.90, 143.85, 143.82, 136.36, 132.75, 124.86, 111.95, 104.05, 100.76, 72.70, 65.35, 63.90, 56.95, 56.41, 55.89, 52.35, 51.75, 50.55, 49.78, 46.76, 28.25, 22.66, 14.15

MS(ESI) : m/z: found 604.05[M+H]$^+$, calculated 604.51[M+ H]$^+$

7.2.55 Synthesis of (1S,5S,6R)-10-(3,5-dichlorophenylsulfonyl)-5-(1,2-dihydroxyethyl)-3-(2-(3,4-dimethoxyphenoxy)ethyl)-3,10-diazabicyclo [4.3.1] decan-2-one __73__ diastereomeric mixture

To a solution of (1S,5S,6R)-10-(3,5-dichlorophenylsulfonyl)-3-(2-(3,4-dimethoxyphenoxy)ethyl)-5-vinyl-3,10-diazabicyclo[4.3.1]decan-2-one **71** (20mg, 0.04mmol) in 2ml t-BuOH and water (1:1) was added AD-mix-beta (88mg) at room temperature and stirred overnight. The pure product was obtained by preparative TLC with 1% AcOH in cyclohexane: EtOAc 1:4.

TLC [1% AcOH in cyclohexane: EtOAc 1:4]: R$_f$ = 0.35

HPLC [0-100% Solvent B, 30 min]: R$_t$ = 21.6 min, purity (280 nm) = 99%

Yield: 20mg, 0.03mmol (94%)

^{1}HNMR (300 MHz, CDCl$_3$) δ= 7.68-7.72(m,2H), 7.52-7.56(m,1H), 6.74-6.81(m,1H), 6.54-6.58(m,1H), 6.38-6.44(m,1H), 4.67-4.74(m,1H), 3.90-4.35(m,6H), 3.85(s,3H), 3.82(s,3H), 3.30-3.80(m,6H), 2.08-2.30(m,3H), 1.35-1.55(m,3H), 0.82-0.85(m,1H)

^{13}C NMR (75 MHz, CDCl$_3$) δ=169.95, 153.09, 149.90, 143.85, 143.82, 136.36, 132.75, 124.86, 111.95, 104.05, 100.76, 72.70, 65.35, 63.90, 56.95, 56.41, 55.89, 52.35, 51.75, 50.55, 49.78, 46.76, 28.25, 22.66, 14.15

MS(ESI) : m/z: found 604.05[M+H]$^+$, calculated 604.51[M+ H]$^+$

7.2.56 Synthesis of (1R,5S,6S)-10-(3,5-dichlorophenylsulfonyl)-3-(2-(3,4-dimethoxyphenoxy)ethyl)-5-(2,2,3,3,8,8,9,9-octamethyl-4,7-dioxa-3,8-disiladecan-5-yl)-3,10-diazabicyclo[4.3.1]decan-2-one 74 diastereomeric mixture

To a solution of (1S,5S,6R)-10-(3,5-dichlorophenylsulfonyl)-5-(1,2-dihydroxyethyl)-3-(2-(3,4-dimethoxyphenoxy)ethyl)-3,10-diazabicyclo[4.3.1]decan-2-one **73** (20mg, 0.03mmol) in 1ml DCM at 0℃ was added 2,6-lutidine (18mg, 0.17mmol) and tert-Butyldimethylsilyl trifluoromethanesulfonate (88mg, 0.33mmol). After stirring for 29 h, no **73** was still existed. The organic layers were concentrated *in vacuo*. The attempt to purify with preparative HPLC using a gradient of 80-90% buffer B in 16 minutes was failed. As a test reaction, further efforts for purification were not put forth.

MS(ESI) : m/z: found 831.98[M+H]$^+$, calculated 832.31[M+ H]$^+$

7.2.57 Synthesis of (2S)-1-benzyl 2-methyl 6-hydroxypiperidine-1,2-dicarboxylate 66 and (S)-methyl 2-(benzyloxycarbonylamino)-6-hydroxyhexanoate 67

To a solution of (S)-1-benzyl 2-methyl 6-oxopiperidine-1,2-dicarboxylate **65** (100 mg, 0.34 mmol) in 2ml MeOH at 0℃ was added NaBH$_4$ (29 mg, 0.76 mmol) and stirred for 6 h. The pure products were obtained by flash chromatography with cyclohexane: EtOAc 4:1

TLC [cyclohexane: EtOAc 1:1]: R$_f$ = 0.64 for **66** and R$_f$ = 0.25 for **67**

Yield: 26mg, 0.09mmol (26%) for **66** and 22mg, 0.07mmol (21%) for **67**

^{1}HNMR (300 MHz, CDCl$_3$) of **66** δ= 7.3-7.45(m,5H), 5.75-5.85(m,0.5H), 5.1-5.3(m,2H), 4.8-4.9(m,0.5H), 4.70-4.80(m,0.5H), 4.25-4.35(m,0.5H), 3.6-3.9(m,3H), 2.2-2.3(m,0.5H), 1.5-1.8(m,2.5H), 1.2-1.4(m,3H),

^{1}HNMR (300 MHz, CDCl$_3$) of **67** δ= 7.3-7.4(m,5H), 5.3-5.4(m,1H), 5.05-5.15(m,2H), 4.35-4.45(m,1H), 3.7-3.8(s,3H), 3.56-3.7(m,2H), 1.8-1.95(m,1H), 1.65-1.8(m,1H), 1.5-1.65(m,2H), 1.35-1.5(m,2H)

MS(ESI) : m/z: found 316.87[M+Na]$^+$, calculated 316.32[M+ Na]$^+$ for **66**

m/z: found 318.87[M+Na]$^+$, calculated 318.33[M+ Na]$^+$ for **67**

7.2.58 Synthesis of N-(2-(3,4-dimethoxyphenoxy)ethyl)prop-2-en-1-amine 58

To a solution of tert-butyl allyl(2-(3,4-dimethoxyphenoxy)ethyl)carbamate **48** (285mg, 0.85mmol) in 5ml DCM at room temperature were added 2.5 ml TFA. The reaction mixture was stirred for 1 h, concentrated *in vacuo*, dissolved in H_2O (5 ml) and extracted with EtOAc (3 x 5 ml). The aqueous layers were basified with saturated Na_2CO_3 solution and extracted with EtOAc (6 x 6 ml). The collected organic layers were dried over $MgSO_4$ and concentrated *in vacuo*. This crude product was used for next reaction without further purification.

TLC [10% MeOH in $CHCl_3$]: $R_f = 0.46$

Yield: 200mg, 0.85mmol (100%)

^1HNMR (300 MHz, $CDCl_3$) δ= 6.78 (d, 1H, J=8.75 Hz), 6.54 (d, 1H, J=2.8 Hz), 6.41 (d, 1H, J=8.73 Hz), 5.85-6.0 (m, 1H), 5.1-5.3(m,2H), 4.0-4.1(m,2H), 3.86 (s, 3H), 3.84 (s, 3H), 3.3-3.4(m,2H), 3.0-3.05(m,2H), 2.6-2.8(m,1H)

^{13}C NMR (75 MHz, $CDCl_3$) δ= 153.37, 149.87, 143.66, 135.93, 116.70, 111.82, 103.85, 100.97, 67.58, 56.43, 55.82, 52.06, 48.06

7.2.59 Synthesis of (S)-N-allyl-N-(2-(3,4-dimethoxyphenoxy)ethyl)-6-oxopiperidine-2-carboxamide 59

To a solution of (S)-6-oxo-2-piperidinecarboxylic acid **52** (50mg, 0.35mmol) in 5ml DCM was added sequentially with TEA (42mg, 0.42mmol), HATU(160mg, 0.42mmol) and stirred for 30 min at room temperature followed by addition of N-(2-(3,4-dimethoxyphenoxy)ethyl)prop-2-en-1-amine **58** (83mg, 0.35mmol). After 6 h, brine (10ml) was added and extracted with DCM (5 x 10 ml), dried over $MgSO_4$, filtered and concentrated *in vacuo*. The pure product was obtained by flash chromatography with 1% TEA in EtOAc.

TLC [1% TEA in EtOAc]: $R_f = 0.1$

Yield: 116mg, 0.32mmol (91%)

^1HNMR (300 MHz, $CDCl_3$) δ= 6.75-6.8 (m, 1H), 6.5-6.55 (m, 1H), 6.35-6.4 (m, 1H), 5.7-5.85 (m, 1H), 5.1-5.3(m,2H), 4.55-4.65(m, 0.4H), 4.35-4.4 (m, 0.6H), 4.25-4.3 (m,

0.4H), 4.0-4.1(m,3H), 3.8-3.9(m,6.6H), 3.73-3.8(m,1H), 3.55-3.65 (m,1H), 2.3- 2.35 (m, 2H), 1.8- 2.1 (m, 2H), 1.6- 1.8 (m, 2H)

^{13}C NMR (75 MHz, CDCl$_3$) δ= 173.55, 171.82, 153.02, 149.84, 143.61, 132.65, 117.65, 111.93, 103.97, 100.68, 66.26, 56.42, 55.88, 52.70, 51.30, 47.09, 30.57, 25.53, 18.62

MS(ESI) : m/z: found 363.47[M+H]$^+$, calculated 363.42[M+H]$^+$

7.2.60 Synthesis of (S)-benzyl 2-(allyl(2-(3,4-dimethoxyphenoxy)ethyl) carbamoyl)-6- oxopiperidine-1-carboxylate 60

To a solution of (S)-N-allyl-N-(2-(3,4-dimethoxyphenoxy)ethyl)-6-oxopiperidine-2-carboxamide **59** (2.33g, 6.43mmol) in 70ml THF was added BuLi (0.5g, 7.71mmol) dropwise and catalyttical amount of 4-Dimethylaminopyridine under argon at -78°C and stirred for 1 h followed by addition of Cbz-Cl (2.2g, 12.86mmol). After 2 h at -78°C, a saturated NH$_4$Cl solution (50ml) was added at room temperature and extracted with DCM (6 x 70ml), dried over MgSO$_4$, filtered and concentrated *in vacuo*. The pure product was obtained by flash chromatography with cyclohexane: EtOAc 1:2.

TLC [hexane: EtOAc 1:2]: R$_f$ = 0.3

Yield: 1.92g, 3.87mmol (60%), purity >98%

^{1}HNMR (600 MHz, CDCl$_3$) δ= 7.26-7.44 (m, 5H), 6.73-6.78 (m, 1H), 6.47-6.53 (m, 1H), 6.33-6.40 (m, 1H), 6.05-6.2 (m, 1H), 5.7-5.9 (m, 2H), 5.2-5.3 (m, 2H), 5.1-5.2 (m, 1H), 4.0-4.3 (m, 4H), 3.8-3.88 (m, 6H), 3.52-3.78 (m, 2H), 2.45-2.55 (m, 1H), 2.25-2.45 (m, 1H), 1.8-2.1 (m, 2H), 1.5-1.8 (m, 2H).

^{13}C NMR (150 MHz, CDCl$_3$) δ= 173.20, 171.18, 153.10, 154.50, 149.84, 143.66, 153.23, 132.85, 128.49, 128.45, 128.21, 127.97, 127.88, 118.08, 111.87, 104.00, 100.81, 68.72, 66.75, 56.42, 56.11, 55.87, 51.84, 46.26, 34.42, 25.76, 18.10

MS (ESI): m/z= 519.47 [M + Na]$^+$, calculated: 519.21[M + Na]$^+$.

7.2.61 Synthesis of (S)-benzyl 2-((2-(3,4-dimethoxyphenoxy)ethyl)(4-(trimethylsilyl) but-2-enyl)carbamoyl)-6-oxopiperidine-1-carboxylate 62

To a solution of (S)-N-(2-(3,4-dimethoxyphenoxy)ethyl)-6-oxo-N-(4-(trimethylsilyl)but-2-enyl)piperidine-2-carboxamide **53** (923mg, 2.06mmol) in 10ml THF was added 1M BuLi solution in hexanes (158mg, 2.47mmol) dropwise under argon at -78°C and stirred for 1 h followed by addition of Cbz-Cl (421mg, 2.47mmol). After 7 h at -78°C, a saturated NH_4Cl solution (20ml) was added at room temperature and extracted with DCM (6 x 20ml), dried over $MgSO_4$, filtered and concentrated *in vacuo*. The pure product was obtained by flash chromatography with cyclohexane: EtOAc 1:1.

TLC [cyclohexane: EtOAc 1:1]: $R_f = 0.4$

Yield: 871mg, 1.49mmol (73%)

^{1}HNMR (400 MHz, $CDCl_3$) δ= 7.26-7.42(m,5H), 6.74-6.78(m,1H), 6.47-6.52(m,1H), 6.34-6.39(m,1H), 5.55-5.7(m,1H), 5.25-5.33(m,2H), 5.2-5.25(m,2H), 5.05-5.15(m,1H), 4.05-4.2(m,2H), 3.9-4.05(m,2H), 3.8-3.87(m,6H), 3.70-3.75(m,1H), 3.5-3.6(m,1H), 2.6-2.7(m,1H), 2.4-2.5(m,1H), 2.2-2.4(m,1H), 2-2.1 (m,1H), 1.7-2.0(m,2H), 1.4-1.5 (m,2H), 0.01(t,9H,J=13.53,13.53Hz)

^{13}C NMR (100 MHz, $CDCl_3$) δ= 171.24, 170.84, 154.66, 153.14, 149.83, 143.60, 135.33, 132.13, 128.48, 128.16, 128.03, 127.92, 127.84, 122.38, 111.87, 104.03, 100.83, 68.68, 66.64, 56.42, 56.13, 55.85, 51.38, 45.26, 34.43, 25.73, 22.92, 18.14, -1.77

MS(ESI) : m/z: found 607.37 $[M+H]^+$, calculated 607.76$[M+H]^+$

8. Abbrevations

ACTH	Adrenocorticotropic Hormone
AR	Androgen Receptor
Brine	Saturated NaCl solution
BuLi	n-butyllithium
CN	Calcineurin
CRH	Corticotropin Releasing Hormone
DCM	Dichlormethane
DCC	N,N′-Dicyclohexylcarbodiimide
DIPEA	N,N-Diisopropylethylamine
EDC	1-Ethyl-3-(3-dimethylaminopropyl)carbodiimid
EE	Ethylacetate
ER	Estrogen Receptor
F	Phenylalanine
FKBP	FK506 binding protein
FP	Fluorescence Polarisation
GR	Glucocorticoid receptor
HOAt	1-Hydroxy-7-azabenzotriazole
HATU	2-(1H-7-Azabenzotriazol-1-yl)--1,1,3,3-tetramethyl uronium hexafluorophosphate Methanaminium
HPA	Hypothalamus pituitary adrenal
HPLC	High Pressure Liquid Chromatography
Hsp90	Heat shock protein 90
LDC	Lead Discovery Center
LiHMDS	Lithium hexamethyl disilazid
LiOH	Lithiumhydroxid
LMU	Ludwigs-Maximilians-University
MeOH	Methanol
MD	Major depression
MPI	Max-Planck-Institute
MR	Mineralcorticoid Receptor
NaHMDS	Natrium hexamethyl disilazid
n-Hex	n-Hexane
NMR	Nuclear magnetic resonance
PPIase	Peptidyl-prolyl-cis/trans-Isomerase
PR	Progesterone Receptor
PTSD	Post-traumatic stress disorder
Rap	Rapamycin
RT	Room Temperature
SAR	Structure Activity Relationship
SHR	Steroid Hormone Receptor
TFA	Trifluoroacetic acid
TEA	Triethylamine
TLC	Thin layer chromatography
THF	Tetrahydrofuran
V	Valine
WT	Wildtype

9. References

1.   Breiman, A.; Camus, I., The involvement of mammalian and plant FK506-binding proteins (FKBPs) in development. *Transgenic Res* **2002,** 11, (4), 321-35.
2.   Bharatham, N.; Chang, M. W.; Yoon, H. S., Targeting FK506 binding proteins to fight malarial and bacterial infections: current advances and future perspectives. *Curr Med Chem* **2011,** 18, (12), 1874-89.
3.   Dornan, J.; Taylor, P.; Walkinshaw, M. D., Structures of immunophilins and their ligand complexes. *Curr Top Med Chem* **2003,** 3, (12), 1392-409.
4.   Wedemeyer, W. J.; Welker, E.; Scheraga, H. A., Proline cis-trans isomerization and protein folding. *Biochemistry* **2002,** 41, (50), 14637-44.
5.   Yang, W. M.; Inouye, C. J.; Seto, E., Cyclophilin A and FKBP12 interact with YY1 and alter its transcriptional activity. *J Biol Chem* **1995,** 270, (25), 15187-93.
6.   Ochocka, A. M.; Kampanis, P.; Nicol, S.; Allende-Vega, N.; Cox, M.; Marcar, L.; Milne, D.; Fuller-Pace, F.; Meek, D., FKBP25, a novel regulator of the p53 pathway, induces the degradation of MDM2 and activation of p53. *FEBS Lett* **2009,** 583, (4), 621-6.
7.   Nelson, C. J.; Santos-Rosa, H.; Kouzarides, T., Proline isomerization of histone H3 regulates lysine methylation and gene expression. *Cell* **2006,** 126, (5), 905-16.
8.   Kuzuhara, T.; Horikoshi, M., A nuclear FK506-binding protein is a histone chaperone regulating rDNA silencing. *Nat Struct Mol Biol* **2004,** 11, (3), 275-83.
9.   Jin, Y. J.; Burakoff, S. J., The 25-kDa FK506-binding protein is localized in the nucleus and associates with casein kinase II and nucleolin. *Proc Natl Acad Sci U S A* **1993,** 90, (16), 7769-73.
10.   Noguchi, J.; Ozawa, M.; Nakai, M.; Somfai, T.; Kikuchi, K.; Kaneko, H.; Kunieda, T., Affected homologous chromosome pairing and phosphorylation of testis specific histone, H2AX, in male meiosis under FKBP6 deficiency. *J Reprod Dev* **2008,** 54, (3), 203-7.
11.   Kumar, P.; Mark, P. J.; Ward, B. K.; Minchin, R. F.; Ratajczak, T., Estradiol-regulated expression of the immunophilins cyclophilin 40 and FKBP52 in MCF-7 breast cancer cells. *Biochem Biophys Res Commun* **2001,** 284, (1), 219-25.
12.   Desmetz, C.; Bascoul-Mollevi, C.; Rochaix, P.; Lamy, P. J.; Kramar, A.; Rouanet, P.; Maudelonde, T.; Mange, A.; Solassol, J., Identification of a new panel of serum autoantibodies associated with the presence of in situ carcinoma of the breast in younger women. *Clin Cancer Res* **2009,** 15, (14), 4733-41.
13.   Pei, H.; Li, L.; Fridley, B. L.; Jenkins, G. D.; Kalari, K. R.; Lingle, W.; Petersen, G.; Lou, Z.; Wang, L., FKBP51 affects cancer cell response to chemotherapy by negatively regulating Akt. *Cancer Cell* **2009,** 16, (3), 259-66.
14.   Li, L.; Lou, Z.; Wang, L., The role of FKBP5 in cancer aetiology and chemoresistance. *Br J Cancer* **2011,** 104, (1), 19-23.
15.   Jinwal, U. K.; Koren, J., 3rd; Borysov, S. I.; Schmid, A. B.; Abisambra, J. F.; Blair, L. J.; Johnson, A. G.; Jones, J. R.; Shults, C. L.; O'Leary, J. C., 3rd; Jin, Y.; Buchner, J.; Cox, M. B.; Dickey, C. A., The Hsp90 cochaperone, FKBP51, increases Tau stability and polymerizes microtubules. *J Neurosci* **2010,** 30, (2), 591-9.
16.   Barth, S.; Nesper, J.; Hasgall, P. A.; Wirthner, R.; Nytko, K. J.; Edlich, F.; Katschinski, D. M.; Stiehl, D. P.; Wenger, R. H.; Camenisch, G., The peptidyl prolyl cis/trans isomerase FKBP38 determines hypoxia-inducible transcription factor prolyl-4-hydroxylase PHD2 protein stability. *Mol Cell Biol* **2007,** 27, (10), 3758-68.
17.   Choi, B. H.; Feng, L.; Yoon, H. S., FKBP38 protects Bcl-2 from caspase-dependent degradation. *J Biol Chem* **2010,** 285, (13), 9770-9.

18. Ahearn, I. M.; Tsai, F. D.; Court, H.; Zhou, M.; Jennings, B. C.; Ahmed, M.; Fehrenbacher, N.; Linder, M. E.; Philips, M. R., FKBP12 binds to acylated H-ras and promotes depalmitoylation. *Mol Cell* **2011,** 41, (2), 173-85.

19. Shirane, M.; Nakayama, K. I., Inherent calcineurin inhibitor FKBP38 targets Bcl-2 to mitochondria and inhibits apoptosis. *Nat Cell Biol* **2003,** 5, (1), 28-37.

20. Riggs, D. L.; Roberts, P. J.; Chirillo, S. C.; Cheung-Flynn, J.; Prapapanich, V.; Ratajczak, T.; Gaber, R.; Picard, D.; Smith, D. F., The Hsp90-binding peptidylprolyl isomerase FKBP52 potentiates glucocorticoid signaling in vivo. *Embo J* **2003,** 22, (5), 1158-67.

21. Cameron, A. M.; Steiner, J. P.; Sabatini, D. M.; Kaplin, A. I.; Walensky, L. D.; Snyder, S. H., Immunophilin FK506 binding protein associated with inositol 1,4,5-trisphosphate receptor modulates calcium flux. *Proc Natl Acad Sci U S A* **1995,** 92, (5), 1784-8.

22. Jayaraman, T.; Brillantes, A. M.; Timerman, A. P.; Fleischer, S.; Erdjument-Bromage, H.; Tempst, P.; Marks, A. R., FK506 binding protein associated with the calcium release channel (ryanodine receptor). *J Biol Chem* **1992,** 267, (14), 9474-7.

23. Shim, S.; Yuan, J. P.; Kim, J. Y.; Zeng, W.; Huang, G.; Milshteyn, A.; Kern, D.; Muallem, S.; Ming, G. L.; Worley, P. F., Peptidyl-prolyl isomerase FKBP52 controls chemotropic guidance of neuronal growth cones via regulation of TRPC1 channel opening. *Neuron* **2009,** 64, (4), 471-83.

24. Galat, A., Peptidylprolyl cis/trans isomerases (immunophilins): biological diversity--targets--functions. *Curr Top Med Chem* **2003,** 3, (12), 1315-47.

25. Pemberton, T. J.; Kay, J. E., Identification and comparative analysis of the peptidyl-prolyl cis/trans isomerase repertoires of H. sapiens, D. melanogaster, C. elegans, S. cerevisiae and Sz. pombe. *Comp Funct Genomics* **2005,** 6, (5-6), 277-300.

26. Kay, L. E.; Muhandiram, D. R.; Farrow, N. A.; Aubin, Y.; Forman-Kay, J. D., Correlation between dynamics and high affinity binding in an SH2 domain interaction. *Biochemistry* **1996,** 35, (2), 361-8.

27. Clardy, J., Borrowing to make ends meet. *Proc Natl Acad Sci U S A* **1999,** 96, (5), 1826-7.

28. Wu, B.; Li, P.; Liu, Y.; Lou, Z.; Ding, Y.; Shu, C.; Ye, S.; Bartlam, M.; Shen, B.; Rao, Z., 3D structure of human FK506-binding protein 52: Implications for the assembly of the glucocorticoid receptor/Hsp90/immunophilin heterocomplex *PNAS* **2004** 101, (22), 8348-8353.

29. Sinars, C. R., Structure of the Large FK506-Binding Protein FKBP51, an Hsp90-Binding Protein and a Component of Steroid Receptor Complexes. *PNAS* **2003,** 100 868-873

30. Pirkl, F.; Buchner, J., Functional analysis of the Hsp90-associated human peptidyl prolyl cis/trans isomerases FKBP51, FKBP52 and Cyp40. *J Mol Biol* **2001,** 308, (4), 795-806.

31. Riggs, D. L.; Cox, M. B.; Tardif, H. L.; Hessling, M.; Buchner, J.; Smith, D. F., Noncatalytic role of the FKBP52 peptidyl-prolyl isomerase domain in the regulation of steroid hormone signaling. *Mol Cell Biol* **2007,** 27, (24), 8658-69.

32. Taipale, M.; Jarosz, D. F.; Lindquist, S., HSP90 at the hub of protein homeostasis: emerging mechanistic insights. *Nat Rev Mol Cell Biol* **2011,** 11, (7), 515-28.

33. Sanchez, E. R., Hsp56: a novel heat shock protein associated with untransformed steroid receptor complexes. *J Biol Chem* **1990,** 265, (36), 22067-70.

34. Smith, D. F.; Faber, L. E.; Toft, D. O., Purification of unactivated progesterone receptor and identification of novel receptor-associated proteins. *J Biol Chem* **1990,** 265, (7), 3996-4003.

35. Marc B. Cox; Smith., D. F., *Functions of the Hsp90-Binding FKBP Immunophilins*. Austin: 2007.

36.   Cheung-Flynn, J.; Prapapanich, V.; Cox, M. B.; Riggs, D. L.; Suarez-Quian, C.; Smith, D. F., Physiological role for the cochaperone FKBP52 in androgen receptor signaling. *Mol Endocrinol* **2005,** 19, (6), 1654-66.

37.   Tranguch, S.; Cheung-Flynn, J.; Daikoku, T.; Prapapanich, V.; Cox, M. B.; Xie, H.; Wang, H.; Das, S. K.; Smith, D. F.; Dey, S. K., Cochaperone immunophilin FKBP52 is critical to uterine receptivity for embryo implantation. *Proc Natl Acad Sci U S A* **2005,** 102, (40), 14326-31.

38.   Ni, L.; Yang, C. S.; Gioeli, D.; Frierson, H.; Toft, D. O.; Paschal, B. M., FKBP51 promotes assembly of the Hsp90 chaperone complex and regulates androgen receptor signaling in prostate cancer cells. *Mol Cell Biol* **2010,** 30, (5), 1243-53.

39.   Periyasamy, S.; Hinds, T., Jr.; Shemshedini, L.; Shou, W.; Sanchez, E. R., FKBP51 and Cyp40 are positive regulators of androgen-dependent prostate cancer cell growth and the targets of FK506 and cyclosporin A. *Oncogene* **2010,** 29, (11), 1691-701.

40.   Chen, S.; Sullivan, W. P.; Toft, D. O.; Smith, D. F., Differential interactions of p23 and the TPR-containing proteins Hop, Cyp40, FKBP52 and FKBP51 with Hsp90 mutants. *Cell Stress Chaperones* **1998,** 3, (2), 118-29.

41.   Morishima, Y.; Kanelakis, K. C.; Murphy, P. J.; Lowe, E. R.; Jenkins, G. J.; Osawa, Y.; Sunahara, R. K.; Pratt, W. B., The hsp90 cochaperone p23 is the limiting component of the multiprotein hsp90/hsp70-based chaperone system in vivo where it acts to stabilize the client protein: hsp90 complex. *J Biol Chem* **2003,** 278, (49), 48754-63.

42.   Storer, C. L.; Dickey, C. A.; Galigniana, M. D.; Rein, T.; Cox, M. B., FKBP51 and FKBP52 in signaling and disease. *Trends Endocrinol Metab* **2011,** 22, (12), 481-90.

43.   Galigniana, M. D.; Echeverria, P. C.; Erlejman, A. G.; Piwien-Pilipuk, G., Role of molecular chaperones and TPR-domain proteins in the cytoplasmic transport of steroid receptors and their passage through the nuclear pore. *Nucleus* **2010,** 1, (4), 299-308.

44.   de Kloet, E. R.; Joels, M.; Holsboer, F., Stress and the brain: from adaptation to disease. *Nat Rev Neurosci* **2005,** 6, (6), 463-75.

45.   Holsboer, F., The corticosteroid receptor hypothesis of depression. *Neuropsychopharmacology* **2000,** 23, (5), 477-501.

46.   Wochnik, G. M.; Ruegg, J.; Abel, G. A.; Schmidt, U.; Holsboer, F.; Rein, T., FK506-binding Proteins 51 and 52 Differentially Regulate Dynein Interaction and Nuclear Translocation of the Glucocorticoid Receptor in Mammalian Cells. *J. Biol. Chem.* **2005,** 280, (6), 4609-4616.

47.   Binder, E. B.; Salyakina, D.; Lichtner, P.; Wochnik, G. M.; Ising, M.; Putz, B.; Papiol, S.; Seaman, S.; Lucae, S.; Kohli, M. A.; Nickel, T.; Kunzel, H. E.; Fuchs, B.; Majer, M.; Pfennig, A.; Kern, N.; Brunner, J.; Modell, S.; Baghai, T.; Deiml, T.; Zill, P.; Bondy, B.; Rupprecht, R.; Messer, T.; Kohnlein, O.; Dabitz, H.; Bruckl, T.; Muller, N.; Pfister, H.; Lieb, R.; Mueller, J. C.; Lohmussaar, E.; Strom, T. M.; Bettecken, T.; Meitinger, T.; Uhr, M.; Rein, T.; Holsboer, F.; Muller-Myhsok, B., Polymorphisms in FKBP5 are associated with increased recurrence of depressive episodes and rapid response to antidepressant treatment. *Nat Genet* **2004,** 36, (12), 1319-25.

48.   Kirchheiner, J.; Lorch, R.; Lebedeva, E.; Seeringer, A.; Roots, I.; Sasse, J.; Brockmöller, J. r., Genetic variants in FKBP5 affecting response to antidepressant drug treatment. *Pharmacogenomics* **2008,** 9, (7), 841-846.

49.   Lekman, M.; Laje, G.; Charney, D.; Rush, A. J.; Wilson, A. F.; Sorant, A. J. M.; Lipsky, R.; Wisniewski, S. R.; Manji, H.; McMahon, F. J.; Paddock, S., The FKBP5-Gene in Depression and Treatment Response - an Association Study in the Sequenced Treatment Alternatives to Relieve Depression (STAR*D) Cohort. *Biological Psychiatry* **2008,** 63, (12), 1103-1110.

50.   Willour, V. L.; Chen, H.; Toolan, J.; Belmonte, P.; Cutler, D. J.; Goes, F. S.; Zandi, P. P.; Lee, R. S.; MacKinnon, D. F.; Mondimore, F. M.; Schweizer, B.; DePaulo, J. R., Jr.;

Gershon, E. S.; McMahon, F. J.; Potash, J. B., Family-based association of FKBP5 in bipolar disorder. *Mol Psychiatry* **2009,** 14, (3), 261-8.

51.   Brent, D.; Melhem, N.; Ferrell, R.; Emslie, G.; Wagner, K. D.; Ryan, N.; Vitiello, B.; Birmaher, B.; Mayes, T.; Zelazny, J.; Onorato, M.; Devlin, B.; Clarke, G.; DeBar, L.; Keller, M., Association of FKBP5 polymorphisms with suicidal events in the Treatment of Resistant Depression in Adolescents (TORDIA) study. *Am J Psychiatry* **2010,** 167, (2), 190-7.

52.   Supriyanto, I.; Sasada, T.; Fukutake, M.; Asano, M.; Ueno, Y.; Nagasaki, Y.; Shirakawa, O.; Hishimoto, A., Association of FKBP5 gene haplotypes with completed suicide in the Japanese population. *Prog Neuropsychopharmacol Biol Psychiatry* **2011,** 35, (1), 252-6.

53.   Roy, A.; Gorodetsky, E.; Yuan, Q.; Goldman, D.; Enoch, M. A., Interaction of FKBP5, a stress-related gene, with childhood trauma increases the risk for attempting suicide. *Neuropsychopharmacology* **2010,** 35, (8), 1674-83.

54.   Roy, A.; Hodgkinson, C. A.; Deluca, V.; Goldman, D.; Enoch, M. A., Two HPA axis genes, CRHBP and FKBP5, interact with childhood trauma to increase the risk for suicidal behavior. *J Psychiatr Res* **2012,** 46, (1), 72-9.

55.   Ising, M.; Depping, A. M.; Siebertz, A.; Lucae, S.; Unschuld, P. G.; Kloiber, S.; Horstmann, S.; Uhr, M.; Muller-Myhsok, B.; Holsboer, F., Polymorphisms in the FKBP5 gene region modulate recovery from psychosocial stress in healthy controls. *Eur J Neurosci* **2008,** 28, (2), 389-98.

56.   Koenen, K. C.; Saxe, G.; Purcell, S.; Smoller, J. W.; Bartholomew, D.; Miller, A.; Hall, E.; Kaplow, J.; Bosquet, M.; Moulton, S.; Baldwin, C., Polymorphisms in FKBP5 are associated with peritraumatic dissociation in medically injured children. *Mol Psychiatry* **2005,** 10, (12), 1058-1059.

57.   Ozer, E. J.; Best, S. R.; Lipsey, T. L.; Weiss, D. S., Predictors of posttraumatic stress disorder and symptoms in adults: a meta-analysis. *Psychol Bull* **2003,** 129, (1), 52-73.

58.   Yehuda, R.; Cai, G.; Golier, J. A.; Sarapas, C.; Galea, S.; Ising, M.; Rein, T.; Schmeidler, J.; Muller-Myhsok, B.; Holsboer, F.; Buxbaum, J. D., Gene expression patterns associated with posttraumatic stress disorder following exposure to the World Trade Center attacks. *Biol Psychiatry* **2009,** 66, (7), 708-11.

59.   Attwood, B. K.; Bourgognon, J. M.; Patel, S.; Mucha, M.; Schiavon, E.; Skrzypiec, A. E.; Young, K. W.; Shiosaka, S.; Korostynski, M.; Piechota, M.; Przewlocki, R.; Pawlak, R., Neuropsin cleaves EphB2 in the amygdala to control anxiety. *Nature* **2011,** 473, (7347), 372-5.

60.   Touma, C.; Gassen, N. C.; Herrmann, L.; Cheung-Flynn, J.; Bull, D. R.; Ionescu, I. A.; Heinzmann, J. M.; Knapman, A.; Siebertz, A.; Depping, A. M.; Hartmann, J.; Hausch, F.; Schmidt, M. V.; Holsboer, F.; Ising, M.; Cox, M. B.; Schmidt, U.; Rein, T., FK506 Binding Protein 5 Shapes Stress Responsiveness: Modulation of Neuroendocrine Reactivity and Coping Behavior. *Biol Psychiatry* **2011**.

61.   Hartmann, J.; Wagner, K. V.; Liebl, C.; Scharf, S. H.; Wang, X. D.; Wolf, M.; Hausch, F.; Rein, T.; Schmidt, U.; Touma, C.; Cheung-Flynn, J.; Cox, M. B.; Smith, D. F.; Holsboer, F.; Muller, M. B.; Schmidt, M. V., The involvement of FK506-binding protein 51 (FKBP5) in the behavioral and neuroendocrine effects of chronic social defeat stress. *Neuropharmacology* **2011**.

62.   O'Leary, J. C., 3rd; Dharia, S.; Blair, L. J.; Brady, S.; Johnson, A. G.; Peters, M.; Cheung-Flynn, J.; Cox, M. B.; de Erausquin, G.; Weeber, E. J.; Jinwal, U. K.; Dickey, C. A., A New Anti-Depressive Strategy for the Elderly: Ablation of FKBP5/FKBP51. *PLoS One* **2011,** 6, (9), e24840.

63.   Scharf, S. H.; Liebl, C.; Binder, E. B.; Schmidt, M. V.; Muller, M. B., Expression and regulation of the Fkbp5 gene in the adult mouse brain. *PLoS One* **2011,** 6, (2), e16883.

64.   Belmaker, R. H., Major Depressive Disorder

The New England Journal of Medicine **2008,** 358, (3), 55-68.

65.   Liu, T. M.; Martina, M.; Hutmacher, D. W.; Hui, J. H.; Lee, E. H.; Lim, B., Identification of common pathways mediating differentiation of bone marrow- and adipose tissue-derived human mesenchymal stem cells into three mesenchymal lineages. *Stem Cells* **2007,** 25, (3), 750-60.

66.   Menicanin, D.; Bartold, P. M.; Zannettino, A. C.; Gronthos, S., Genomic profiling of mesenchymal stem cells. *Stem Cell Rev* **2009,** 5, (1), 36-50.

67.   Yeh, W. C.; Li, T. K.; Bierer, B. E.; McKnight, S. L., Identification and characterization of an immunophilin expressed during the clonal expansion phase of adipocyte differentiation. *Proc Natl Acad Sci U S A* **1995,** 92, (24), 11081-5.

68.   Yeh, W. C.; Bierer, B. E.; McKnight, S. L., Rapamycin inhibits clonal expansion and adipogenic differentiation of 3T3-L1 cells. *Proc Natl Acad Sci U S A* **1995,** 92, (24), 11086-90.

69.   Jiang, W.; Cazacu, S.; Xiang, C.; Zenklusen, J. C.; Fine, H. A.; Berens, M.; Armstrong, B.; Brodie, C.; Mikkelsen, T., FK506 binding protein mediates glioma cell growth and sensitivity to rapamycin treatment by regulating NF-kappaB signaling pathway. *Neoplasia* **2008,** 10, (3), 235-43.

70.   Daudt, D. R.; Yorio, T., FKBP51 protects 661w cell culture from staurosporine-induced apoptosis. *Mol Vis* **2011,** 17, 1172-81.

71.   Avellino, R.; Romano, S.; Parasole, R.; Bisogni, R.; Lamberti, A.; Poggi, V.; Venuta, S.; Romano, M. F., Rapamycin stimulates apoptosis of childhood acute lymphoblastic leukemia cells. *Blood* **2005,** 106, (4), 1400-6.

72.   Romano, S.; D'Angelillo, A.; Pacelli, R.; Staibano, S.; De Luna, E.; Bisogni, R.; Eskelinen, E. L.; Mascolo, M.; Cali, G.; Arra, C.; Romano, M. F., Role of FK506-binding protein 51 in the control of apoptosis of irradiated melanoma cells. *Cell Death Differ* **2010,** 17, (1), 145-57.

73.   Staibano, S.; Mascolo, M.; Ilardi, G.; Siano, M.; De Rosa, G., Immunohistochemical analysis of FKBP51 in human cancers. *Curr Opin Pharmacol* **2011,** 11, (4), 338-47.

74.   Stechschulte, L. A.; Sanchez, E. R., FKBP51-a selective modulator of glucocorticoid and androgen sensitivity. *Curr Opin Pharmacol* **2011,** 11, (4), 332-7.

75.   O'Malley, K. J.; Dhir, R.; Nelson, J. B.; Bost, J.; Lin, Y.; Wang, Z., The expression of androgen-responsive genes is up-regulated in the epithelia of benign prostatic hyperplasia. *Prostate* **2009,** 69, (16), 1716-23.

76.   Hubler, T. R.; Denny, W. B.; Valentine, D. L.; Cheung-Flynn, J.; Smith, D. F.; Scammell, J. G., The FK506-binding immunophilin FKBP51 is transcriptionally regulated by progestin and attenuates progestin responsiveness. *Endocrinology* **2003,** 144, (6), 2380-7.

77.   Reynolds, P. D.; Ruan, Y.; Smith, D. F.; Scammell, J. G., Glucocorticoid resistance in the squirrel monkey is associated with overexpression of the immunophilin FKBP51. *J Clin Endocrinol Metab* **1999,** 84, (2), 663-9.

78.   Denny, W. B.; Valentine, D. L.; Reynolds, P. D.; Smith, D. F.; Scammell, J. G., Squirrel monkey immunophilin FKBP51 is a potent inhibitor of glucocorticoid receptor binding. *Endocrinology* **2000,** 141, (11), 4107-13.

79.   Febbo, P. G.; Lowenberg, M.; Thorner, A. R.; Brown, M.; Loda, M.; Golub, T. R., Androgen mediated regulation and functional implications of fkbp51 expression in prostate cancer. *J Urol* **2005,** 173, (5), 1772-7.

80.   Romano, S.; Di Pace, A.; Sorrentino, A.; Bisogni, R.; Sivero, L.; Romano, M. F., FK506 binding proteins as targets in anticancer therapy. *Anticancer Agents Med Chem* **2010,** 10, (9), 651-6.

81.   Mukaide, H.; Adachi, Y.; Taketani, S.; Iwasaki, M.; Koike-Kiriyama, N.; Shigematsu, A.; Shi, M.; Yanai, S.; Yoshioka, K.; Kamiyama, Y.; Ikehara, S., FKBP51 expressed by both

normal epithelial cells and adenocarcinoma of colon suppresses proliferation of colorectal adenocarcinoma. *Cancer Invest* **2008,** 26, (4), 385-90.

82.   Rees-Unwin, K. S.; Craven, R. A.; Davenport, E.; Hanrahan, S.; Totty, N. F.; Dring, A. M.; Banks, R. E.; G, J. M.; Davies, F. E., Proteomic evaluation of pathways associated with dexamethasone-mediated apoptosis and resistance in multiple myeloma. *Br J Haematol* **2007,** 139, (4), 559-67.

83.   Romano, M. F.; Avellino, R.; Petrella, A.; Bisogni, R.; Romano, S.; Venuta, S., Rapamycin inhibits doxorubicin-induced NF-kappaB/Rel nuclear activity and enhances the apoptosis of melanoma cells. *Eur J Cancer* **2004,** 40, (18), 2829-36.

84.   Lin, J. F.; Xu, J.; Tian, H. Y.; Gao, X.; Chen, Q. X.; Gu, Q.; Xu, G. J.; Song, J. D.; Zhao, F. K., Identification of candidate prostate cancer biomarkers in prostate needle biopsy specimens using proteomic analysis. *Int J Cancer* **2007,** 121, (12), 2596-605.

85.   De Leon, J. T.; Iwai, A.; Feau, C.; Garcia, Y.; Balsiger, H. A.; Storer, C. L.; Suro, R. M.; Garza, K. M.; Lee, S.; Kim, Y. S.; Chen, Y.; Ning, Y. M.; Riggs, D. L.; Fletterick, R. J.; Guy, R. K.; Trepel, J. B.; Neckers, L. M.; Cox, M. B., Targeting the regulation of androgen receptor signaling by the heat shock protein 90 cochaperone FKBP52 in prostate cancer cells. *Proc Natl Acad Sci U S A* **2011,** 108, (29), 11878-83.

86.   Sivils, J. C.; Storer, C. L.; Galigniana, M. D.; Cox, M. B., Regulation of steroid hormone receptor function by the 52-kDa FK506-binding protein (FKBP52). *Curr Opin Pharmacol* **2011,** 11, (4), 314-9.

87.   Warrier, M.; Hinds, T. D., Jr.; Ledford, K. J.; Cash, H. A.; Patel, P. R.; Bowman, T. A.; Stechschulte, L. A.; Yong, W.; Shou, W.; Najjar, S. M.; Sanchez, E. R., Susceptibility to diet-induced hepatic steatosis and glucocorticoid resistance in FK506-binding protein 52-deficient mice. *Endocrinology* **2010,** 151, (7), 3225-36.

88.   Yang, Z.; Wolf, I. M.; Chen, H.; Periyasamy, S.; Chen, Z.; Yong, W.; Shi, S.; Zhao, W.; Xu, J.; Srivastava, A.; Sanchez, E. R.; Shou, W., FK506-binding protein 52 is essential to uterine reproductive physiology controlled by the progesterone receptor A isoform. *Mol Endocrinol* **2006,** 20, (11), 2682-94.

89.   Yong, W.; Yang, Z.; Periyasamy, S.; Chen, H.; Yucel, S.; Li, W.; Lin, L. Y.; Wolf, I. M.; Cohn, M. J.; Baskin, L. S.; Sanchez, E. R.; Shou, W., Essential role for Co-chaperone Fkbp52 but not Fkbp51 in androgen receptor-mediated signaling and physiology. *J Biol Chem* **2007,** 282, (7), 5026-36.

90.   Matsushita, R.; Hashimoto, A.; Tomita, T.; Yoshitawa, H.; Tanaka, S.; Endo, H.; Hirohata, S., Enhanced expression of mRNA for FK506-binding protein 5 in bone marrow CD34 positive cells in patients with rheumatoid arthritis. *Clin Exp Rheumatol* **2010,** 28, (1), 87-90.

91.   Park, J.; Kim, M.; Na, G.; Jeon, I.; Kwon, Y. K.; Kim, J. H.; Youn, H.; Koo, Y., Glucocorticoids modulate NF-kappaB-dependent gene expression by up-regulating FKBP51 expression in Newcastle disease virus-infected chickens. *Mol Cell Endocrinol* **2007,** 278, (1-2), 7-17.

92.   Baker, R. G.; Hayden, M. S.; Ghosh, S., NF-kappaB, inflammation, and metabolic disease. *Cell Metab* **2011,** 13, (1), 11-22.

93.   Hayden, M. S.; Ghosh, S., NF-kappaB in immunobiology. *Cell Res* **2011,** 21, (2), 223-44.

94.   Holownia, A.; Mroz, R. M.; Kolodziejczyk, A.; Chyczewska, E.; Braszko, J. J., Increased FKBP51 in induced sputum cells of chronic obstructive pulmonary disease patients after therapy. *Eur J Med Res* **2009,** 14 Suppl 4, 108-11.

95.   Imai, A.; Sahara, H.; Tamura, Y.; Jimbow, K.; Saito, T.; Ezoe, K.; Yotsuyanagi, T.; Sato, N., Inhibition of endogenous MHC class II-restricted antigen presentation by tacrolimus (FK506) via FKBP51. *Eur J Immunol* **2007,** 37, (7), 1730-8.

96.   Baughman, G.; Wiederrecht, G. J.; Campbell, N. F.; Martin, M. M.; Bourgeois, S., FKBP51, a novel T-cell-specific immunophilin capable of calcineurin inhibition. *Mol Cell Biol* **1995,** 15, (8), 4395-402.

97.   Weiwad, M.; Edlich, F.; Kilka, S.; Erdmann, F.; Jarczowski, F.; Dorn, M.; Moutty, M. C.; Fischer, G., Comparative analysis of calcineurin inhibition by complexes of immunosuppressive drugs with human FK506 binding proteins. *Biochemistry* **2006,** 45, (51), 15776-84.

98.   Blatch, G. L., Chaperones. *Networking of Chaperones by Co-Chaperones* **2006**.

99.   Charters, A. R.; Kobayashi, M.; Butcher, S. P., Immunochemical analysis of FK506 binding proteins in neuronal cell lines and rat brain. *Biochem Soc Trans* **1994,** 22, (4), 411S.

100.   Coss, M. C.; Stephens, R. M.; Morrison, D. K.; Winterstein, D.; Smith, L. M.; Simek, S. L., The immunophilin FKBP65 forms an association with the serine/threonine kinase c-Raf-1. *Cell Growth Differ* **1998,** 9, (1), 41-8.

101.   Chambraud, B.; Belabes, H.; Fontaine-Lenoir, V.; Fellous, A.; Baulieu, E. E., The immunophilin FKBP52 specifically binds to tubulin and prevents microtubule formation. *Faseb J* **2007,** 21, (11), 2787-97.

102.   Fusco, D.; Vargiolu, M.; Vidone, M.; Mariani, E.; Pennisi, L. F.; Bonora, E.; Capellari, S.; Dirnberger, D.; Baumeister, R.; Martinelli, P.; Romeo, G., The RET51/FKBP52 complex and its involvement in Parkinson disease. *Hum Mol Genet* **2010,** 19, (14), 2804-16.

103.   Chambraud, B.; Sardin, E.; Giustiniani, J.; Dounane, O.; Schumacher, M.; Goedert, M.; Baulieu, E. E., A role for FKBP52 in Tau protein function. *Proc Natl Acad Sci U S A* **2010,** 107, (6), 2658-63.

104.   Elbi, C.; Walker, D. A.; Lewis, M.; Romero, G.; Sullivan, W. P.; Toft, D. O.; Hager, G. L.; DeFranco, D. B., A novel in situ assay for the identification and characterization of soluble nuclear mobility factors. *Sci STKE* **2004,** 2004, (238), pl10.

105.   Galas, M. C.; Dourlen, P.; Begard, S.; Ando, K.; Blum, D.; Hamdane, M.; Buee, L., The peptidylprolyl cis/trans-isomerase Pin1 modulates stress-induced dephosphorylation of Tau in neurons. Implication in a pathological mechanism related to Alzheimer disease. *J Biol Chem* **2006,** 281, (28), 19296-304.

106.   Sanokawa-Akakura, R.; Dai, H.; Akakura, S.; Weinstein, D.; Fajardo, J. E.; Lang, S. E.; Wadsworth, S.; Siekierka, J.; Birge, R. B., A novel role for the immunophilin FKBP52 in copper transport. *J Biol Chem* **2004,** 279, (27), 27845-8.

107.   Hamza, I.; Faisst, A.; Prohaska, J.; Chen, J.; Gruss, P.; Gitlin, J. D., The metallochaperone Atox1 plays a critical role in perinatal copper homeostasis. *Proc Natl Acad Sci U S A* **2001,** 98, (12), 6848-52.

108.   Barnham, K. J.; Bush, A. I., Metals in Alzheimer's and Parkinson's diseases. *Curr Opin Chem Biol* **2008,** 12, (2), 222-8.

109.   Sanokawa-Akakura, R.; Cao, W.; Allan, K.; Patel, K.; Ganesh, A.; Heiman, G.; Burke, R.; Kemp, F. W.; Bogden, J. D.; Camakaris, J.; Birge, R. B.; Konsolaki, M., Control of Alzheimer's amyloid beta toxicity by the high molecular weight immunophilin FKBP52 and copper homeostasis in Drosophila. *PLoS One* **2010,** 5, (1), e8626.

110.   Manabe, Y.; Warita, H.; Murakami, T.; Shiote, M.; Hayashi, T.; Omori, N.; Nagano, I.; Shoji, M.; Abe, K., Early decrease of the immunophilin FKBP 52 in the spinal cord of a transgenic model for amyotrophic lateral sclerosis. *Brain Res* **2002,** 935, (1-2), 124-8.

111.   Crabtree, G. R.; Schreiber, S. L., SnapShot: Ca2+-calcineurin-NFAT signaling. *Cell* **2009,** 138, (1), 210, 210 e1.

112.   Xu, X.; Su, B.; Barndt, R. J.; Chen, H.; Xin, H.; Yan, G.; Chen, L.; Cheng, D.; Heitman, J.; Zhuang, Y.; Fleischer, S.; Shou, W., FKBP12 is the only FK506 binding protein mediating T-cell inhibition by the immunosuppressant FK506. *Transplantation* **2002,** 73, (11), 1835-8.

113.   Gaali, S.; Gopalakrishnan, R.; Wang, Y.; Kozany, C.; Hausch, F., The chemical biology of immunophilin ligands. *Curr Med Chem* **2011,** 18, (35), 5355-79.

114.   Hui, K. K.; Liadis, N.; Robertson, J.; Kanungo, A.; Henderson, J. T., Calcineurin inhibition enhances motor neuron survival following injury. *J Cell Mol Med* **2010,** 14, (3), 671-86.

115.   Park, K. K.; Liu, K.; Hu, Y.; Smith, P. D.; Wang, C.; Cai, B.; Xu, B.; Connolly, L.; Kramvis, I.; Sahin, M.; He, Z., Promoting axon regeneration in the adult CNS by modulation of the PTEN/mTOR pathway. *Science* **2008,** 322, (5903), 963-6.

116.   Ruan, B.; Pong, K.; Jow, F.; Bowlby, M.; Crozier, R. A.; Liu, D.; Liang, S.; Chen, Y.; Mercado, M. L.; Feng, X.; Bennett, F.; von Schack, D.; McDonald, L.; Zaleska, M. M.; Wood, A.; Reinhart, P. H.; Magolda, R. L.; Skotnicki, J.; Pangalos, M. N.; Koehn, F. E.; Carter, G. T.; Abou-Gharbia, M.; Graziani, E. I., Binding of rapamycin analogs to calcium channels and FKBP52 contributes to their neuroprotective activities. *Proc Natl Acad Sci U S A* **2008,** 105, (1), 33-8.

117.   Edlich, F.; Weiwad, M.; Wildemann, D.; Jarczowski, F.; Kilka, S.; Moutty, M. C.; Jahreis, G.; Lucke, C.; Schmidt, W.; Striggow, F.; Fischer, G., The specific FKBP38 inhibitor N-(N',N'-dimethylcarboxamidomethyl)cycloheximide has potent neuroprotective and neurotrophic properties in brain ischemia. *J Biol Chem* **2006,** 281, (21), 14961-70.

118.   Kupina, N. C.; Detloff, M. R.; Dutta, S.; Hall, E. D., Neuroimmunophilin ligand V-10,367 is neuroprotective after 24-hour delayed administration in a mouse model of diffuse traumatic brain injury. *J Cereb Blood Flow Metab* **2002,** 22, (10), 1212-21.

119.   Yamazaki, S.; Yamaji, T.; Murai, N.; Yamamoto, H.; Price, R. D.; Matsuoka, N.; Mutoh, S., FK1706, a novel non-immunosuppressive immunophilin ligand, modifies the course of painful diabetic neuropathy. *Neuropharmacology* **2008,** 55, (7), 1226-30.

120.   Liu, D.; McIlvain, H. B.; Fennell, M.; Dunlop, J.; Wood, A.; Zaleska, M. M.; Graziani, E. I.; Pong, K., Screening of immunophilin ligands by quantitative analysis of neurofilament expression and neurite outgrowth in cultured neurons and cells. *J Neurosci Methods* **2007,** 163, (2), 310-20.

121.   Summers, M. Y.; Leighton, M.; Liu, D.; Pong, K.; Graziani, E. I., 3-normeridamycin: a potent non-immunosuppressive immunophilin ligand is neuroprotective in dopaminergic neurons. *J Antibiot (Tokyo)* **2006,** 59, (3), 184-9.

122.   Costantini, L. C.; Cole, D.; Pravin, C.; Isacson, O., Immunophilin ligands can prevent progressive dopaminergic degeneration in animal models of Parkinson's disease. *European Journal of Neuroscience* **2001,** 13, (6), 1085-1092.

123.   Steiner, J. P.; Connolly, M. A.; Valentine, H. L.; Hamilton, G. S.; Dawson, T. M.; Hester, L.; Snyder, S. H., Neurotrophic actions of nonimmunosuppressive analogues of immunosuppressive drugs FK506, rapamycin and cyclosporin A. *Nat Med* **1997,** 3, (4), 421-8.

124.   Revill, W. P.; Voda, J.; Reeves, C. R.; Chung, L.; Schirmer, A.; Ashley, G.; Carney, J. R.; Fardis, M.; Carreras, C. W.; Zhou, Y.; Feng, L.; Tucker, E.; Robinson, D.; Gold, B. G., Genetically engineered analogs of ascomycin for nerve regeneration. *J Pharmacol Exp Ther* **2002,** 302, (3), 1278-85.

125.   Voda, J.; Yamaji, T.; Gold, B. G., Neuroimmunophilin ligands improve functional recovery and increase axonal growth after spinal cord hemisection in rats. *J Neurotrauma* **2005,** 22, (10), 1150-61.

126.   Gold, B. G.; Armistead, D. M.; Wang, M. S., Non-FK506-binding protein-12 neuroimmunophilin ligands increase neurite elongation and accelerate nerve regeneration. *J Neurosci Res* **2005,** 80, (1), 56-65.

127.   Armistead, D. M.; Badia, M. C.; Deininger, D. D.; Duffy, J. P.; Saunders, J. O.; Tung, R. D.; Thomson, J. A.; DeCenzo, M. T.; Futer, O.; Livingston, D. J.; Murcko, M. A.; Yamashita, M. M.; Navia, M. A., Design, synthesis and structure of non-macrocyclic

inhibitors of FKBP12, the major binding protein for the immunosuppressant FK506. *Acta Crystallogr D Biol Crystallogr* **1995,** 51, (Pt 4), 522-8.

128. Germann, U. A.; Shlyakhter, D.; Mason, V. S.; Zelle, R. E.; Duffy, J. P.; Galullo, V.; Armistead, D. M.; Saunders, J. O.; Boger, J.; Harding, M. W., Cellular and biochemical characterization of VX-710 as a chemosensitizer: reversal of P-glycoprotein-mediated multidrug resistance in vitro. *Anticancer Drugs* **1997,** 8, (2), 125-40.

129. Birge, R. B.; Wadsworth, S.; Akakura, R.; Abeysinghe, H.; Kanojia, R.; MacIelag, M.; Desbarats, J.; Escalante, M.; Singh, K.; Sundarababu, S.; Parris, K.; Childs, G.; August, A.; Siekierka, J.; Weinstein, D. E., A role for schwann cells in the neuroregenerative effects of a non-immunosuppressive fk506 derivative, jnj460. *Neuroscience* **2004,** 124, (2), 351-66.

130. Bocquet, A.; Lorent, G.; Fuks, B.; Grimee, R.; Talaga, P.; Daliers, J.; Klitgaard, H., Failure of GPI compounds to display neurotrophic activity in vitro and in vivo. *Eur J Pharmacol* **2001,** 415, (2-3), 173-80.

131. Graziani, F.; Aldegheri, L.; Terstappen, G. C., High Throughput Scintillation Proximity Assay for the Identification of FKBP-12 Ligands. *J Biomol Screen* **1999,** 4, (1), 3-7.

132. Rabinowitz, M.; Seneci, P.; Rossi, T.; Dal Cin, M.; Deal, M.; Terstappen, G., Solid-phase/solution-phase combinatorial synthesis of neuroimmunophilin ligands. *Bioorg Med Chem Lett* **2000,** 10, (10), 1007-10.

133. Sich, C.; Improta, S.; Cowley, D. J.; Guenet, C.; Merly, J. P.; Teufel, M.; Saudek, V., Solution structure of a neurotrophic ligand bound to FKBP12 and its effects on protein dynamics. *Eur J Biochem* **2000,** 267, (17), 5342-55.

134. Gopalakrishnan, R.; Kozany, C.; Gaali, S.; Kress, C.; Hoogeland, B.; Bracher, A.; Hausch, F., Evaluation of Synthetic FK506 Analogs as Ligands for the FK506-Binding Proteins 51 and 52. *J Med Chem* **2012**.

135. Gerard, M.; Deleersnijder, A.; Demeulemeester, J.; Debyser, Z.; Baekelandt, V., Unraveling the role of peptidyl-prolyl isomerases in neurodegeneration. *Mol Neurobiol* **2011,** 44, (1), 13-27.

136. Marshall, V. L. G., D. G. , GPI-1485 (Guilford). *Curr Opin Investig Drugs* **2004,** 5, 107-112.

137. Hamilton, G. S. N., M. H.; Wu, Y.-Q. Carboxylic acids and carboxylic acid isosters of N-heterocyclic compounds. . 2000.

138. Gold, B. G.; Densmore, V.; Shou, W.; Matzuk, M. M.; Gordon, H. S., Immunophilin FK506-binding protein 52 (not FK506-binding protein 12) mediates the neurotrophic action of FK506. *J Pharmacol Exp Ther* **1999,** 289, (3), 1202-10.

139. Hudack, R. A., Jr.; Barta, N. S.; Guo, C.; Deal, J.; Dong, L.; Fay, L. K.; Caprathe, B.; Chatterjee, A.; Vanderpool, D.; Bigge, C.; Showalter, R.; Bender, S.; Augelli-Szafran, C. E.; Lunney, E.; Hou, X., Design, synthesis, and biological activity of novel polycyclic aza-amide FKBP12 ligands. *J Med Chem* **2006,** 49, (3), 1202-6.

140. Gaali, S.; Gopalakrishnan, R.; Wang, Y.; Kozany, C.; Hausch, F., The Chemical Biology of Immunophilin Ligands. *Current Medicinal Chemistry* **2011,** 18.

141. Kozany, C.; März, A.; Kress, C.; Hausch, F., Fluorescent Probes to Characterise FK506-Binding Proteins. *ChemBioChem* **2009,** 10, (8), 1402-1410.

142. Keenan, T.; Yaeger, D. R.; Courage, N. L.; Rollins, C. T.; Pavone, M. E.; Rivera, V. M.; Yang, W.; Guo, T.; Amara, J. F.; Clackson, T.; Gilman, M.; Holt, D. A., Synthesis and activity of bivalent FKBP12 ligands for the regulated dimerization of proteins. *Bioorg Med Chem* **1998,** 6, (8), 1309-35.

143. Gopalakrishnan, R.; Kozany, C.; Wang, Y.; Schneider, S.; Hoogeland, B.; Bracher, A.; Hausch, F., Exploration of Pipecolate Sulfonamides as Binders of the FK506-Binding Proteins 51 and 52. *J Med Chem* **2012**.

144. Dennis A. Holt, Design, synthesis, and kinetic evaluation of high-affinity FKBP ligands and the X-ray crystal structures of their complexes with FKBP12. *Journal of the American Chemical Society* **1993** 115, (22), 9925-9938.

145. Wang, X. J., Peptidyl-prolyl isomerase inhibitors. *Current Trends in Peptide Science* **2004,** 84, 125-146.

146. Andreas Bracher, C. K., Ann-Katrin Thost,Felix Hausch, Structural characterization of the PPIase domain of FKBP51, a cochaperone of human Hsp90. *Acta Crystallographica Section D* **2011,** 67, (6), 549–559.

147. Hopkins, A. L.; Groom, C. R.; Alex, A., Ligand efficiency: a useful metric for lead selection. *Drug Discov Today* **2004,** 9, (10), 430-1.

148. Abad-Zapatero, C., Ligand efficiency indices for effective drug discovery. *Expert Opinion on Drug Discovery* **2007,** 2, (4), 136-488.

149. Holt, D. A.; Luengo, J. I.; Yamashita, D. S.; Oh, H. J.; Konilian, A. L.; Yen, H. K.; Rozamus, L. W.; Brandt, M.; Bossard, M. J.; Levy, M. A.; Eggleston, D. S.; Liang, J.; Schultz, W.; Stout, T. J.; Clardy, J., Design, synthesis, and kinetic evaluation of high-affinity FKBP ligands and the X-ray crystal structures of their complexes with FKBP 12. *J Am Chem Soc* **1993,** 115, (22), 9925-38.

150. Mannhold, R., *Molecular Drug Properties: Measurement and Prediction.* Wiley-VCH: 2007; Vol. 37.

151. Hao, M.-H.; Haq, O.; Muegge, I., Torsion Angle Preference and Energetics of Small-Molecule Ligands Bound to Proteins. *Journal of Chemical Information and Modeling* **2007,** 47, (6), 2242–2252.

152. Perola, E.; Charifson, P. S., Conformational Analysis of Drug-Like Molecules Bound to Proteins:☐ An Extensive Study of Ligand Reorganization upon Binding. *Journal of Medicinal Chemistry* **2004,** 47, (10), 2499–2510.

153. Tirado-Rives, J.; Jorgensen, W. L., Contribution of Conformer Focusing to the Uncertainty in Predicting Free Energies for Protein–Ligand Binding. *Journal of Medicinal Chemistry* **2006,** 49 (20), 5880–5884.

154. Sitzmann, M.; Weidlich, I. E.; Filippov, I. V.; Liao, C.; Peach, M. L.; Ihlenfeldt, W.-D.; Karki, R. G.; Borodina, Y. V.; Cachau, R. E.; Nicklaus, M. C., PDB Ligand Conformational Energies Calculated Quantum-Mechanically. *Journal of Chemical Information and Modeling* **2012,** 52, (3), 739–756.

155. Paulini, R.; Dr., K. M. P.; Dr., F. D. P., Orthogonal Multipolar Interactions in Structural Chemistry and Biology. *Angewandte Chemie International Edition* **2005,** 44, (12), 1788–1805.

156. Robert E Babine, S. L. B., Molecular Recognition of Protein–Ligand Complexes: Applications to Drug Design. *Chemical Reviews* **1997,** 97, (5), 1359-1472.

157. J. P. Devlin, O. E. E., P. R. Gorham, N. R. Hunter, R. K. Pike, B. Stavric Anatoxin-a, a toxic alkaloid from Anabaena flos-aquae NRC-44h. *Canadian Journal of Chemistry* **1977,** 55, (8), 1367-1371.

158. Clarke, R. L., Chapter 2 The Tropane Alkaloids. *The Alkaloids: Chemistry and Physiology* **1977,** 16, 83–180.

159. Tatsuya Shono; Yoshihiro Matsumura; Kenshi Uchida; Tagami, K., A New Method of Formation of 9-Azabicyclo[4.2.1]nonane Skeleton and Its Application to Synthesis of (±)-Anatoxin a. *Chemistry Letters* **1987,** 16, (5), 919-922

160. Karen H Melching; Henk Hiemstra; Wim J Klaver; Speckamp, W. N., Total synthesis of (±)-anatoxin-a via N-acyliminium intermediates. *Tetrahedron Letters* **1986,** 27, (39), 4799–4802.

161. Peter M. Esch, H. H., Wim J. Klaver, and W. Nico Speckamp, An N-Acyliminium Route to the 8-Azabicyclo[3.2.1]octane (Tropane) and the 9-Azabicyclo[4.2.1]nonane Ring System Synthesis of (±)-Anatoxin-A. **1987,** 26, (1), 75-79.

162.   W.N. Speckamp; Hiemstra, H., Intramolecular reactions of N-acyliminium intermediates. *Tetrahedron* **1985,** 41, (20), 4367–4416.

163.   Henk Hiemstra; Speckamp, W. N., *4.5 – Additions to N-Acyliminium Ions*. 1991; Vol. 2, p 1047–1082.

164.   Charles M. Marson, U. G., Timothy Walsgrove, Drake S. Eggleston, Paul W. Baures, Stereoselective syntheses of substituted .gamma.-lactams from 3-alkenamides. *The journal of organic chemistry* **1991,** 56 (8), 2603–2605.

165.   Charles M. Marson; Urszula Grabowska; Walsgrove, T., Stereocontrolled syntheses of substituted unsaturated .delta.-lactams from 3-alkenamides. *The journal of organic chemistry* **1992,** 57, (19), 5045–5047.

166.   Shono, T., Electroorganic chemistry in organic synthesis. *Tetrahedron* **1984,** 40, (5), 811–850.

167.   Peter M.M. Nossin; Speckamp, W. N., Stereochemical control by remote substituents in α-acyliminium olefin cyclisations *Tetrahedron Letters* **1980,** 21, (20), 1991–1994.

168.   David A. Evans; Edward W. Thomas; Cherpeck, R. E., A stereoselective synthesis of (.+-.)-H12-histrionicotoxin and related photoaffinity-labeled congeners. *Journal of the American Chemical Society* **1982,** 104, (13), 3695–3700.

169.   Horst Böhme; Hartke, K., Über N-α-Halogenalkyl-carbonsäureamide, VII Die Umsetzung Schiffscher Basen mit Carbonsäurehalogeniden. *Chemische Berichte* **1963,** 96, (2), 600–603.

170.   Krow, G. R.; Pyun, C.; Leitz, C.; Marakowski, J.; Ramey, K., Heterodienophiles. VI. Structure of protonated aldimines. *The Journal of Organic Chemistry* **1974,** 39, (16), 2449–2451.

171.   Henk Hiemstra; Hendrikus P. Fortgens; Speckamp, W. N., Intramolecular reactions of acyclic n-acyliminium ions II allyl silanes as nucleophiles. *Tetrahedron Letters* **1985,** 26, (26), 3155–3158.

172.   Hendrik H Mooiweer; Henk Hiemstra; Hendrikus P Fortgens; Speckamp, W. N., Intramolecular reactions of acyclic n-acyliminium ions III silicon assisted cyclocondensation of glyoxylic esters to proline and pipecolic acid derivatives. *Tetrahedron Letters* **1987,** 28, (28), 3285–3288.

173.   Overman, L. E.; Malone, T. C.; Meier, G. P., Iminium ion and acyl iminium ion initiated cyclizations of vinylsilanes. Regiocontrolled construction of unsaturated azacyclics. *Journal of the American Chemical Society* **1983,** 105 (23), 6993–6994.

174.   Ent, H.; Koning, H. D.; Speckamp, W. N., 2-azonia-Cope rearrangement in N-acyliminium cyclizations. *The Journal of Organic Chemistry* **1986,** 51, (10), 1687–1691.

175.   Charles M. Marson; Pink, J. H., Convergent stereocontrolled construction of 5-7-6 tricyclic aza analogues of phorbol and aconite alkaloids. *Tetrahedron Letters* **1995,** 36, (44), 8107–8110.

176.   Tanis, S. P.; Deaton, M. V.; Dixon, L. A.; McMills, M. C.; Raggon, J. W.; Collins, M. A., Furan-Terminated N-Acyliminium Ion Initiated Cyclizations in Alkaloid Synthesis. *The Journal of Organic Chemistry* **1998,** 63, (20), 6914–6928.

177.   Henk Hiemstra, M. H. A. M. S., Robert J. Vijn, W. Nico Speckamp, Silicon directed N-acyliminium ion cyclizations. Highly selective syntheses of (.+-.)-isoretronecanol and (.+-.)-epilupinine. *J. Org. Chem.* **1985,** 50 (21), 4014–4020.

178.   D.A. Evans; Thomas, E. W., A formal synthesis of (±)-perhydrohistrionicotoxin View the MathML source α-acylimmonium ion-olefin cyclizations. *Tetrahedron Letters* **1979,** 20, (5), 411–414.

179.   Flynn, G. A.; Giroux, E. L.; Dage, R. C., An acyl-iminium ion cyclization route to a novel conformationally restricted dipeptide mimic: applications to angiotensin-converting enzyme inhibition. *Journal of the American Chemical Society* **1987,** 109, (25), 7914–7915.

180.   Daniel L. Comins; Paresh M. Thakker; Matthew F. Baevsky; Badawi, M. M., Chiral auxiliary mediated pictet-spengler reactions: Asymmetric syntheses of (−)-laudanosine, (+)-glaucine and (−)-xylopinine. *Tetrahedron* **1997,** 53, (48), 16327–16340.

181.   Fukuyama, T.; Nunes, J. J., Stereocontrolled total synthesis of (.+-.)-quinocarcin. *Journal of the American Chemical Society* **1988,** 110 (15), 5196–5198.

182.   Shono, T.; Matsumura, Y.; Uchida, K.; Kobayashi, H., A new [3 + 3]-type annelation useful for the formation of piperidine skeletons. *The Journal of Organic Chemistry* **1985,** 50, (17), 3243–3245.

183.   Hart, D. J., Vinylogous N-acyliminium ion cyclizations: application to the synthesis of depentylperhydrogephyrotoxin. *The Journal of Organic Chemistry* **1981,** 46, (2), 367–373.

184.   Tamelen, E. E. V.; Shamma, M.; Burgstahler, A. W.; Wolinsky, J.; Tamm, R.; Aldrich, P. E., Total synthesis of yohimbine. *Journal of the American Chemical Society* **1969,** 91, (26), 7315–7333.

185.   Loegers, M.; Overman, L. E.; Welmaker, G. S., Mannich Biscyclizations. Total Synthesis of (-)-Ajmalicine. *Journal of the American Chemical Society* **1995,** 117, (36), 9139–9150.

186.   Veenstra, S. J.; Speckamp, W. N., A stereoselective synthesis of indole alkaloid intermediates via N-acyliminium cyclizations. *Journal of the American Chemical Society* **1981,** 103, (15), 4645–4646.

187.   Andrew Madin; Christopher J. O'Donnell; Taeboem Oh; David W. Old; Larry E. Overman; Sharp, M. J., Total Synthesis of (±)-Gelsemine. *Angewandte Chemie International Edition* **1999,** 38, (19), 2934–2936.

188.   Downham, R.; Ng, F. W.; Overman, L. E., Asymmetric Construction of the Diazatricyclic Core of the Marine Alkaloids Sarains A−C. *The Journal of Organic Chemistry* **1998,** 63 (23), 8096–8097.

189.   Ismail, M. A.; Brun, R.; Easterbrook, J. D.; Tanious, F. A.; Wilson, W. D.; Boykin, D. W., Synthesis and antiprotozoal activity of aza-analogues of furamidine. *J Med Chem* **2003,** 46, (22), 4761-9.

190.   Stephen Hanessian, G. Y., Jean-Michel Rondeau, Ulf Neumann, Claudia Betschart, and Marina Tintelnot-Blomley, Structure-Based Design and Synthesis of Macroheterocyclic Peptidomimetic Inhibitors of the Aspartic Protease -Site Amyloid Precursor Protein Cleaving Enzyme (BACE). *journal in Medicinal Chemistry* **2006,** 49, (15), 4544-4567.

191.   Skerlj, R. T., Facile Cyanomethylation of Bromopyridines by Nucleophilic Substitution with Lithioacetonitrile *Synlett* **2000** 1488-1490.

192.   Lim, M. H., Direct Nitric Oxide Detection in Aqueous Solution by Copper(II) Fluorescein Complexes. *J. Am. Chem. Soc.* **2006,** 128 (44), 14364 -14373.

193.   Edward M. Engler, J. D. A., and Paul V. R. Schleyer, Critical evaluation of molecular mechanics. *Journal of the American Chemical Society* **1973,** 95, (24), 8005 - 8025.

194.   Dubowchik, G. M. M., CT) United States Patent 6818643. **11/16/2004**

195.   Guo, C.; Dong, L.; Kephart, S.; Hou, X., An efficient synthesis of sulfamides. *Tetrahedron Letters* **2010,** 51, (21), 2909–2913.

196.   Gopalakrishnan, R.; Kozany, C.; Gaali, S.; Kress, C.; Hoogeland, B.; Bracher, A.; Hausch, F., Evaluation of Synthetic FK506 Analogs as Ligands for the FK506-Binding Proteins 51 and 52. *J Med Chem*.

197.   Gopalakrishnan, R.; Kozany, C.; Wang, Y.; Schneider, S.; Hoogeland, B.; Bracher, A.; Hausch, F., Exploration of Pipecolate Sulfonamides as Binders of the FK506-Binding Proteins 51 and 52. *J Med Chem*.

198.   Schmidt, M. V.; Paez-Pereda, M.; Holsboer, F.; Hausch, F., The Prospect of FKBP51 as a Drug Target. *ChemMedChem* **2012**.

199.   G. Klebe; F. Dullweber; Böhm, H. J., *Drug-Receptor Thermodynamics: Introduction and Applications*. John Wiley & Sons: 2001; p 83.

200.   Martin, S. F., Preorganization in biological systems: Are conformational constraints worth the energy? *Pure and Applied Chemistry* **2007,** 79, (2), 193.

201.   Benfield, A. P.; Teresk, M. G.; Plake, H. R.; DeLorbe, J. E.; Millspaugh, L. E.; Martin, S. F., Ligand preorganization may be accompanied by entropic penalties in protein-ligand interactions. *Angew Chem Int Ed Engl* **2006,** 45, (41), 6830-5.

202.   Edwards, A. A.; Mason, J. M.; Clinch, K.; Tyler, P. C.; Evans, G. B.; Schramm, V. L., Altered enthalpy-entropy compensation in picomolar transition state analogues of human purine nucleoside phosphorylase. *Biochemistry* **2009,** 48, (23), 5226-38.

203.   Edwards, A. A.; Tipton, J. D.; Brenowitz, M. D.; Emmett, M. R.; Marshall, A. G.; Evans, G. B.; Tyler, P. C.; Schramm, V. L., Conformational states of human purine nucleoside phosphorylase at rest, at work, and with transition state analogues. *Biochemistry* **2010,** 49, (9), 2058-67.

204.   Hanessian, S.; Tremblay, M.; Petersen, J. F., The N-acyloxyiminium ion aza-Prins route to octahydroindoles: total synthesis and structural confirmation of the antithrombotic marine natural product oscillarin. *J Am Chem Soc* **2004,** 126, (19), 6064-71.

205.   Ivan Collado, J. E., Concepcion Pedregal, Stereoselective Addition of Grignard-Derived Organocopper Reagents to N-Acyliminium Ions: Synthesis of Enantiopure 5- and 4,5-Substituted Prolinates. *J. Org. Chem.,* **1995,** 60, (16), 5011–5015.

206.   J.C. Hubert, J. B. P. A. W., W.Nico Speckamp, NaBH4 reduction of cyclic imides. *Tetrahedron* **1975,** 31, (11–12), 1437–1441.

207.   Neuenschwander, G. A. K. a. K., Amidoalkylations with allylic silanes: a facile synthesis of the carbapenem system. *J. Chem. Soc., Chem. Commun.* **1982**, 134-135.

208.   Henk Hiemstra, W. J. K., W. Nico Speckamp, .omega.-Alkoxy lactams as dipolar synthons. Silicon-assisted synthesis of azabicycles and a .gamma.-amino acid. *The Journal of Organic Chemistry* **1984,** 49 (6), 1149–1151.

209.   Bracher, A.; Kozany, C.; Thost, A. K.; Hausch, F., Structural characterization of the PPIase domain of FKBP51, a cochaperone of human Hsp90. *Acta Crystallogr D Biol Crystallogr* **2011,** 67, (Pt 6), 549-59.

210.   Banks, P., Understanding fluorescence polarization and its data analysis. *Physical Principles Of Fluorescence Polarization.*

211.   Hudack, R. A., Design, Synthesis, and Biological Activity of Novel Polycyclic Aza-Amide FKBP12 Ligands *journal of Medicinal Chemistry* **2006,** 49, 1202-1206.

10.Curriculum Vitae

YANSONG, WANG

Research Group Chemical Genomics

Max Planck Institute of Psychiatry

Kraepelinstr. 2-10, 80804, Munich, Germany

Email address: yansong@mpipsykl.mpg.de

Phone: +49-(0)17621895586

Education:

2008-2012	Ph.D study, Max Planck Institute of Psychiatry, Munich, Germany.
2006-2008	Master of Sciences (M.Sc), Molecular Biosciences at the University of Heidelberg, Germany.
1999 - 2003	B.S., College of Pharmacy, The Second Military Medical University, Shanghai, China.

Grants and Fellowships:

- Max-Planck doctoral fellowship for doctoral research at the Max Planck Institute of Psychiatry, Munich, Germany. 2008 to present
- MCB scholarship from MCB program Heidelberg University, Heidelberg, Germany 2006-2008

Talks:

1. MPIP Institute PhD seminar series, 2011
2. Ligands for FKBP51 and FKBP52. MPI Psychiatry Ringberg symposium 2011.
3. Chemical exploration of the FK506-binding protein 51. MPI Psychiatry summer symposium 2012.

Patent filing:

1. **Wang Y**, Hausch.F. [3.3.1] and [4.3.1] bicyclic pipecolate analogs as FKBP51 and FKBP52 ligands.

10.Curriculum Vitae

Publications and Manuscripts:

1. **Wang Y**, Kirschner A, Fabian A, Gopalakrishnan R, Kress C, Hoogeland B, Koch U, Kozany C, Bracher A, Hausch F*. **Increasing Ligand Efficiency by Conformational Control.** Submitted to Nature Chemistry

2. Gopalakrishnan R, Kozany C, **Wang Y**, Schneider S, Hoogeland B, Bracher A, Hausch F. **Exploration of Pipecolate Sulfonamides as Binders of the FK506-Binding Proteins 51 and 52.** J. Medicinal Chemistry. 2012 May 10;55(9):4123-31. DOI: 10.1021/jm201747c

3. Gaali S, Gopalakrishnan R, **Wang Y**, Kozany C, Hausch F. **The chemical biology of immunophilin ligands**. Current Medicinal Chemistry, 2011,18,5355-5379

4. Ming G, Zhao J, **Wang Y,** Duan Q. **Recent advances in treatment of HIV-infected patients.** Medical Journal of National Defending forces in Southwest China, 2005, 1, 107-110 in chinese.

5. Zhi J, Zhang G, **Wang Y, Clinical Significance of Detecting C-Reactive Protein and IL-6 on Patients with Acute Pancreatitis**. Journal of Dali Univerity, 2005, 4, 43-44 in chinese.

6. **Wang Y,** Ming G, Zhao J. **Medical research progress of Ganoderma lucidum.** Medical Journal of National Defending forces in Southwest China, 2004, 14, 680-682 in chinese.